THE SURFACE EXCHANGE OF TRACE GASES IN THE TROPICS AND SAVANNAS

vorgelegt von / by

Grant A. Kirkman

Dissertation zur Erlangung des Grades „Doktor der Naturwissenschaften“ / A thesis submitted in fulfillment of the requirements for the degree of Doctor of Natural Sciences

am Fachbereich Geowissenschaften der Johannes Gutenberg-Universität Mainz, Deutschland / Faculty of Geosciences, Johannes Gutenberg University, Mainz, Germany

Mai / May 2001

geboren Kapstadt / born Cape Town

Berichterstatter 1:

Berichterstatter 2:

Tag der mündlichen Prüfung: _____ 6 Juli 2001

ERKLÄRUNG

Hiermit versichere ich gemäß § 11(3) der Promotionsordnung vom 30. April 1990, dass ich diese als Dissertation vorgelegte Arbeit selbständig verfasst und alle benutzten Hilfsmittel und Quellen in der Arbeit angegeben habe. Sie ist weder als Prüfungsarbeit für andere Prüfungen noch ganz oder teilweise als Dissertation an einer anderen Fakultät oder einem anderen Fachbereich eingereicht worden.

Mainz, den 02.05.2001

(Grant A. Kirkman)

Abstract

THE SURFACE EXCHANGE OF TRACE GASES IN THE TROPICS AND SAVANNAS

by Grant A. Kirkman

The tropospheric trace gases NO_x (Nitric Oxide (NO) and Nitrogen Dioxide (NO_2)) control the production of the Hydroxyl Radical (OH) and Ozone (O_3). Soil sources of NO_x are largely uncertain. The objective of this work was to study the processes responsible for soil NO emissions using laboratory-, field measurements and model simulations so as to estimate soil emissions for two regions, the tropical forests of Rondônia (Brazil) and the subtropical savannas of Zimbabwe. Measured NO emissions data were used in a modified process-oriented trace gas model, which showed that forest clearing in the tropics caused periods of elevated soil NO release, which declined over time. The up scaled simulations for 1999 revealed that emissions have doubled since the area was entirely covered by forest. The combination of both land-use and soil moisture were shown to be useful NO emission predictors on the dystrophic tropic and eutrophic savanna soils. Annual soil NO emission rates for the tropics (0.49 kg N ha yr^{-1}) were approximately half those estimated for the subtropical savannas (0.86 kg N ha yr^{-1}). However, the tropics are expected to play an important role in future tropospheric chemistry as long as forests continue to be cleared.

Zusammenfassung

THE SURFACE EXCHANGE OF TRACE GASES IN THE TROPICS AND SAVANNAS

vorgelegt von Grant A. Kirkman

Die Spurengase NO_x (Stickstoffoxid (NO) und Stickstoffdioxid (NO_2)) haben massgeblichen Einfluss auf die Produktion von OH (Hydroxylradikal) und Ozon (O_3) in der Troposphäre. Die Bodenemissionen dieser Gase sind weitgehend unbekannt. Das Ziel dieser Arbeit war, die für die NO Bodenemissionen relevanten Prozesse durch Labor und Feldmessungen zu untersuchen und diese durch Modellsimulationen für zwei Regionen, ein tropisches Regenwaldgebiet in Rondônia (Brasilien) und subtropische Savannen in Zimbabwe abzuschätzen. Unter Verwendung der gemessenen NO Werte ergaben die Simulationen mit einem modifizierten prozessorientierten Modell, dass Abholzung in den Tropen nach einer kurzzeitigen Erhöhung zu einer langfristigen Abnahme der Bodenemissionen führt. Ein "up scaling" der Modellresultate ergab ausgehend von der ursprünglichen Bewaldung der Region eine Verdopplung der NO Bodenemission bis 1999. Sowohl für nährstoffarme Böden der Tropen als auch für die nährstoffreichen Savannenböden waren Landnutzung und Bodenfeuchte die wichtigsten Einflussgrössen für die Regulierung der Emissionen. Über den Zeitraum eines Jahres waren die Emissionsraten der Tropen (0.49 kg N ha yr^{-1}) ungefähr halb so gross wie die der subtropischen Savannen (0.86 kg N ha yr^{-1}). Solange die Abholzung der Regenwälder voranschreitet werden die Tropen starken Einfluss auf die troposphärische Chemie haben.

TABLE OF CONTENTS

LIST OF FIGURES

ACKNOWLEDGMENT AND DEDICATION

The author wishes to acknowledge the contribution of my 'Doktorvater' Prof. Dr. Dietmar Schenk for accepting to be examiner of this thesis. I am also especially indebted to Prof. Dr. Franz X. Meixner who initiated my interest in this fascinating field and provided me with encouragement, friendship and the opportunity to work in an interdisciplinary environment with a high degree of independence. I am also indebted to several who added constructive critic and logistical support without which this monograph would not be possible; Dr. Christof Amman, Dr. Andreas Gut, Mr Udo Rummel, Mr Micheal Welling and, Prof. Dr. Beth Holland. The co-examiners Prof. Dr. J. Preuß and Prof. Dr. A. Seitz are also acknowledged. The present study was carried out at the Biogeochemistry Department of the Max Planck Institute for Chemistry in Mainz and was financially supported by of the Graduate College *"Kreisläufe, Austauschprozesse und Wirkungen von Stoffen in der Umwelt"* (Gutenburg University, Mainz, Germany) and the Max Planck Society, Germany.

This work is dedicated to our blue planet and to my ever supportive and loving parents, Chris and Priscilla Kirkman and companion Sabine Seitz.

THE SURFACE EXCHANGE OF TRACE GASES IN THE TROPICS AND SAVANNAS

Approximately 99 % of the earths atmosphere is made up of three gases; nitrogen, oxygen and argon. The remaining 1 % comprises trace gases; most of whose surface sources and sinks are only partly understood in the developed world. Among these trace gases are nitric oxide (NO) and nitrogen dioxide (NO_2), (collectively NO_x) whose presence plays a particularly important role in tropospheric photochemistry, by controlling the production and destruction of the greenhouse gas ozone (O_3) and the atmospheric cleanser hydroxyl radical (OH) [*Crutzen*, 1974, 1979]. Slight increases (parts per trillion) in tropospheric concentrations of NO_x trigger the production of O_3 and OH in the presence of reactive hydrocarbons such as methane (CH_4) and carbon monoxide (CO), whilst O_3 can be destroyed, when NO_x concentrations are low, during the oxidation of these compounds [*Fishman et al.*, 1979, *Lin et al.*, 1988]. NO_x is also an effective acidifier of the environment when photo-chemically oxidized to gaseous and particulate nitrate (HNO_3, NO_3^-) and then deposited (dry and/or wet) to land surfaces. The significant emission of NO_x both from anthropogenic (fire, fossil fuel combustion) and natural sources (soils, lightning), production of tropospheric O_3, and resultant deposition of these gases can significantly alter atmospheric and ecosystem chemistry thereby affecting biomass growth, production and human health [*Chameides et al.*, 1994; IPCC, 1995; *Wesely & Hicks*, 2000].

Soil NO Emissions

There are six primary global sources of NO_x; these include fossil fuel combustion, soil biogenic emissions, biomass burning, lightning discharge, upper tropospheric aircraft emissions, and stratospheric intrusions. The most prominent sources are fossil fuel-, biomass burning and soil biogenic emissions. The former two sources are largely anthropogenically produced. Fossil fuel combustion sources generally confined to industrial areas and biomass burning sources to rural areas with a strong seasonal bias [*Kirkman et al.*, 1998, 2000]. These anthropogenic sources are the primary cause of changes in present day tropospheric NO_x concentrations [*Matson*, 1997, *Delmas et al.*, 1997] and global

estimates have been place at 22 ± 7 Tg N year^{-1} [*Dignon*, 1992] and 6.7 ± 3.7 Tg N year^{-1} [*Delmas et al.*, 1997] for fossil fuel and biomass combustion NO_x emissions respectively.

NO_x emissions estimates from soil biogenic processes are much more uncertain, due to the difficulties faced in quantifying them at spatial scales [*Davidson & Kingerlee*, 1997; *Ludwig et al.*, 2001, *Holland & Larmarque*, 1997]. Soils act predominantly as a source of NO but can under elevated ambient mixing ratios, become a NO_x sink [*Meixner*, 1994a, *Conrad*, 1994]. They are governed by a complex interplay of soil processes at scales < 1 cm, which are in turn governed by climate at the synoptic scale and land-use at interannual scales. Complete information on soil microbial populations, species, metabolism, and environmental responses are at present not forthcoming and probably will remain so due to the shear multitude of biota found in a single gram of soil [*Conrad*, 1996]. Global estimates of soil NO emissions are proposed to be approximately 21 ± 10 Tg N-NO yr^{-1}, or 13 ± 6 Tg N-NO yr^{-1} after correction for the plant uptake mechanism commonly known as *canopy reduction factor* (CRF). This refers to the uptake by canopy biomass of soil NO emissions, which reduces its net flux to the tropospheric boundary layer [*Jacob & Bakwin*, 1991]. The above global soil NO emission estimates were derived by simply summing the product of the area and the mean measured (from an inventory of field measurements) soil NO exchange rate for a set of global biomes [*Davidson & Kingerlee*, 1997].

Soil NO is largely produced by soil microbial action (biotic) with a smaller contribution from chemical processes (abiotic) within the soil matrix. The microbial production pathway is the result of primarily two processes; nitrification and denitrification, which are influenced by soil environmental conditions [*Conrad*, 1996]. These conditions are exclusively related to the top 5–10 cm of the non-polar continental soil surfaces of the globe. They include (a) soil– temperature, (b) moisture, (c) fertility, (d) vegetative biomass cover, and (e) fire. These environmental controlling factors vary spatio-temporally, often in contradiction to one another, but can make useful predictors of the microbial scale processes responsible for NO emissions from soils [*Hutchinson et al.*, 1997]. Using these environmental predictors to model or scale up strategically selected soil NO emission measurements provides a more accountable and meaningful method to simply summing the product of area and emission rate. For example soil temperature can be used to predict the diel pattern of soil NO emissions when soil moisture is not limiting [*Ludwig et al.*, 2001]. At larger temporal scales, a 10 °C rise in soil temperature produces a 2-5 fold increase in NO emission rates [*Williams & Fehsenfeld*, 1991; *Valente & Thornton*, 1993]. Soil moisture (cf. Fig. 2.2 in chapter 2), which controls soil oxygen and substrate and gas transport, thereby soil microbial processes (nitrification and denitrification) is also an extremely

useful predictor of soil NO emissions imparting a measure of seasonal variance in model or up scaled estimates [*Potter et al.*, 1996]. It can influence soil behavior so dramatically that NO production can revert to NO consumption in a matter of hours after rainfall [*Davidson*, 1991]. Soil moisture also affects the gas diffusive properties of soils and abrupt changes in soil moisture (particularly rainfall after a dry period) can result in large "pulses" of NO [*Davidson*, 1991].

Soil fertility (ammonium (NH_4^+), and nitrate (NO_3^-) concentrations) and organic matter (OM) turnover rates are equally reasonable indicators of NO emission rates, particularly in those ecosystems deprived of such reserves (i.e. the tropics). Land-use practices, such as deforestation, which can alter soil fertility, are good indicators of soil nitrogen status and therefore NO emissions at long temporal scales [*Davidson et al.*, 2000]. Vegetative biomass, which is largely related to land-use, affects NO emissions in two ways; (a) directly via the CRF and (b) indirectly by controlling the input of soil nutrients from the decomposition of litterfall, roots and organic matter. The canopy uptake of NO (CRF) can reduce soil NO emissions by up to 75 %. This takes place by O_3 titration of NO to NO_2 and the consequent uptake of NO_2 via the stomata and/or cuticle within the plant canopy [*Jacob & Bakwin*, 1991]. Fire is often used to eradicate cut and felled vegetation and results in a temporary reduction in the plant and microbial sink of soil inorganic nitrogen by removing live biomass and dead litter with high C:N ratios. This results in favorable conditions for biotic (nitrification and denitrification) and abiotic (chemodenitrification) NO production and recent observations have shown that significant amount of NO can be produced after fire events [*Poth et al.*, 1995; *Keller et al.*, 1993; *Keller & Rieners*, 1994; *Neff et al.*, 1995; *Weitz et al.*, 1998; *Verchot et al.*, 1999]. This source has seldom been accounted for in emission inventory and model based soil NO estimates [*Davidson*, 1991].

Trace Gas Deposition

Surface deposition is the process whereby atmospheric trace substances are transferred by turbulent air motions (dry) and precipitation (wet) to vegetated and soil surfaces. Besides SO_2, oxides of nitrogen and O_3 deposition have been blamed for losses of biodiversity in recent decades and may be acting to influence the atmosphere indirectly by altering the global carbon cycle [*Fishman et al.*, 1979; *Ramanathan et al.*, 1987; *Galloway*, 1995]. The impacts of nitrogen deposition are tightly linked to other rapidly changing human-driven variables such as fossil fuel burning, vehicular traffic, shifts in land-use, climate, atmospheric carbon dioxide (CO_2) and O_3 levels [*Vituosek et al.*, 1997].

The deposition of nitrogen to the earth surfaces includes [1]NO_y and [2]NH_x, with NO_y constituting the smaller fraction of total nitrogen deposited to the surface [*Holland & Larmarque*, 1997]. The dry and wet deposition of NH_3, HNO_3 and NO_2 to land surfaces is a significant means of gaseous nitrogen removal within the planetary boundary layer and typically occurs onto vegetation (plant stomata/cuticle), bare soil surfaces or into solution with surface water [*Meixner*, 1994a]. Of these very little is known about the mechanisms responsible for and magnitudes of NO_2 and O_3 dry deposition [*Lerdau et al.*, 2000], and no studies have specifically addressed this phenomenon over deforested landscapes in the tropics. An explicit evaluation of the mechanisms governing NO_2 and O_3 deposition and NO emissions are necessary for the prediction of their effects on regional land surface C and N cycles and tropospheric chemistry [*Matson*, 1997; *Vitousek et al*, 1997].

Current estimates of mankind's contribution to global NO_x emissions stand at approximately 80 % [*Vitousek et al.*, 1997]. An improvement in the estimation of the largest natural source of NO (soils) and an understanding of NO_2 and O_3 removal processes, is essential to improving the evaluation of the anthropogenic effects on global NO_x and O_3 chemistry. Two mutually inclusive approaches are available for achieving this—field and laboratory measurements and model simulation of trace gas exchanges.

Measurement of Trace Gas Exchanges

Surface to atmosphere exchange of trace gases and in particular NO_x and O_3 have been studied on a range of scales from a few square meters in the field [*Williams et al.*, 1992a; *Meixner et al.*, 1997; *Gut et al.*, submitted, 2001a; Chapter 1] to entire countries and continents in models [*Yienger & Levy*, 1995; *Potter et al.*, 1996, 1998; Chapter 2 & 3]. Typically measurement of the surface exchange of these gases in the field is made using an enclosed chamber, of various designs (without or without exchange of air within the chamber), placed over the plant/soil surface. The use of flow through or dynamic chambers (with air exchange) provides the least disturbance to field conditions and allows for measurements to proceed for longer periods at one location than a closed or static system (without air exchange) [*Matson & Harris*, 1995]. A second approach to the field measurement of trace gas exchanges includes the micrometeorological method, which represents the least disturbance to the ecosystem but is restricted to selected areas with uniform, level terrain. Similar to the chamber method, measurements of trace gas exchanges with the micrometeorological method are also particularly

[1] $NO_y = NO_x + HNO_2 + HNO_3 + HO_2NO_2 + NO_3 + 2N_2O_5 + PAN$ (peroxyacetyl nitrate)

[2] $NH_x = (NH_4^+ + NH_3 + (NH_4)_2SO_4)$

sensitive to the interference from chemical reactions that take place at rates faster than turbulent transport times [*Villá-Guerrau de Arellano & Duynkerke,* 1992].

Several studies have assessed the emission of NO from soils and surface uptake of NO_2 and O_3 [*Hicks & Matt*, 1988; *Huebert & Roberts*, 1985; *Johansson*, 1987], but none have specifically addressed the net ecosystem exchange of the NO-NO_2-O_3 gas triad over soil and plant surfaces in the degraded tropics. The first measurements of this kind, spanning a period of ca. one month at a half-hour time resolution, from a 22-year-old cattle pasture in southwestern Brazil (Rondônia), are presented in chapter 1. Details on measurement techniques, errors, chemical corrections, findings and implications are discussed therein.

Laboratory measurements of soil NO emissions is a specialized field described in detail by *Remde et al.* [1993] and *Yang et al.* [submitted, 1998] and is summarized in chapter 4. It provides an alternative to field measurements as a high data return rate can be achieved with a relatively small sampling strategy. It generally involves the observation of NO production by subjecting small amounts of soil sample to a range of environmentally controlled conditions. It has recently been perfected to such an extent that results from laboratory studies can be used in models to successfully emulate the magnitudes of NO fluxes observed by field measurements [*Yang et al.*, submitted, 1998; *van Dijk et al.*, submitted, 2001].

Simulation of Soil NO_x Exchange

Tropospheric NO is a highly reactive gas (~1 day) [*Conrad*, 1996; *Kramlich & Linak*, 1994], which is in part produced and consumed by soil microbes and influenced by climatic conditions and anthropogenic land-use practice, making soil source contributions extremely difficult to quantify at large scales. Simulating soil NO emissions requires innovative approaches and is best achieved at a regional scale. Quantification at the global scale can mask the relative importance of soil NO sources at the scale where NO predictors (soil moisture etc.) are likely to offer predictability and where emissions might make the most impact on atmospheric chemistry and global biogeochemical cycles [*Matson*, 1997]. In addition by resolving regional emissions, effects such as seasonal, spatio-temporal or anthropogenic influences, which otherwise would be hidden in global estimates, are resolved. For example elevated NO emissions during cool-dry to hot-wet transitions periods of the year may coincide with periods where meteorological conditions are ripe for the production of O_3. Studies at regional scales [*Parkin*, 1993] are also useful for validating proxy variables and boundary assumptions for use in larger scale model (GCM) studies [*Hutchinson et al.*, 1997].

The regional estimation of soil NO emissions are only possible through the use of some form of spatial extrapolation method [*Stewart et al.*, 1989]. The simplest approach is to conduct field measurements of soil NO emissions randomly and to estimate the area flux based upon the random sample. An improvement might be to sample strategically, based on sub-regional classes [*Davidson & Kingerlee*, 1997], and a further improvement might be to estimate regional emissions according to parameters that control trace gas fluxes [*Matson et al.*, 1989]. Because trace gas fluxes can be highly variable in time and space, a prohibitively large number of samples are required to achieve an estimate with an acceptable level of confidence, with these approaches [*Folorunso & Rolston*, 1984]. Since field-sampling experiments are expensive and time consuming, the number of field measurements is desirably kept to a minimum. A compromise is therefore to use a selection of the most significant environmental predictors of soil NO emissionsfor a particular region. To then use these predictors in semi-empirical model schemes to scale up (spatial extrapolation) a minimum number of strategically sampled field measurements to arrive at an estimate of regional soil NO emissions.

Two regions or global biomes, which are believed to make up a significant contribution to global tropospheric NO concentrations, have been highlighted as deserving of further research attention [*Ludwig et al.*, 2001; *Davidson & Kingerlee*, 1997; *Matson*, 1997; *Potter et al.*, 1996; *Yienger & Levy*, 1995]. These are the seasonally dry savanna/agriculture biomes of the subtropics (ca. 7.4 Tg N-NO yr^{-1}) and the forest/secondary forest/pasture biomes of the tropics (ca. 1.6 Tg N-NO yr^{-1}) [*Davidson & Kingerlee*, 1997; *Delmas et al.*, 1997, *Matson*, 1997].

Tropical Soil NO

Soils in the Amazon basin are predominantly dystrophic, as their nutrients have long since been washed out by the high annual precipitation. Therefore soil nutrient status and in particular nitrogen availability, which is strongly coupled to land-use and age since primary deforestation, provide for useful environmental predictors of soil NO emissions for this region. The state of Rondônia (Brazil) is unique, as conversion of rainforest to agriculture has taken place at an unprecedented rate in the last 20 years, resulting in vast areas of degraded and recovering land. This area is ideal for the studies of the effects of land-use change on soil NO emissions in this region and provides an insight into the future Amazon.

Field measurements of soil NO emission, NO_2 and O_3 deposition from a 22-year old cattle pasture in Rondônia are presented in chapter 1. These measurements

and those from a forest from co-authored work [*Gut et al.*, submitted, 2001a, 2001b] in Rondônia were used in a 1-D plant-soil ecosystem based trace gas model to predict soil NO emissions in response to various land-use and agricultural management practices in chapter 2. Results from these model integrations, which include soil NO emissions for a transition from forest to pasture, were used in conjunction with satellite imagery to up scale to regional NO emissions for an area of Rondônia in chapter 3.

Subtropical Soil NO

The subtropical savannas of Africa are characterized by long dry seasons followed by periods of interspersed rain and dry spells. The soils are generally eutrophic in contrast to the highly leached soils of the tropics [*Aubert & Tavanier*, 1972]. As a result the environmental predictor most limiting soil NO emissions in this region is soil moisture [*Scholes & Andreae*, 2000]. Laboratory measurements of soil NO emissions in response to soil moisture and temperatures were conducted by *Yang & Meixner* [1997]. They also showed that their laboratory experiments were able to reasonably reproduce field measurements of NO from the same soils in Zimbabwe [*Ludwig et al*, 2001]. These results were used in an empirically based up scaling scheme for the savanna/woodland/agriculture land-use complex of legal Zimbabwe (southern Africa). This was achieved using a GIS (geographic information system) with observed and remotely sensed data. The up scaling scheme included soil moisture, soil temperature, land-use class, vegetative biomass, rainfall induced NO pulsing and a CRF sub-model. This approach explicitly excluded soil nutrient dynamics as an environmental predictor, as its influence paled in significance to soil water content on the nutrient rich soils of subtropical Zimbabwe.

Objectives

The primary objective of this work was to scale up soil NO emissions for two tropospheric chemically important regions of the globe—subtropical southern Africa and tropical South America. These regions were chosen as they are considered important contributors to the global NO_x and O_3 budgets, and include the savanna/woodland/agriculture complex of Zimbabwe, and the forest/secondary forest/pasture transition of the state of Rondônia in Brazil. This work also aimed to pioneer an approach to quantifying soil NO emissions, which facilitated a minimum of field measurements by using current understanding of the processes governing NO_x exchanges from literature, laboratory–, field measurements and empirical models at the regional scale. Results from these approaches are also compared with existing soil NO flux inventories and model estimates in an effort to verify their utility. The objectives

were achieved by making use of NO flux environmental predictors that were specific and central to controlling most of the NO_x exchange for the two regions studied. For example land-use patterns coupled to soil nutrient dynamics in the tropics and soil water distribution in response to seasonal climatology in the subtropics.

In addition this work aimed to address an area of research not previously attempted in the tropics by investigating the exchange dynamics and contributions of the NO-NO_2-O_3 trace gas triad over aged tropical soils. This field experiment in Rondônia was also conducted in order to provide valuable input into the up scaling scheme for the tropics. The concepts demonstrated in the up scaling sections [Chapters 2–4] and results from measurements made in the field [Chapter 1] are presented such that they may be easily incorporated into larger scale biosphere or photochemical models.

A summary of these objectives, results and their significance to trace gas research are discussed in the concluding section, chapter 5.

C h a p t e r 1

SURFACE EXCHANGE OF NO_X AND O_3 IN RONDÔNIA, BRAZIL

The study of NO–NO_2–O_3 trace gas exchange over established tropical pastures, is fundamental to our understanding of how deforested environments affect regional trace gas budgets, and consequently global tropospheric chemistry. The study of NO_x (NO_x = NO + NO_2) and O_3 exchange provides an insight into soil microbial ecology, and the nitrogen cycling of these disturbed ecosystems. Diurnal observations of uptake (NO_2 and O_3) resistances over a soil and grassland environment in the tropics also have important implications for multi-resistance– climate– and regional biogeochemical modeling. Measurements of NO–NO_2–O_3 trace gas exchange were performed for two-transition season periods during 1999 (30 April to 17 May, "wet–dry", and 24 September to 27 October, "dry–wet") over a cattle pasture in Rondônia. A dynamic chamber system (applied during the "dry–wet" season) was used to measure emission fluxes of NO and surface resistances for NO_2 and O_3 deposition directly. In order to determine ecosystem-representative NO_2 and O_3 deposition fluxes for both measurement periods, an inferential method (multi-resistance model) was applied to measured ambient NO_2 and O_3 concentrations using observed quantities of turbulent transport. Supplementary measurements included soil NO diffusivity and soil nutrient analysis. The observed NO soil emission fluxes were nine times lower than old-growth rainforest emissions under similar soil moisture and temperature conditions and were attributed to the combination of a conservative soil N–cycle and lower effective soil NO diffusion at the pasture. Canopy resistances (R_c) of both gases controlled the deposition processes during the day for both measurement periods. Day and night NO_2 canopy resistances were significantly similar ($\alpha = 0.05$) during the "dry–wet" period. Ozone canopy resistances revealed significantly higher daytime resistances of 106 s m^{-1} versus 65 s m^{-1} at night due to plant, soil and wet skin uptake processes, accentuated by stomatal activity at night and aqueous phase chemistry on vegetative and soil surfaces. The surface of the pasture was a net NO_x sink during 1999 removing seven times more NO_2 from the atmosphere as was emitted as NO.

1.1 Background

Over the last 25 years more than 70 million ha of the native vegetation in Brazil have been replaced by pastures for beef production mostly planted to grasses of the African genus *Brachiaria*. Rondônia has seen a large proportion of this development and stands today as one of the best examples of how rapidly South American tropical ecosystems are undergoing anthropogenic change. Several

years after deforestation and establishment of agriculture there is a marked decline in soil productivity, reported as declining yields forcing farmers to either abandon their land or establish permanent agriculture [*Moran*, 1993]. Along and in strong interaction with changes in soil productivity are also changes in soil-atmosphere exchange of trace gases such as nitrogen oxides (NO_x = NO + NO_2) and ozone.

The measurement of all three species of the NO-NO_2-O_3 triad is a precondition for studying and making inferences on these exchange process at the landscape scale. This is firstly due to the fast chemical reactions of nitric oxide (NO) with ozone (O_3) or peroxyl radicals, which form nitrogen dioxide (NO_2) [*Crutzen*, 1974, *Kolar*, 1990], and the reverse photo-dissociation of NO_2 during the day (< 400 nm). Time scales for these reactions are in the order of minutes and can consequently be in the same order as time scales for turbulence mixing at the surface [*Kramm et al.*, 1991]. Secondly, these gases are governed by quite different air-surface exchange regulating processes. For instance the predominant natural source of NO is the soil where biotic (nitrification and denitrification) and abiotic (chemodenitrification) processes produce this gas. Within the soil environment the aerobic process of nitrification (predominant at < 60% water filled pore space–WFPS) is maintained primarily by autotrophic bacteria resulting in the conversion of ammonium (NH_4^+) to nitrate (NO_3^-) via nitrite (NO_2^-). There are two groups of nitrifiers namely the ammonium-oxidizing nitrifiers, which convert NH_4^+ via hydroxylamine to NO_2^- and the nitrite-oxidizing nitrifiers, which oxidize NO_2^- to NO_3^-. Denitrification on the other hand is an anaerobic process (predominant at > 60% WFPS) where denitrifiers reduce NO_3^- via NO_2^-, NO and nitrous oxide (N_2O) to molecular nitrogen (N_2). The complete denitrification pathway results in the reduction of NO_3^- to N_2, but significant amounts of NO can be emitted before complete reduction to N_2 [*Remde et al.*, 1989, *Remde & Conrad*, 1991; *Cardenas et al.*, 1993]. Soil pH, metallic ion composition, and soil organic matter (SOM) all control the abiotic process of chemodenitrification, whereby microbially produced NO_2^- is decomposed to NO and NO_2 [*VanCleemput & Baert*, 1984; *Davidson*, 1992]. Recent work in Rondônia has shown that NO fluxes from old pastures are 25 times lower than adjacent forest fluxes [*Garcia-Montiel et al.*, 1999]. Further, *Davidson et al.* [2000] confirmed from a variety of tropical sites in Costa Rica, Puerto Rica and Brazil that old tropical pastures produce consistently lower NO fluxes than old-growth tropical forests. The reasons for these differences are changes in the factors controlling NO emissions between the two ecosystems. These include a combination of soil water, –temperature, –nutrient status, –pH, diffusion, plant biomass characteristics, and ambient atmospheric conditions [*Davidson et al.*, 2000; *Ludwig et al.*, 2001].

The exchange of O_3 and NO_2 occurs via dry deposition onto vegetation (plant stomata/cuticle), onto bare soil surfaces or into solution with surface water

[*Meixner*, 1994a]. The rate at which plant stomatal uptake occurs is determined by the concentration gradient between the gas phase inside and outside the leaf, leaf temperature, water vapor deficit and intensity of photosynthetic radiation, although some uncertainty surrounds the magnitude of this process, particularly for NO_2 [*Lerdau et al.*, 2000]. Removal rates of O_3 by soils with high levels of organic matter and moderate moisture content have been shown to be significant [*Wesely & Hicks*, 2000]. Less is known about bare soil as a NO_2 sink, however there are reports of NO_2 reactions with humic acids and phenols on dry soils and stone surfaces [*Baumgartner et al.*, 1992] and chemical scavenging ($NO_2 + NO_2^- \rightarrow O_3^- + NO$) in low pH, high SOM content soils [*van Cleemput & Baert*, 1976]. Recent work also suggests that some ammonia oxidizers are able consume NO_2 and produce NO and NO_2^- under both oxic and anoxic soil conditions [*Zart & Bock*, 1998, *Schmidt & Bock*, 1997]. Equally unclear are the effects of wet surface uptake, where aqueous phase chemistry has been reported to enhance O_3 deposition to foliage [*Fuentes et al.*, 1992].

The study of $NO–NO_2–O_3$ trace gas exchange over Amazonian landscapes, which have undergone extreme ecosystem modification, is fundamental to understanding how deforested environments affect regional trace gas budgets, and consequently global tropospheric chemistry. Further it improves our understanding of the soil microbiological ecology and thereby our understanding of the nitrogen cycle. In close association with NO_x the study of O_3 surface exchange has implications on regional climate and biology [*Fishman et al.*, 1979; *Ramanathan et al.*, 1987]. Elevated ambient concentrations are hazardous to biological life; contribute to the greenhouse effect and to the formation of photochemical smog.

As part of the LBA-EUSTACH project (*European Studies on Trace gases and Atmospheric Chemistry* within the *Large Scale Biosphere-Atmosphere Experiment in Amazonia*), results from measurements over a cattle pasture in Rondônia (cf. Section 1.2.1) are presented. Measurements were performed during both, the LBA-EUSTACH-1 and LBA-EUSTACH-2 campaigns [*Andreae et al.*, submitted, 2001], i.e. for two transition seasons during 1999 (30 April to 17 May, "wet–dry", and 24 September to 27 October, "dry–wet"). The objectives of this study were to (a) quantify the exchange of $NO–NO_2–O_3$ for an established cattle pasture for two distinct seasons, (b) propose possible reasons for the diminutive NO emission fluxes in contrast to an old growth primary forest for the same period, (c) examine and discuss the surface resistances and deposition fluxes of NO_2 and O_3 and their possible environmental controlling factors.

1.2 Experimental

The primary tool used for gas exchange measurements was a dynamic chamber system (applied during LBA–EUSTACH-2), which measured emission fluxes of NO and surface resistances for NO_2 and O_3 deposition directly (cf. Section 1.2.3). In order to determine ecosystem-representative NO_2 and O_3 deposition fluxes for both, the LBA–EUSTACH–1 and -2 periods, an inferential method (multi-resistance model) was applied to measured ambient NO_2 and O_3 concentrations using observed quantities of turbulent transport (cf. Section 1.2.4). In the case of O_3, the resulting fluxes could be compared to a limited data set of independent flux measurements by the aerodynamic gradient approach (cf. Section 1.2.5). Supplementary measurements included soil NO diffusivity and soil nutrient analysis (cf. Section 1.2.6).

1.2.1 Site description

Rondônia is situated on the fringe of the Amazon basin and comprises of seasonally dry tropical rainforest (*floresta ombrõfila aberta*) and various forms of degraded land (*floresta de transição*), cultivation (*plantação*) and pasture (*pastagem*). It is also situated along the "arc of deforestation" of Brazil, and is renown for its characteristic "fishbone" deforestation pattern and rapid land conversion rates [*Andreae et al.*, submitted, 2001]. Human settlement increased considerably after construction of the *Cuiabã-Porto Velho* highway (*BR 364*) in 1968, which cut through some of the more fertile parts of the weathered soils in this region [*Moran*, 1993]. Paving of this road was completed in 1984, which increased immigration and stimulated markets for agriculture and forest products [*Browder & Godfrey*, 1997]. With it came slash-and-burn agriculture, cropping and established cattle pasture and abandonment.

The measurement site was located on one of the camps on the commercial cattle ranch *Fazendha Nossa Senhora da Aparecida* (FNS) (Fig. 1.1), which lies between the unpaved roads *Linha* 12 and 16 off the paved *RO-470* at 10°45' 44" S, 62°21' 27" W and at a elevation of ca. 315 m. Soils at FNS are highly weathered, predominately sandy (> 75 %) red yellow podzols (*Podzõlico vermelho amarelo a moderado textura media* - Brasil or *Orthic acrisol* - FAO) [*Hodnett et al.*, 1996]. The nearest town is *Ouro Preto d'Oeste*, situated on the paved federal highway *BR364* between the towns *Jaru* and *Ji-Paranã* ca. 8 km NE from the site. A small charcoal kiln was in operation during the wet–dry season off the *BR 364* ca. 8 km from the site.

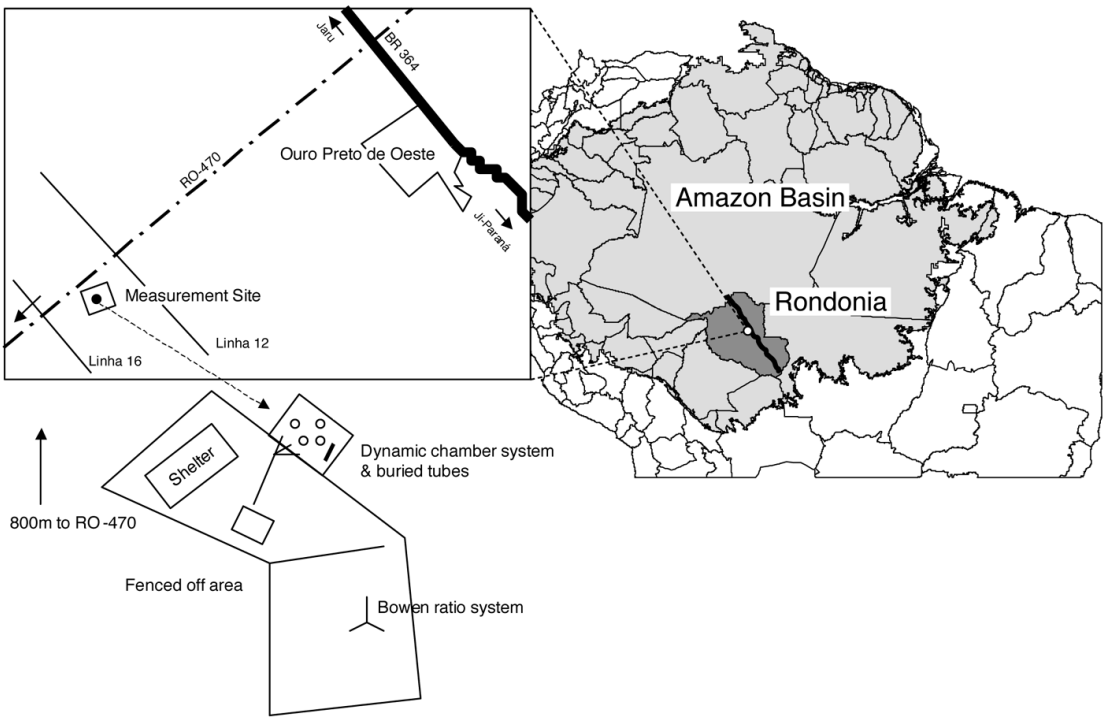

Figure 1.1. Location of the LBA-EUSTACH measurement site *Fazendha Nossa Senhora da Aparecida* (FNS) in Rondônia Brazil.

The land was first deforested in 1977 by the current owner and planted to rice (*Oriza sativa, Agulhinha / IAC (comum)*), beans (*Phaseolus vulgaris, Carioquinha, Rosinha, Tibagi*) and maize (*Zea mays, Asteca e Hibridos*). Fire was used as the primary deforestation tool and all burns typically took place between June and September. Combustion of slashed material was generally considered to be partial or poor. The first two seasons of cropping were the most lucrative with yields surpassing those of later years. Thereafter the land underwent a pattern of burn and *Brachiaria decumbens* pasture grass (*Australiano Braquiaria, Braquiaria Comum, Braquiaria de Alho, Capim*) for 12 seasons, after which a disk harrow (20 cm) was used in 1992 to liberate the old growth forest soil organic matter below the grass root zone. One season of beans was planted resulting in yields that equaled the first two seasons after deforestation. The camp was then burned for two seasons and planted to a predominantly homogenous sward of *Brachiaria brizantha* (A. Rich.) Stapf., (*Brachiarão, Brizantao, Brizantha, Braquiarao, Capim Braquiaria, Capim Marandu, Capim Ocinde*) and there after was never burned again. The camp has never been fertilized.

B. brizantha is a fire sensitive exotic perennial grass species with stout erect culms and broadly lanceolate leaf-blades, which can reach a height if left ungrazed of up to 120 cm. It produces poor seed and it propagates vegetatively. The sward at FNS had a leaf area index of 1.2 $m^2\ m^{-2}$ [*Kirkman G.A.*, unpublished data, 2000] during the "dry–wet" season and 2.1 $m^2\ m^{-2}$ during the "wet–dry" season [*Waterloo, M.J.*, personal communication, 2000]. Assuming a leaf nitrogen content of ca. 0.67 %, as found by *Davidson E.A.* [personal communication, 2000] at the *Fazenda Vitoria* in Parã, the total above ground nitrogen for FNS was estimated to 21 kg ha^{-1}.

During the measurement campaign the camp was stocked with a breeding herd of *Blanco* cattle (*Bos indicus* hybrid). The grass sward had a carrying capacity of ca. 2 animal units per hectare (1 A.U. = 450 kg). Soon after deforestation, and for a period after the plough event in 1992, the carrying capacity was in the order of 3–4 A.U. ha^{-1}. The 4 camps were typically rotated every 3 months, resulting in a camp utilization of 3–4 months per year dependent on sward conditions. Data from *Fazenda Vitoria* has shown that export of nitrogen as cattle harvesting is estimated at about 7 kg N $ha^{-1}\ yr^{-1}$ including returns from feces and urine (excluding NH_3 volatilization). At the time of measurement the camp was stocked with a breeding herd comprising cows and heifers with bull.

1.2.2 Trace gas monitoring

During LBA-EUSTACH-1 and -2 campaigns, concentrations of NO, NO_2, and O_3 were monitored at FNS. A glass tube (2 cm dia.) of a total length of 2.0 m, continuously purged by an auxiliary pump with a flow rate of 28 L min^{-1}, was used as sample intake system. The rain protected sampling head was mounted 3.5 m above ground on top of an instrument trailer. From a glass manifold mounted inside the trailer, sample air was fed through ¼" PTFE-tubing (2 m) to corresponding 47 mm PTFE-filters (0.5 μm) mounted on the sample intake ports of the NO/NO_X, and O_3 analyzers. Commercial gas-phase-chemiluminescence and spectrometric analyzers were used to measure NO-, NO_2-, and O_3-concentrations, respectively (Table A1, cf. Appendix A). NO and NO_2 calibrations were conducted with the use of a *Thermo Environmental Instruments Inc.*, *Model 146C Gas Phase Titration & Ozone Generator* instrument by mixing known concentrations of NO calibration gas with non-dried zero air from a *Thermo Environmental Instruments Inc.*, *Model 111 Zero Air Supply*. To this, a lesser amount of O_3 was added and the amount of NO_2 produced was then determined by the measured loss of NO. Subsequently O_3 was calibrated by assuming that the loss of NO was equivalent to the concentration of O_3 produced such that,

$$NO + O_3 \rightarrow NO_2 + O_2 \qquad (1.1)$$

The NO_x analyzer employed was equipped with a Molybdenum (*Mo*) NO_2 to NO converter, which is nonspecific for determination of NO_2 [*Winer et al.*, 1974]. The instrument also converts other reactive nitrogen compounds to NO, in particular, nitric acid (HNO_3), nitrous acid (HONO), the nitrate radical (NO_3), dinitrogen pentaoxide (N_2O_5), peroxyacetyl nitrate (PAN), and other organic nitrates. PAN is a thermally unstable compound at temperatures well below those found at FNS. HNO_3 is probably the most important of these interfering nitrogenous compounds at FNS. However, it is also known for its high affinity to the inner walls of intake systems, especially if these (a) consist of glass and/or stainless steel and (b) are covered with a molecular layer of water, which was certainly the case for the humid conditions at FNS. It is therefore assumed that HNO_3 (and also HNO_2, if present) was completely destroyed within the glass sample line (described above) and stainless steel fittings inside the instruments. Any interference from gaseous ammonia (NH_3) is most unlikely, since the *Mo*-converter was operated at 300 °C and any substantial conversion of NH_3 is usually not observed for temperatures below 400 °C. The other interfering nitrogenous compounds mentioned above are assumed to be negligible compared to NO_2.

1.2.3 Dynamic chamber system

During the LBA-EUSTACH-2 campaign, a second set of identical NO-, NO_X-, and O_3-analyzers (Table A1, cf. Appendix A) were applied to a dynamic chamber system. This system was similar to that described by *Gut et al.* [submitted 2001a, 2001b]. Weekly NO and NO_2 calibrations were conducted with the same gas-phase-titration/zero-air-supply system as described above.

Chamber measurements were used (a) to quantify surface emission fluxes of NO directly and (b) evaluate surface resistances for NO_2 and O_3 by relating chamber fluxes to chamber concentrations (cf. Section 1.2.4). The system comprised of three chambers placed over a previously grazed *B. brizantha* sward sealed to the surface with TEFLON® foil weighted by small sandbags (Fig. 1.2) such that no root destructive frames were necessary. Ambient air flow through the chambers was controlled by small air entry fans producing an average flow rate (Q) of ca. 28 L min^{-1} such that the average air residence time was ca. 25 s. Air inside the chamber was continuously mixed with an additional ventilator fan to prevent concentration gradients [*Meixner et al.*, 1997]. A fourth "blank" chamber, closed at the bottom, was employed for *in-situ* quantification of chemical reactions and chamber wall deposition effects (cf. below). A sample inlet for measurement of ambient NO^-, NO_2^-, and O_3^- concentrations was positioned close to the inlet of one of the chambers (10 cm above the soil surface). The chambers were constructed from polycarbonate, which is transparent to light of wavelengths above 420 nm, with a cross section area (A) of 0.066 m^2 and a height of 0.18 m

giving a total volume of 11.8 L. Solenoid valves controlled the flow of sample air (4 L min^{-1}) to the analyzers through blue colored PTFE tubing. All fittings in contact with the sample air were constructed of TEFLON®.

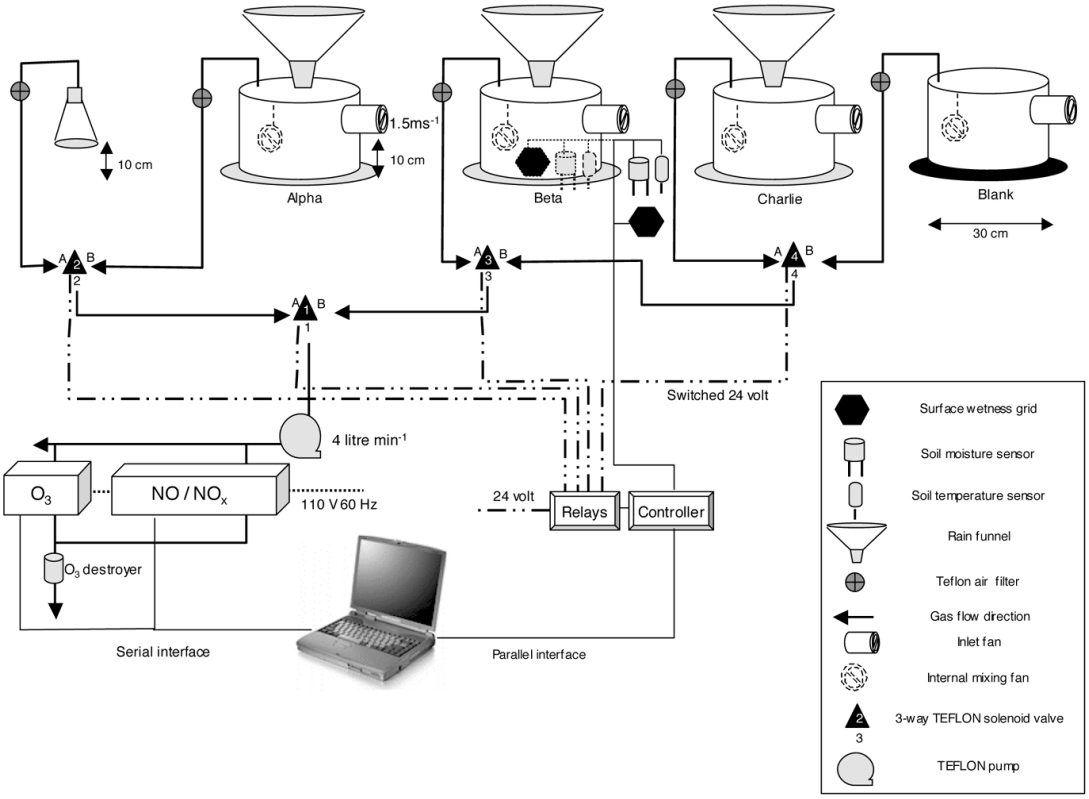

Figure 1.2 Dynamic chamber system.

The concentrations of all trace gas species *j* inside the chambers ($C(j)_{chamber}$) were measured sequentially for the three minutes interspersed by two minutes of ambient air ($C(j)_{ambient}$) measurements. Half a minute flush time was discarded prior to each measurement such that fluxes for each of the four chambers could be determined once every 24 minutes. Chamber fluxes ($F(j)_{chamber}$) of each trace gas *j* were determined by the mass balance,

$$F(j)_{chamber} = Q / A\ [C(j)_{chamber} - C(j)_{ambient}]\ (j = NO, NO_2, O_3) \quad (1.2)$$

which accounted for the individual losses to the chamber walls, and gains and losses due to NO-NO_2-O_3 reactions within the air sample while passing the

through the dynamic chamber. A complete and detailed description of the flux evaluation procedure is given in *Meixner et al.* [1997].

Uncertainty of the chamber flux measurements was determined by the sum of the errors due to non-stationarity (trend) in the ambient concentrations and instrument drift/noise such that,

$$\sigma(F(j)_{\text{chamber}}) = Q/A\,[(\sigma(C(j)_{\text{trend}})^2 + 2\,(\sigma(C(j)_{\text{instrument}})^2]^{1/2} \quad (1.3)$$

The trend related error $\sigma(C(j)_{\text{trend}})$ in the data was quantified as half the absolute difference between ambient concentrations $C(j)_{\text{ambient}}$ measured directly before and after the measurement of chamber air. It ranged between 0–0.13 ppb for NO, 0–0.25 ppb for NO_2 and 0–2.9 ppb for O_3. The standard deviation of all the zero air measurements, during calibration, was used for the determination of the instrument error $\sigma(C(j)_{\text{instrument}})$ (Table A1, cf. Appendix A).

Thereafter flux data whose total error exceeded their magnitude or whose trend error exceeded the instrument error were removed in accordance with,

$$(\sigma(F(j)_{\text{chamber}}) > |F(j)_{\text{chamber}}|)\ OR\ (\sigma(C(j)_{\text{trend}}) > \sigma(C(j)_{\text{instrument}}) \quad (1.4)$$

Due to power failures, instrument failure, and the above data rejection criteria dynamic chamber flux data were reduced to 9 % for NO, 32 % for NO_2 and 23 % for O_3 during LBA-EUSTACH-2.

Chamber flux measurements were also accompanied by measurements of soil temperature, soil moisture, and soil surface wetness inside and outside the chambers (Table A1, cf. Appendix A). Identical concurrent measurements were conducted at the EUSTACH forest site at *Reserva Biológica do Jaru*, (RBJ) 80 km NE of FNS [*Andreae et al.*, submitted, 2001; *Gut et al.*, submitted, 2001a, 2001b].

1.2.4 Inferential method

The emission flux of NO ($F(NO)_{\text{chamber}}$) as determined by the dynamic chamber system (above) is considered to be representative of the camp. This holds true as NO emission is predominantly controlled by soil nutrients, diffusivity, moisture and temperature [*Davidson et al.*, 2000; *Ludwig et al.*, 2001]. In contrast, dry deposition fluxes of NO_2 and O_3, depend on surface uptake characteristics, surface concentrations and turbulent transfer conditions close to the surface. The design of the chamber and particularly the rapid exchange (2.4 times min^{-1}) of the headspace air volume ensured that air temperature, relative humidity, and light intensity were close to ambient conditions [*Ludwig*, 1994; *Meixner et al.*, 1997]. However turbulent transfer conditions controlling the supply of trace gases to the

surface may differ from conditions outside the chamber. Therefore chamber NO_2 and O_3 fluxes were not representative for ambient field conditions. In order to account for this difference, an inferential method based on the ´big leaf multiple resistance approach´ [*Wesely & Hicks*, 1977, *Hicks et al.*, 1987] was applied. The dry deposition flux $F(j)$ of a non-reactive trace gas compound j, for which the surface represents a general sink at all ambient conditions, may be expressed as,

$$F(j) = C(j) / R_{tot}(j) \tag{1.5}$$

where $C(j)$ is the ambient mixing ratio of the trace gas compound j at the reference height and $R_{tot}(j)$ a gas transfer resistance in analogy to an electrical resistance according to Ohm's law. Correspondingly, $R_{tot}(j)$ is split into a series of partial resistances,

$$R_{tot}(j) = R_a + R_b + R_c(j) \tag{1.6}$$

such that R_a is the resistance against turbulent exchange in the air, R_b the molecular-turbulent boundary layer resistance close to the surface elements, and $R_c(j)$ the canopy resistance of the trace gas compound j comprising stomata, cuticle, soil, water and other surface related resistances. The general idea of this resistance concept in the context of chamber measurements is, that due to the artificial ventilation of the chamber the transport related resistances (aerodynamic) R_a and R_b differ from natural (outside) conditions, whereas the surface related resistance $R_c(j)$ is the same inside and outside the chamber. Thus for a transfer of chamber deposition measurements to representative natural conditions, R_a and R_b inside and outside the chamber must be quantified.

The aerodynamic resistance inside the chamber ($R_{aero,chamber}$), which is the sum of the turbulent resistance and molecular-turbulent boundary layer resistance inside the well-mixed chamber,

$$R_{aero,chamber} = R_{a,chamber} + R_{b,chamber} \tag{1.7}$$

was determined experimentally. The soil surface enclosed by a dynamic chamber was replaced by a saturated potassium-iodide (KI) solution, which represents a virtually ideal sink for ozone, i.e. its surface resistance to O_3 uptake is virtually zero [*Ludwig,* 1994]. Dividing the chamber O_3 concentration by the flux (given by the flow rate through the chamber, the surface area of the KI-solution, and the difference between ambient and chamber O_3 concentrations according to eq. (1.2) yielded a $R_{aero,chamber}$ of 60 s m^{-1}. Consequently the surface resistance for NO_2 and O_3 deposition in the chamber ($R_c(NO_2)$ and $R_c(O_3)$) was derived from

concentrations $C(NO_2)_{chamber}$ and $C(O_3)_{chamber}$, the chamber fluxes $F(NO_2)_{chamber}$ and $F(O_3)_{chamber}$ such that,

$$R_c(NO_2) = C(NO_2)_{chamber} / F(NO_2)_{chamber} - R_{aero,chamber} \quad (1.8a)$$

$$R_c(O_3) = C(O_3)_{chamber} / F(O_3)_{chamber} - R_{aero,chamber} \quad (1.8b)$$

According to eq. (1.6), the R_c have to be added to R_a and R_b, determined for ambient conditions outside the chamber, to yield representative values for $R_{tot}(NO_2)$ and $R_{tot}(O_3)$. From FNS wind speed and air temperature profile data (cf. Section 1.2.5), representative turbulent resistances (R_a) and molecular-turbulent boundary layer resistances (R_b) were estimated according to *Hicks et al.* [1987]. R_a was determined using friction velocities (u_*) and Monin-Obukhov lengths (L) calculated using a generalized algorithm [*Ammann*, 1999] from wind speed and air temperature profiles such that,

$$R_a = (k\, u_*)^{-1} [\ln (z_{ref} / z_{(0)}) - \Psi_c (z_{ref} / L)] \quad (1.9)$$

where the *von Karmán* constant (k) was 0.4, $z_{(0)}$ was the roughness length (LBA-EUSTACH-1: 0.15 m; LBA-EUSTACH-2: 0.11 m), z_{ref} was the reference height of 3.5 m, and $\Psi_c(z_{ref} / L)$ is a function, which corrects for atmospheric non-neutral stability conditions [*Ammann*, 1999].

The molecular-turbulent boundary layer resistance (R_b) is described by

$$R_b = (2 / k\, u^*) (Sc / Pr)^p \quad (1.10)$$

where the *Schmidt* number (Sc) was 1.07 for the trace gases of interest, the *Prandtl* number (Pr) was 0.72 and p was 2/3.

Substitution of eqs. (1.8 to 1.10) into eq. (1.6) delivers $R_{tot}(NO_2)$ and $R_{tot}(O_3)$. According to eq. (1.5), ecosystem-wide dry deposition fluxes of $F(NO_2)$ and $F(O_3)$ were then calculated using the NO_2 and O_3 concentrations, which were measured at a reference height of 3.5 m above the surface of FNS. (cf. Section 1.2.2).

As previously mentioned, the application of the inferential method is strictly valid for non-reactive trace gases only. An inferential method for reactive trace gases has to consider chemical reactions/transformations of these trace gases during the turbulent transport between the reference height and the surface [*Kramm et al.*, 1996]. However, the "non-reactive" flux-resistance relationship expressed by eq. (1.5) can also be applied, as a sufficient proxy, in the case of reactive trace gases, if "slow chemistry" is prevalent [*Villá-Guerrau de Arellano & Duynkerke,*

1992], i.e. if characteristic chemical reactions times are much larger than corresponding turbulent transport times. Following *Villá-Guerrau de Arellano & Duynkerke* [1992], the characteristic time of turbulent transport (τ_{turb}) was calculated by

$$\tau_{turb} = k\,(z_{ref} + z_0)\,(\sigma_w^2 / u^*)^{-1} \tag{1.11}$$

approximating σ_w/u^* by $1.25\,(1-3\,z_{ref}/L)^{1/3}$ and $1.25\,(1+0.2\,z_{ref}/L)$ for unstable and stable atmospheric conditions, respectively [*Ammann*, 1999]. The overall characteristic time scales for the NO-NO_2-O_3 triad (τ_{chem}) are given by the combination of $\tau_{NO} = (k_{13}\,[O_3])^{-1}$, $\tau_{NO2} = k_{12}^{-1} = j(NO_2)^{-1}$, and $\tau_{O3} = (k_{13}\,[NO])^{-1}$, with the reaction constants $k_{12} = j(NO_2)$ [s^{-1}] and $k_{13} = 2 \times 10^{-12} \exp(-1400 / T)$ [cm^3 $molecules^{-1}$ s^{-1}] for the reactions,

$$NO_2 + h\nu \rightarrow NO + O_3 \tag{1.12}$$

$$NO + O_3 \rightarrow NO_2 + O_2 \tag{1.13}$$

NO_2 photolysis rate $j(NO_2)$ was calculated from global radiation data (Table. A1, cf. Appendix A) using a relationship derived from simultaneous measurements of global radiation and NO_2 photolysis rate at RBJ during LBA-EUSTACH-1 and -2 [*Ammann et al.*, submitted, 2001]. Monitored NO, NO_2, and O_3-concentrations and micrometeorological data (cf. Sections 1.2.2 & 1.2.5) were used to calculate mean diel variations of τ_{turb} and τ_{chem} for the LBA-EUSTACH-1 and -2 periods. Results are shown in figure 1.3. Turbulent transport times were generally found to be at least one order of magnitude faster than chemical reaction times. "Slow chemistry" between $z_{ref} = 3.5$ m and the surface could therefore be assumed, justifying the application of eq. (1.5) to infer NO_2 and O_3 dry deposition fluxes for conditions at FNS during LBA-EUSTACH-1 and -2.

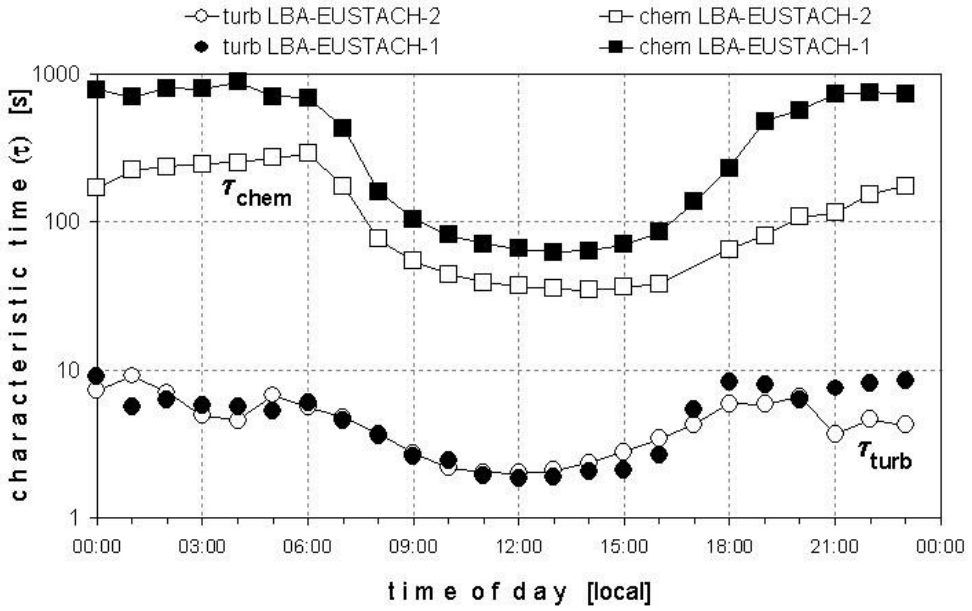

Figure 1.3 Chemical and turbulent characteristic times scales

1.2.5 Micrometeorological gradient system

Profiles of wind speed and air temperature were obtained from corresponding continuous measurements at four levels on a 5 m tall tripod-mast, which was set up 15 m south of the dynamic chamber system and 25 m south-east of the NO, NO_2, and O_3-monitoring intake system (Fig 1.1). Wind direction was measured at 4.5 m and global radiation at 2.02 m above ground. Data acquisition and averaging (30 min) was performed by a micrologger (*21X, Campell Sci. Ltd, U.K.*). Micrometeorological sensors and their precision are listed in table A1. Profile data have been rejected for wind sectors 217°—265 and 301°—322, for which substantial flow distortions for the profile measurements were observed due to instrument shelters and other nearby structures. A generalized algorithm by *Ammann* [1999] was used to infer surface roughness (z_0), friction velocities (u^*), Monin-Obukhov lengths (L), and stability correction functions $\Psi_c(z / L)$ necessary for the calculation of the resistances R_a and R_b (eqs. 1.9 and 1.10, cf. Section 1.2.4). To account for conditions of very low wind speeds and/or high thermal stability (where atmospheric turbulence seldom exists and micrometeorological techniques fail), data were rejected where $u^* < 0.025$ m s^{-1} and $z_{ref} / L > 10$. Stringent application of data rejection criteria reduced daytime

(nighttime) data availability to 76 % (17 %) and 74 % (21 %) during the LBA-EUSTACH-1 and LBA-EUSTACH -2 periods, respectively.

To determine the dry deposition O_3 flux from its vertical gradient, another O_3-analyzer (Table A1, cf. Appendix A) was used for the gradient system during LBA-EUSTACH-1 and -2 campaigns. This O_3-analyzer was cross-compared with the "monitoring" O_3-analyzer (cf. Section 1.2.2) for a total of 96 hours on four different occasions and showed good agreement (within $\pm$ 1 ppb). For the determination of the vertical O_3 gradient, two ¼" PTFE tubes of identical length (6.25m) were installed with inlets at z_4 = 4.5 m and z_1 = 0.52 m above ground. The two intake lines were switched, alternating every 3 minutes, by a stainless steel 3-way valve, which fed into the sample port of the analyzer equipped with a 47 mm PTFE filter (> 2 µm). One minute flush time was discarded prior to each measurement. Every 30 minutes, means and standard deviations of O_3 concentrations from both levels were calculated by the micrologger routine. Thereafter cases with the observed standard deviation of the O_3 concentrations exceeding the magnitude of the gradient were removed. This procedure reduced daytime (nighttime) vertical O_3 gradient data to 38 % (35 %) and 41 % (38 %) during LBA-EUSTACH-1 and LBA-EUSTACH -2 respectively. The O_3 dry deposition flux was calculated by the aerodynamic flux-gradient relationship given by [*Müller et al.*, 1993; *Meixner*, 1994b]. Subsequently the total dry deposition resistance $R_{tot}(O_3)$ was calculated according to eq. (1.5) and the canopy resistance ($R_c(O_3)$) was finally obtained (according to eq. 1.6) by subtracting R_a and R_b. The later were quantified by eqs. (1.9 and 1.10).

Due to the data rejection procedures on both, micrometeorological and O_3 gradient data, daytime (nighttime) availability for $R_{tot}(O_3)$ was reduced to 27 % (8 %) and 28 % (9 %) during LBA-EUSTACH-1 and LBA-EUSTACH -2 respectively. Therefore, nighttime $R_{tot}(O_3)$ data obtained by the micrometeorological technique were not considered for this study.

1.2.6 Determination of soil properties

For the interpretation of the gas-exchange measurements, all important physical and chemical soil properties were determined for the measurement site. Soil diffusivity was determined by measurement of the naturally occurring transport tracer ^{222}Rn with a system identical that used at RBJ [*Gut et al.*, submitted, 2001a, *Gut et al.*, 1999]. It comprised of a closed system of two 1 m gas permeable membrane tubes (Acurrel®) buried at 3 cm, a ^{222}Rn gas detector (Table A1, cf. Appendix A) and a ventilated soil chamber. Determination of the soil bulk diffusion coefficient was estimated according to Fick´s first law using measurements of ^{222}Rn soil-atmosphere gradient and the ^{222}Rn surface flux [*Gut, et al.*, 1998] at 10-minute intervals for 3 days. The top 5 cm of soil from the

chamber measurement site at FNS underwent physical and chemical characterization for organic carbon, total phosphorous, total nitrogen, total sulfur, plant available phosphorous, -potassium, pH ($CaCl_2$), bulk density, texture and cation exchange capacity in accordance with methods described in *Emde & Szöcs* [2000]. Determination of ammonium, nitrate, net mineralization, net nitrification and potential nitrification rates were performed in accordance with methods described in *Hart et al.* [1994].

1.3 Results and Discussion

In the following results section time series data are presented as mean diel courses for reasons of compactness and simplicity. Furthermore data were grouped into one-hour intervals centered at the local time hour. Medians together with first and third quartiles were used to graphically present results for both measurements campaigns LBA-EUSTACH-1 (18 days) and LBA-EUSTACH-2 (34 days). For all trace gas fluxes the micrometeorological convention of negative for downward fluxes and positive for the upward direction have been adopted.

1.3.1 Soil emission of NO and its relation to soil properties

NO emission fluxes. As mentioned previously, NO soil fluxes were determined directly from dynamic chamber measurements during the LBA-EUSTACH-2 campaign (September–October 1999). A statistical summary of the observed results is given in table A5 (b) and average diel cycles are displayed in figure 1.4. The minimum detectable NO emission flux was 0.28 ng N m^{-2} s^{-1}. Soil moisture ranged from 19.5—70.7 % WFPS with a mean of 35.7 % WFPS. Soil temperature averaged 25.5 °C and ranged between 19 °C and 38 °C (Fig. 1.4). The observed NO soil emissions were of the lowest fluxes measured on an established pasture in the Amazon basin [*Garcia-Montiel et al.*, 1999] with a mean of 0.65 ng N m^{-2} s^{-1} ($\pm$ 0.37 ng N m^{-2} s^{-1}). NO emission fluxes also showed no diel dependence on soil temperature and/or soil moisture WFPS ($r^2 = 0.03$, $\alpha = 0.05$; cf. Fig. 1.4(c)). The pronounced early morning peak in ambient NO concentration measured at 10 cm above ground (Fig. 1.4(a)) was most likely due to photolysis of accumulated nighttime NO_2 shortly after sunrise and is not a microbial response to e.g. increased surface wetness.

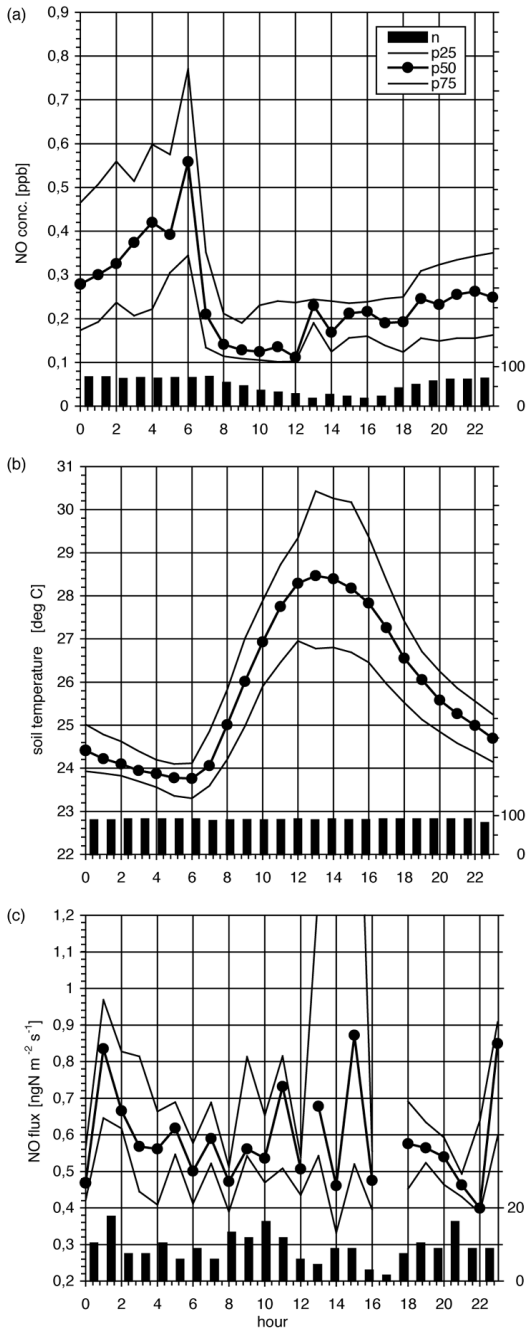

Figure 1.4 Mean diel variation of (a) NO concentration (ppb), (b) soil temperature (ºC), (c) and soil NO emission flux (ng N m^{-2} s^{-1}) at FNS for the "dry–wet" transition season during LBA-EUSTACH-2 (24 September to 27 October 1999).

Median NO emission fluxes at FNS were nine times lower than at the RBJ primary rainforest site under similar soil moisture and temperature conditions [*Gut et al.*, submitted, 2001a; *van Dijk et al.*, submitted, 2001]. To explain this difference, possible influencing factors, namely physical and chemical soil properties (soil gas diffusion and nitrogen-status), are discussed in the following.

Soil diffusivity. Bulk density tends to increase with pasture age [*Feigl et al.*, 1995], which directly affects soil gas diffusion. Compaction through mechanized forest clearing, ploughing, seed drilling and cattle hoof action result in an increase soil bulk density, increasing soil turtousity and thereby the length of time a NO gas molecule takes to diffuse through the soil profile and thus is exposed to consumption by denitrifiers [*Gödde & Conrad*, 2000]. Flux measurements and vertical profiles in soils have shown the half-life of NO to be in the order of minutes [*Rudolph & Conrad*, 1996]. The resultant emission flux is therefore a combination of NO production and consumption in the soil, which is largely soil diffusion dependant [*Remde et al.*, 1993]. Bulk density, for the top 5 cm of soil at FNS was 1.56 Mg m^{-3}, which was considerably higher (41 %) than for the RBJ soil [*Gut et al*, submitted, 2001a] and somewhat higher (16 %) than for pasture soils older than 20 years in Rondônia [*Neill et al.*, 1995, 1996, 1997, 1999; *Feigl et al.*, 1995; *Kirkman G.A.*, unpublished data, 2000]. This is similarly reflected in the NO effective diffusion coefficients measured at FNS, ($6.4 \pm 3.0 \times 10^{-7}$ m^2 s^{-1}), and RBJ, ($7.9 \pm 4.0 \times 10^{-7}$ m^2 s^{-1}), for a range of soil water conditions where maximum NO production is expected (10–20 % WFPS) [*van Dijk & Meixner*, submitted, 2000b]. This represents a 23 % difference in soil diffusion between the two sites and can be attributed to the higher bulk density and the relative absence of soil macro-pores and soil fauna (termite and earthworm passages) at FNS. However this difference is too small to explain the observed difference in the NO emission flux between pasture and forest.

Soil nitrogen status. The repeated effects of slash-and-burn agriculture on tropical ecosystems are postulated to result in reduced overall soil nitrogen cycling and have been shown to result in lower productivity with time [*Palm et al.*, 1996]. Reduced bulk litter inputs result in poor nitrogen availability and a suppression of nitrification and mineralization [*Piccolo et al.*, 1994, 1996; *Neil et al.*, 1999]. This is partly manifested in the high soil C:N ratios (21:1) that were found at FNS.

Inorganic ammonium pools (16.2 μg NH_4^+ g^{-1} soil or 12.6 μg N-NH_4^+ g^{-1} soil) were a factor 10 larger than the inorganic nitrate pools (5.3 μg NO_3^- g^{-1} soil or 1.2 μgN-NO_3^- g^{-1} soil). N-pool sizes are considered to be reasonable indicators of soil nitrogen cycle dynamics, which suggests that FNS had a conservative rather than fast nitrogen soil turnover rate [*Davidson et al.*, 2000]. Nitrogen cycling of the soils at FNS showed similar characteristics to older pastures in Rondônia

(Table A2 and A3, cf. Appendix A). Negative net mineralization (–0.89 μg $NH4^+$ g^{-1} soil d^{-1}) and the weak positive net nitrification rates (0.40 μg NO_3^- g^{-1} soil d^{-1}) suggest a large portion of the nitrogen turnover was immobilized by microbes [*Hart et al.*, 1994]. Potential nitrification rates indicate the maximum rate of NH_4^+ oxidation by ammonium oxidizers [*Besler*, 1979] (Table A3, cf. Appendix A) and rates at FNS (1.69 μg NO_3^- g^{-1} d^{-1}) were found to be within the upper ranges measured by *Verchot, et al.* [1999] in Parã (0.18—1.70 μg NO_3^- g^{-1} d^{-1}) for active and degraded old pastures. They are however a factor three lower than those for forest and secondary forest soils [*Kirkman G.A.*, unpublished data, 2000], indicating that ammonia oxidizers are possibly restrained by conversion from forest to pasture [*Verchot et al.*, 1999]. The low NO emissions measured at FNS during September-October 1999 at FNS are assumed to be a combination of lower NO effective soil diffusion and a conservative N-cycle. This is supported by field measurements of diffusion, a dominant inorganic ammonium nitrogen pool, and lower potential nitrification rates, corroborated by a site history of declining agricultural productivity.

1.3.2 Surface resistances of NO_2 and O_3

The measurement of daytime and nocturnal resistances has important implications for multi-resistance modeling. Results presented here are of the first observations from a soil and grassland (*B. brizantha*) environment in the tropics were uptake resistances were measured on a 24-hour basis. Studies of NO_2 and O_3 uptake resistances over temperate grasslands are often limited to measurements during the day e.g. for lawn 333–769 s m^{-1} [*Delany & Davies*, 1983] and pasture 38–67 s m^{-1} [*Duyzer et al.*, 1983]. Rates of removal of O_3 by grasslands have been reported by *Pio et al.* [2000] at 500 s m^{-1} at night to 200 s m^{-1} during the day and *Massman* [1993] at 100 s m^{-1} over a semi-arid grassland.

Canopy resistance values of ($R_c(NO_2)$ and $R_c(O_3)$) were measured by the dynamic chamber system during the LBA-EUSTACH-2 ("dry–wet") campaign as described in section 1.2.3. In addition, R_a and R_b and a limited (daytime) dataset of R_c values for O_3 were determined from the aerodynamic gradient measurement system during both campaigns (cf. Section 1.2.5). The corresponding median and IQR (inter-quartile range) for daytime and nighttime R_a, R_b, R_c, and v_d (deposition velocities in mm s^{-1}) for NO_2 and O_3 are listed in table A4. Diel resistance courses are presented together with global radiation and relative humidity for the "dry–wet" period in figure 1.5.

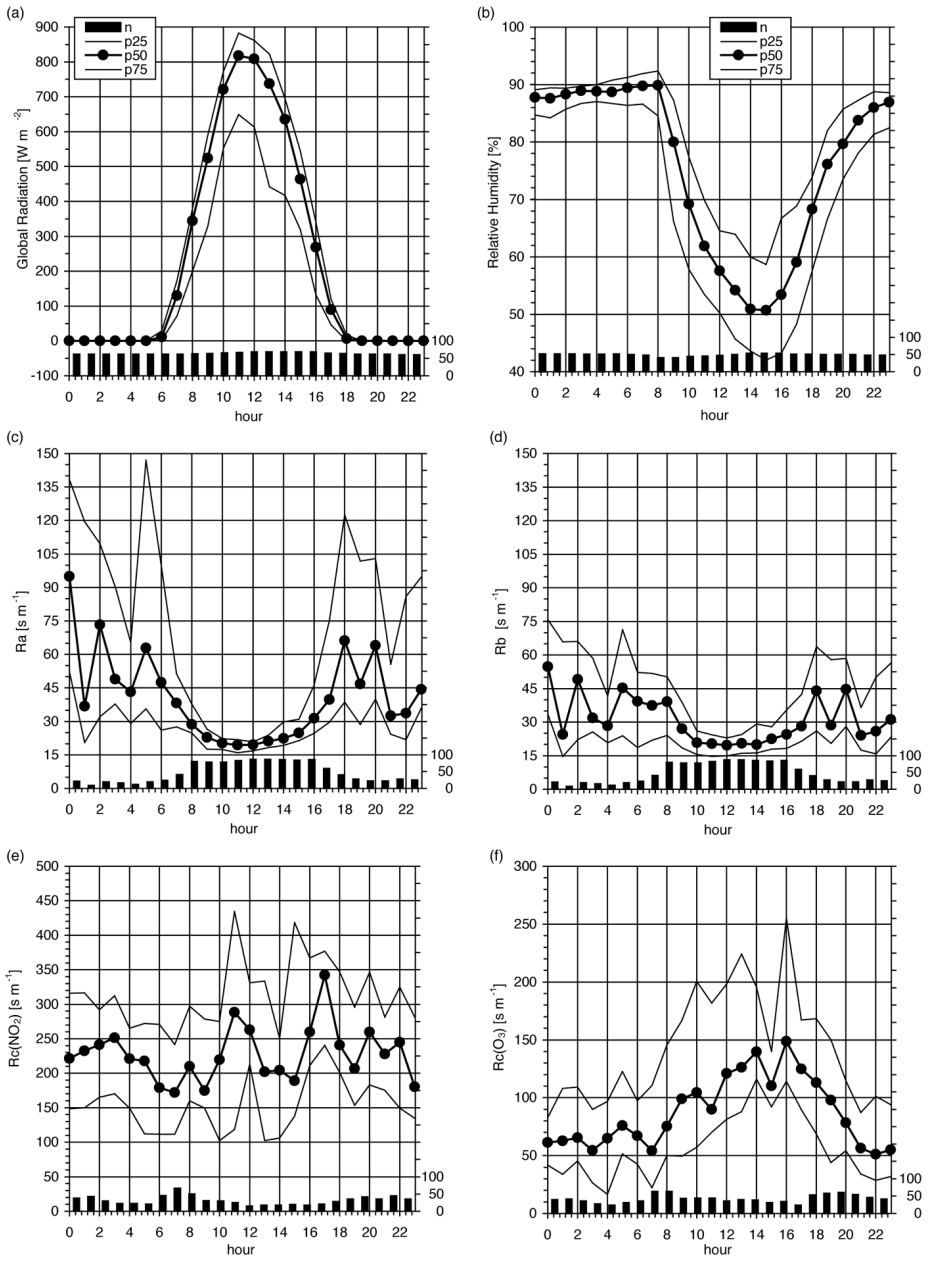

Figure 1.5 Diel (a) global radiation (W m^{-2}), (b) relative humidity (%), (c) R_a, (s m^{-1}) (d) R_b (s m^{-1}), (e) $R_c(NO_2)$ (s m^{-1}), (f) and $R_c(O_3)$ (s m^{-1}) first second and third quartiles for the "dry–wet" transition season during LBA-EUSTACH-2 (24 September to 27 October 1999).

During LBA-EUSTACH-2 ("dry–wet") median turbulent resistances (R_a) were 23 s m^{-1} during the day (06H00–18H00) and 51 s m^{-1} at night, whereas the day and night molecular-turbulent boundary layer resistances (R_b) were 23s m^{-1} and 33 s m^{-1} respectively (Table A4 (b), cf. Appendix A). These near surface boundary layer resistance components (R_a & R_b) followed a typical diel trend in accordance with increased turbulent mixing during daytime due to higher wind speeds and thermal convection (Table A4 (b), cf. Appendix A). However these data only reflect the nights with relatively high wind speeds that passed the rejection criteria described in section 1.2.5. For the major part of the nighttime cases, which did not pass the rejection procedure, much higher resistances have to be assumed indicating a very weak or intermittent turbulence. Canopy resistances of both gases controlled the deposition processes during the day for both measurement periods. Contributing more than 65 % to the total resistance ($R_a + R_b + R_c$). Day and night NO_2 canopy resistance means, during LBA-EUSTACH-2, were significantly similar ($\alpha = 0.05$) at 235 s m^{-1} and 238 s m^{-1} for day and night respectively. Medians were 209 s m^{-1} and 229 s m^{-1} (Table A4 (b), cf. Appendix A). Ozone canopy resistances revealed significantly higher daytime resistances (106 s m^{-1}) versus 65 s m^{-1} at night (Table A4 (a), cf. Appendix A). The highest O_3 resistances (145 s m^{-1}) were observed at 16H00 and at 17H00 for NO_2 (343 s m^{-1}) each day, which coincided with low relative humidity (Fig. 1.5(b)), suggesting stomatal closure due to high water vapor pressure deficit. The gradient and dynamic chamber derived $R_c(O_3)$ values during the "dry–wet" period showed reasonable agreement, with day time medians of 141 s m^{-1} and 106 s m^{-1} (Table A4 (a), cf. Appendix A). During LBA-EUSTACH-1 ("wet–dry") nighttime conditions were even more stable and/or less turbulent resulting in four times larger R_a and two times larger R_b nighttime values. Slightly lower R_a and R_b during the day were observed (Table A4 (a), cf. Appendix A), resulting from higher wind speeds [*Andreae et al.*, submitted, 2001]. Daytime total resistances, determined by the gradient method, ($R_a + R_b + R_c(O_3)$) for both the "wet–dry" and "dry–wet" periods also showed little seasonal difference such that corresponding O_3 deposition velocities ($v_d(O_3) = R_{tot}(O_3)^{-1} = [R_a + R_b + R_c(O_3)]^{-1}$) were within 10 % of each other during 1999 (Table A4 (a), (b), cf. Appendix A).

The diel patterns in NO_2 an O_3 resistances observed at FNS are considered to be the result of a combination of three processes: (a) stomatal, cuticular and mesophylic uptake, (b) soil uptake and (c) uptake into solution of wet surfaces. The daytime comparable $R_c(NO_2)$ and lower nighttime $R_c(O_3)$, when plant stomata are expected to be closed, is possibly due to nighttime uptake of NO_2 and O_3 via stomata and/or foliar cuticle [*Kisser et al.*, 1990] by the *B. brizantha* grass species. Whereas, during the day this stomatal activity gradually decreases as declining leaf water potential would dictate. At around 16H00 when relative humidity was lowest, vapor pressure deficits were highest causing partial stomatal closure and

hence larger resistances. [*Pathre et al.*, 1998]. This would, however, bring into conflict previous understanding that stomatal activity is typically higher during the day for C4 plants. However, a closer look at the dry and transition season (August-September 1992, June 1993) data of *McWilliam et al.* [1996] suggests not much difference between the early and late part of the day. Unfortunately night values were intentionally not measured [*Roberts, J.M.*, personal communication, 2000]. In addition *Jacob & Wofsy* [1990] had to introduce an efficient nighttime mechanism for NO_2 plant uptake in order to balance their NO_y forest budget during ABLE-2B [*Lerdau et al.*, 2000]. A similar mechanism could be assumed for FNS. Soil uptake, on the other hand, is presumed to be diel invariant and a significant contributor to NO_2 and O_3 uptake at FNS. Soil has been shown to contribute as much as 75 % to the total O_3 depositional flux on Colorado semi-arid grasslands [*Massman*, 1993], and ammonia oxidizers are thought to be significant consumers of NO_2 [*Zart & Bock*, 1998, *Schmidt & Bock*, 1997].

Surface wetness might also significantly alter the surface resistances of less soluble trace gases like NO_2 and O_3 [*Baldocchi,* 1993; *Chameides,* 1987; *Fuentes et al.*, 1992; *Schwartz*, 1992; *Wesely*, 1989]. Surface moisture or condensation on soil and grass elements occurred mostly at night (> 70 % of all measurements of surface wetness) and was detectable by the wetness grids during 45 % of all nights during LBA-EUSTACH-2 at FNS. NO_2 and O_3 resistances were 60 and 72 % higher respectively, during these wet nights as opposed to nights where no condensation occurred. Reports of enhanced O_3 deposition due to surface wetness have been noted above deciduous forests by *Fuentes et al.* [1992]. Their observations indicated that mechanisms, other than stomatal uptake contributed to the O_3 deposition when the foliage was wet. Recent chemical models now make a distinction between foliage wetness caused by rain and dew to account for their different aqueous-phase chemical compositions [*Wesely*, 1989]. Therefore nighttime $R_c(NO_2)$ and $R_c(O_3)$ values measured at FNS during the "dry–wet" period could be the competing result of plant, soil and wet skin uptake processes, accentuated by possible stomatal activity at night and aqueous phase chemistry on vegetative and soil surfaces.

Moreover, the canopy resistances for the pasture, which comprised grass vegetation and soil, were compared to surface resistances of the forest floor at RBJ, which comprised of soil, root-mat, and dead plant material. FNS showed 70 % lower $R_c(NO_2)$ and 40 % lower $R_c(O_3)$ 24-hr averages than RBJ for the dry wet season [*Gut et al.*, submitted, 2001b].

1.3.3 NO_2 and O_3 deposition fluxes and the NOx budget at FNS

In order to make a seasonal comparison of NO_2 and O_3 dry deposition fluxes at FNS, fluxes were calculated for both periods by the inferential method described

in section 1.2.4. Essentially for LBA-EUSTACH-2, all NO_2, O_3 day and night R_c from the dynamic chambers were used, while for LBA-EUSTACH-1 only the daytime $R_c(O_3)$ from the aerodynamic method were available directly. Unfortunately number counts rendered nighttime $R_c(O_3)$ calculated with the aerodynamic method non-significant (cf. Section 1.2.5) and these data were substituted with $R_c(O_3)$ measured by the dynamic chamber system during the "dry–wet" period. Correspondingly $R_c(NO_2)$ were estimated by,

$$R_c(NO_2)_{\text{wet–dry}} = R_c(O_3)_{\text{wet–dry}} \left[R_c(NO_2)_{\text{dry–wet}} / R_c(O_3)_{\text{dry–wet}} \right] \quad (1.14)$$

as an empirically adjusted first order estimate of dry deposition flux for the "wet–dry" transition period. Diel NO_2 and O_3 concentrations and inferred diel NO_2 and O_3 dry deposition fluxes for both periods are presented in figure 1.6 and 1.7. In addition mean, standard deviation, count and quartile statistics of NO_2 and O_3 dry deposition fluxes are given in table A5.

During LBA-EUSTACH-2 NO_2 and O_3 concentrations were considerably elevated above those measured during LBA-EUSTACH-1 at FNS. This can be attributed to biomass burning from forest clearing activities, which typically occur in the later part of the dry season [*Andreae et al.*, submitted, 2001]. Nitrogen dioxide concentrations were a factor three higher during "dry–wet" transition season (Fig 1.6) resulting in deposition fluxes six times larger than those of the "wet–dry" period (−3.93 vs. −0.7 ng N m^{-2} s^{-1}) (Table A5, cf. Appendix A). An early evening peak in the NO_2 concentration (more pronounced during the "wet–dry" period) was observed at ca. 19H00 during both measurement periods, which was due to local advection of moderately aged pollution plumes (from nearby vehicular traffic along the RO-47) dispersing in a very shallow, stable, and young nocturnal boundary layer [*Meixner et al.*, 2000]. Ozone concentrations were equally elevated during the "dry–wet" period with deposition $F(O_3)$ fluxes twice as large (−6.11 nmol m^{-2} s^{-1} or 0.13 μg m^{-2} s^{-1}) during the "dry–wet" in contrast to the "wet–dry" (−2.75 nmol m^{-2} s^{-1} or 0.29 μg m^{-2} s^{-1}) season. Since resistance conditions are significantly similar through the year (cf. Section 1.3.2), consideration of seasonal ambient O_3 trace gas conditions is vital for quantifying the deposition of O_3 at expanded spatial and temporal scales in Amazonia. Assuming measurements during LBA-EUSTACH-1 and -2 were representative for both wet and dry seasons and these seasons were equal in length, the mean O_3 dry deposition was 0.24 ± 0.013 s.e. μg m^{-2} s^{-1}, which is higher than 0.19 μg m^{-2} s^{-1} first suggested as a mean for Amazonian pastures by *Sigler et al.* [submitted, 2000] based on measurements for the 1999 "wet" season (January and February 1999 only), at FNS.

NO soil emission fluxes have been shown above (cf. Section 1.3.1, Table A4) to be extremely low during the "dry–wet" period (0.65 ng N m^{-2} s^{-1}). Due to higher soil moisture in the wet season, which limits NO production and inhibits soil diffusion [*van Dijk et al.*, submitted, 2001], it is reasonable to assume that NO fluxes were relatively similar or perhaps slightly lower during the "dry–wet" period. In this case emission of NO and dry deposition of NO_2 would be approximately equal during the "wet–dry" season (Table A5, cf. Appendix A). However, during the "dry–wet" season the surface of FNS removed up to seven times more NO_2 from the atmosphere as was emitted as NO. Assuming that measurements during LBA-EUSTACH-1 and -2 were representative for the wet and dry seasons and these seasons are about equal in length, on a annual basis this constitutes a net NO_2 sink of 0.73 kg N ha^{-1} yr^{-1}, which is a factor four larger than that emitted from the soil as NO (0.17 kg N ha^{-1} yr^{-1}) at FNS. Therefore FNS could be considered as a net NO_x (NO_x = NO + NO_2) sink during 1999.

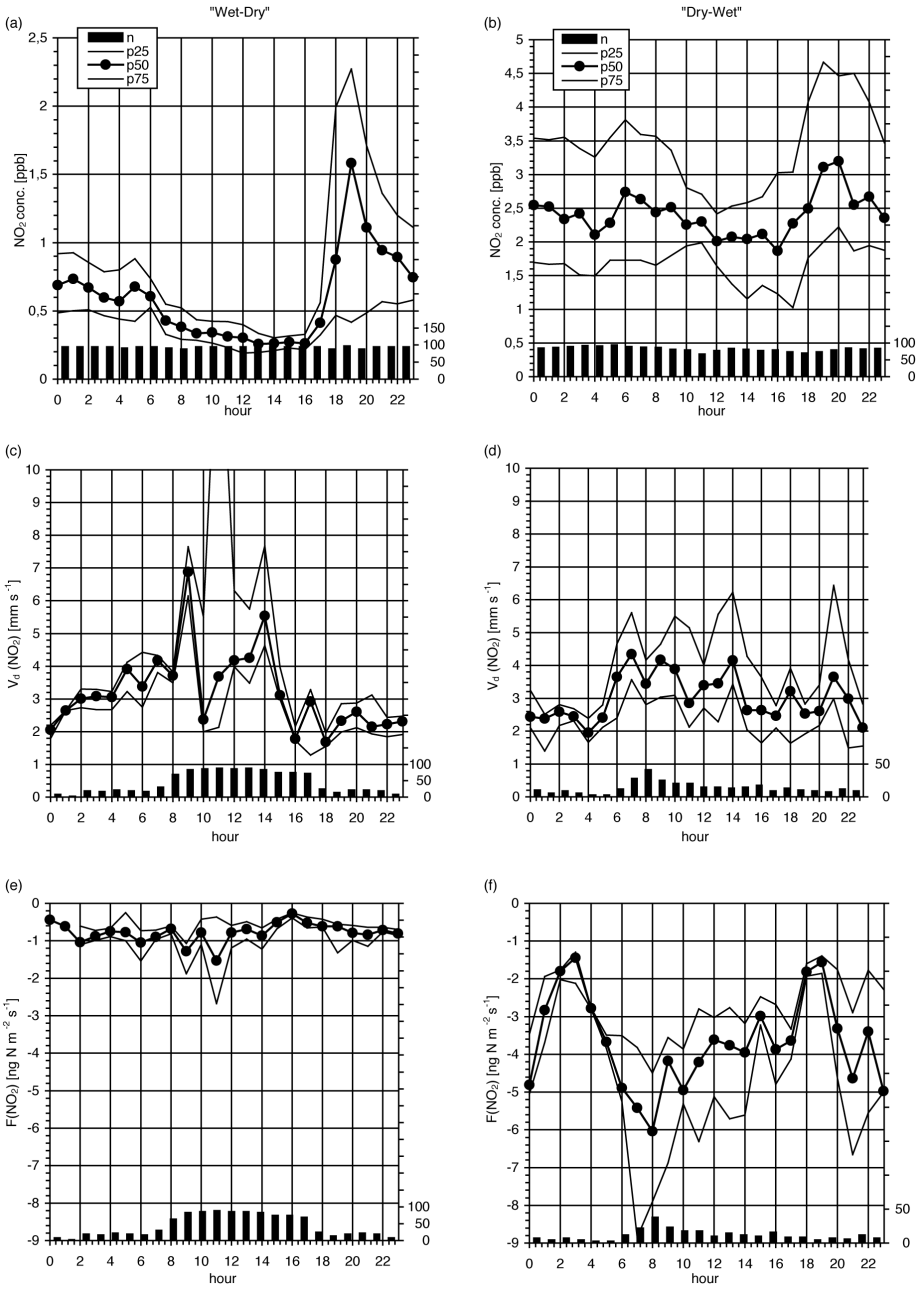

Figure 1.6 Diel (a) (b) NO_2 concentrations (ppb), (c) (d) deposition velocities (mm s^{-1}), and (e) (f) NO2 fluxes (ng N m^{-2} s^{-1}) first, second and third quartiles for LBA-EUSTACH-1 and LBA-EUSTACH-2.

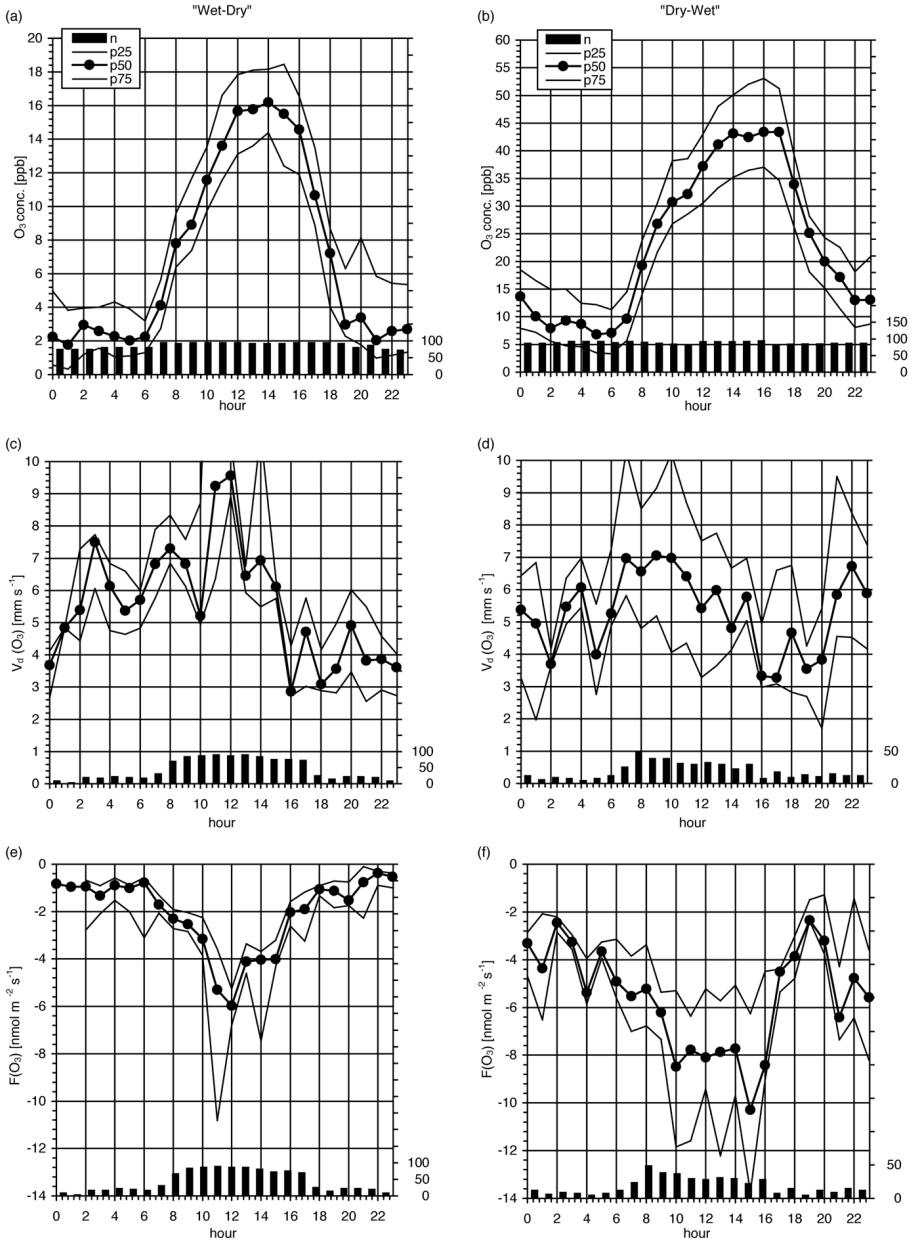

Figure 1.7 Diel (a) (b) O_3 concentrations (ppb), (c) (d) deposition velocities (mm s^{-1}), and (e) (f) O_3 fluxes (nmol m^{-2} s^{-1}) first, second and third quartiles for LBA-EUSTACH-1 and LBA-EUSTACH-2.

1.4 Conclusion

Rondônia state (Brazil) has in recent times undergone rapid replacement of natural forest by commercial and small-scale agriculture. These areas typically decline in productivity within a relatively short period (2-6 yrs) after deforestation and are then either abandoned or planted to grass. Measurements of (a) NO fluxes, (b) NO_2 and O_3 canopy resistances, (c) and NO_2 and O_3 fluxes were conducted for two seasons ("wet–dry" and "dry–wet") on the 22-year old cattle pasture *Fazendha Nossa Senhora da Aperacida* (FNS) in the state of Rondônia, Brazil. The pattern of declining productivity found on old pastures was corroborated by the low NO flux emissions measured during the 1999 "dry–wet" season. At the same time the pasture was shown to be a significant net NO_x sink, corresponding with elevated NO_2 mixing ratios during the "dry–wet" season when biomass burning was most prevalent. There was little seasonal variation in the deposition velocities of both NO_2 and O_3 between the "wet–dry" and "dry–wet" seasons at FNS. Yet, deposition fluxes were up to a factor six larger during the "dry–wet" season. This indicating that ambient concentrations largely control dry deposition of NO_2 and O_3 over established pastures.

A comparison between forest soil surface, which comprised of soil, root-mat layer and dead plant material, and pasture canopy resistances revealed that the pasture surface, which comprised of soil and vegetation, was an effective sink of NO_2 and O_3 during the two transition seasons in 1999. Further work on old-growth forest canopy and pasture soil and plant NO_2 and O_3 uptake processes is required to clarify the diel pattern of canopy resistances observed with the dynamic chamber system and corroborated in part by micrometeorological measurements.

C h a p t e r 2

A MODEL CASE STUDY OF SOIL NO EMISSIONS IN RONDÔNIA

The Brazilian state of Rondônia, situated in the seasonally dry Amazon, is presently undergoing rapid conversion (2 % yr^{-1}) of the terra firme tropical rainforest to land primarily under agriculture. One of the many spin-offs from this land clearing process is the dramatic alteration of soil climate and fertility after deforestation, which effects the natural emissions of soil borne trace gases. The contribution of nitric oxide (NO) emissions from tropical soils (forest and pastures) to global NO_x (NO and NO_2) budgets at time scales longer than 2 years is largely unknown. The disparate time scales at which processes governing soil NO emissions (microbial, climatic and anthropogenic) occur, makes regional quantification extremely difficult without models that account for time scales from days to centuries. In this study the DAYCENT[3] plant-soil ecosystem model was modified for tropical ecosystems and used to study the effects of land-use change on soil NO emissions in Rondônia for a 23-year period. The model was initialized with soil, plant and climatic conditions from a studied primary rainforest, to reproduce soil NO fluxes measured at this site, and then used to predict flux measurements at a 22-year-old pasture. The simulated effect of slash and burn, two years cropping and fire, 12 years grazed pasture and biannual burn, one plough and crop year, and then eight years of grazed pasture on forest C and N pools and cycles was significant. It resulted in a 6-fold decrease in NO emissions from forest to pasture and a significant (19 fold) increase in emissions for a 2-month period after slash and burning. Soil NO fluxes were generally elevated during the dry–wet and wet–dry transition seasons when soil conditions were optimal for NO production. Model optimizations revealed that land-use, soil moisture and nitrogen fixation/deposition, in that order, were significant determinants of soil NO fluxes for this tropical ecosystem. As older pastures and agricultural come to dominate deforested regions of the Amazon, such as in the case of Rondônia, soil nitrogen transformation will slow and resulting in a regional decrease in NO emissions in the long term. However, in the medium to short term model simulations suggest the contrary. As land undergoes conversion to agriculture episodes of high NO emissions after land clearing could complement emissions from biomass burning. This may have important implications for tropical tropospheric chemistry and highlights another unique influence of mankind in the tropics.

[3] *A plant-soil ecosystem and trace gas model [Parton et al., 1998, Parton et al., submitted, 2000; Kelly et al., 2000]*

2.1 Background

Biomass burning associated with tropical land clearing represents a major source of nitric oxide (NO) and is one of the significant ways in which tropical land-use change is contributing to regional tropospheric NO chemistry [*Crutzen & Andreae*, 1990, *Andreae & Merlet*, submitted, 2001]. A less transient but equally important source of NO results from soil emissions and global contributions are placed at 21 Tg N-NO yr^{-1} [*Davidson & Kingerlee*, 1997]. The tropical rainforest soils of the globe are considered to be an important component of this source of NO, with total emissions of between 0.5–1.1 Tg N-NO yr^{-1} [*Davidson & Kingerlee*, 1997]. It is well known that global rainforest ecosystems are under threat and an excellent example of this is found in Southwestern Amazonia. This region, which encompasses the Brazilian state of Rondônia, is currently undergoing rates of deforestation in the order of 2 % yr^{-1} since 1978 [*Roberts et al.*, submitted, 2001].

Typically Brazilian frontier agriculture involves cutting and burning a primary forest stand followed immediately by a cash crop, such as manioc, beans, rice or maize, until soil productivity declines and forces the farmer to either abandon or plant cattle pasture grass [*Jordan*, 1989; *Fujisaka & White*, 1998]. Frontier farmers make use of slash and burning for several reasons; they can (a) take advantage of the (1–3 years) soil nutrient reserve caused by forest clearing, (b) utilize the short lived neutralizing effect of the ash to the soil (1–6 months), (c) kill tree stumps that might shade crops, (d) sterilize the soil against weed infestation, (e) and reinforce their land claim, as fallow land is liable to be seized by authorities [*Nepstad et al.*, 1999a].

2.1.1 The effect of deforestation

The soils in Amazonia are inherently infertile [*Aubert & Tavanier*, 1972], highly weathered, have a low ion absorption capacity, are particularly susceptible to leaching and are generally acidic [*Brinkman & Nascimento,* 1973; *Hecht,* 1982]. Despite this the Amazonian forest ecosystem maintains a high degree of productivity (GPP > 200 g C m^{-2} $month^{-1}$) [*Lloyd et al.*, 1995] and is one of the most biologically diverse ecosystems on the planet. This is due to the efficient biogeochemical cycling of soil-plant nutrients (initially organic components), facilitated by a multitude of conservation and symbiotic mechanisms on the leaf, bark, humus, rootmat surfaces and in the soil [*Brinkman*, 1983; *Brinkman* & *Nascimento*, 1973]. The time lag between biochemical uptake, production and transfer ensures a permanent flux of energy and nutrients for the micro- and macro flora and fauna within the ecosystem [*Stark & Jordan*, 1978, *Smith et al.*, 1998].

When a tropical forest is converted to semi- and/or permanent agriculture by slashing and burning the overstory, significant changes in the surface energy balance, vegetative biomass, soil physical and chemical properties occur [*Nye & Greenland*, 1960; *Jordan,* 1989; *Nepstad et al.*, 1999a, 1999b]. The nutrient conservation and symbiotic mechanisms are destroyed and biogeochemical cycling is temporarily halted [*Palm et al.*, 1996]. The removal of the vegetative canopy results in a temporary build up of soil C and N stocks due to the lack of plant biomass competition and may also result in elevated organic nitrogen mineralization due to higher soil temperatures [*Juo & Manu*, 1996]. Soil microbial production is initially suppressed, due to microbial fire sterilization, but later recovers, tending to proliferate initially due to reduced competition with root mycorrhizae, and greater structural accessibility of high quality litter (lower C:N ratio), after burning [*Mroz et al.*, 1980]. Nitrification also increases soon after deforestation due to increased availability of ammonium and elevated soil pH due to the accompanied release of mineral nutrients from burnt soil horizons [*Mroz et al.*, 1980; *Reiners et al.*, 1994]. The gradual natural encroachment of pioneer plants after deforestation, which have larger nitrogen and lower lignin ratios, also assists in elevating mineralization, particularly if these species are nitrogen-fixers [*Hecht*, 1982, *Rhoades & Coleman*, 1999]. Between 3–12 months after deforestation inorganic C and N stocks start to decline. Mineralization slows down, as microbial populations are out-competed for limited nutrients (primarily N and P) by decomposers and re-growing plant biomass. Nitrogen is also immobilized due to the abundance of resilient roots and woody debris or leached out during the ensuing wet season [*Kauffman et al*, 1995; *Guild et al.*, 1998].

2.1.2 Soil NO emissions

Trace gas emissions of nitric oxide (NO) and nitrous oxide (N_2O) from soils are a by-product of the biotic processes nitrification, denitrification and abiotic chemodenitrification [*Remde & Conrad*, 1991; *Conrad*, 1996a] and are likewise affected by alterations to the plant-soil ecosystem [*Robertson*, 1989, *Keller et al.*, 1993]. Nitrification is an aerobic process carried out by autotrophic (B in Fig. 2.1) or heterotrophic bacteria (C in Fig. 2.1) resulting in the conversion of NH_4^+ to NO_3^- via NO_2^-. Denitrification is an anaerobic soil process where oxides of nitrogen (NO_3^-, NO, N_2O) are used as terminal electron acceptors during organic substrate decomposition. The complete denitrification pathway results in the reduction of NO_3^- to N_2, but significant amounts of NO can be emitted before complete reduction to N_2 [*McKenney et al.*, 1982; *Remde et al.*, 1989; *Remde & Conrad*, 1991; *Cardenas et al.*, 1993]. Chemodenitrification is the production of NO by chemical decomposition of biotically produced nitrite NO_2^- [*Chalk & Smith,* 1983; *VanCleemput & Baert*, 1984; *Blackmer & Cerrato*, 1986]. Tropical forest soils, which are typically wet and acidic, may be more susceptible to heterotrophic

nitrification, denitrification [*Schimel et al.*, 1984] and/or chemodenitrification [*Conrad*, 1990, 1995; *Serça et al.*, 1994].

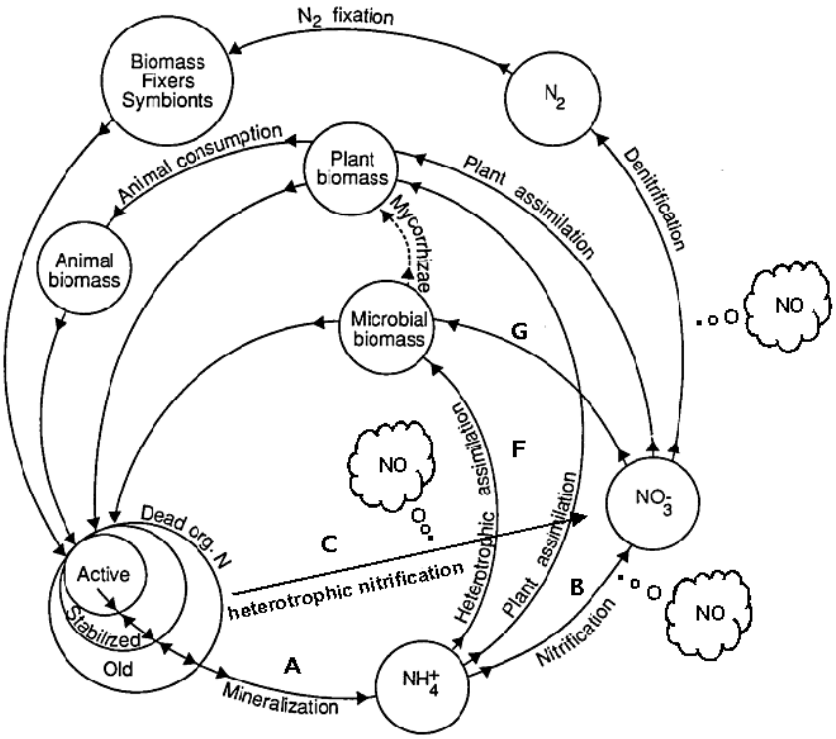

Gross nitrification = (B + C) + G
Gross mineralization = (A + C) + (F + G)

Figure 2.1 A simplified representation of the nitrogen cycle, with production of NO indicated as clouds.

The primary factors controlling NO emissions include: (a) soil temperature, (b) soil water content, and (c) soil inorganic nitrogen (elemental, oxide and ammonium forms) content and turnover rates [*Ludwig et al.*, 2001]. For any given soil temperature there is an optimum soil moisture at which NO emission is a maximum. This concept of optimum soil moisture is well documented and is reported in recent work by *van Dijk et al.*, [submitted, 2001] and *van Dijk & Meixner* [submitted, 2000a, 2000b]. Diffusion of gases in the air phase and inorganic nitrogen in the liquid phase of the soil can have a decisive influence on the soil's chemical and biological processes. Under very dry soil conditions nitrogen substrate transport within microbially active soil microsites is limited by the lack of water surrounding the soil particles, but the diffusion of gas through

the soil medium is optimized [*Linn & Doran*, 1984]. Conversely, under very wet soil conditions, substrate transport is optimized at the expense of gas diffusion [*Skopp et al.*, 1990]. The reduced gas diffusivity of the soil increases the potential for microbial consumption and chemical reduction of NO [*Gödde & Conrad*, 2000; *Conrad* 1996a; *Schuster & Conrad*, 1992]. Optimum soil moisture conditions for the emission of NO are situated between these dry and wet extremes and generally occurs at around 20–30 % water filled pore space (WFPS). Soil microbial activity can also produce significant amounts of nitrous oxide (N_2O) primarily under wetter soil conditions (> 30 % WFPS) primarily via the denitrification pathway. For more information on the production of N_2O in soils the reader is referred to reviews by *Conrad*, [1995, 1996a].

Several key studies have shown that there exists a relationship between the amount of NO and N_2O emitted from soils as a function of soil water content (WFPS) [*Davidson et al.*, 1991, 1993, 2000]. This is illustrated in figure 2.2, where as WFPS increases, NO emissions increase reaching an optimum at between 20–30 % WFPS. They then decline at a rate approximately equal to the increase in N_2O emissions as soil become wetter. The same follows for N_2O, with extremely wet soils producing more N_2 at the expense of N_2O. Generally nitrification is more dominant under aerobic soil conditions, while denitrification is more prevalent under anaerobic conditions, but both process are effectively responsible for the production of NO [*Linn & Doran*, 1984; *Davidson*, 1993; *Conrad* 1996b]. A NO and N_2O emission ratio, which describes these WFPS effects, is useful for simulating nitrogen trace gas production, consumption and diffusion within soil-plant ecosystem models.

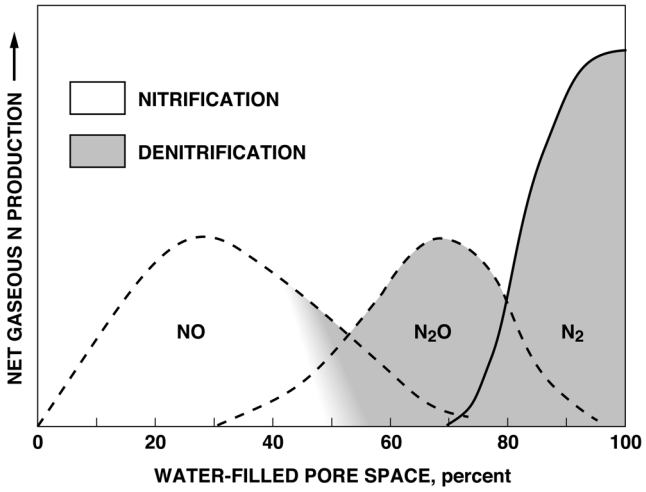

Figure 2.2 The relationship between percent water filled pore space (WFPS) of soil and the relative fluxes of nitrogen trace gases adapted from *Davidson* [1991].

Soil inorganic nitrogen content and turnover rates in the soil are best quantified by the two nitrogen indices; gross– mineralization and nitrification. These indices can be determined in the field [*Hart et al.*, 1994] and are used in soil nitrogen models as measures of soil inorganic nitrogen status [*Potter et al.*, 1996, 1998; *Li et al.*, 2000; *Parton et al.*, 1996]. Gross mineralization is the sum of inorganic nitrogen mineralization (A in Fig. 2.1), heterotrophic nitrification (C), and the immobilization by biomass, heterotrophs (F) and microbes (G). Gross nitrification is the sum of both heterotrophic and autotrophic nitrification (C and B) and microbial immobilization (G).

Early studies in the tropics suggested that deforestation produced elevated nitrogen trace gas emissions that remained constant in time [*Luizáo et al.*, 1989], but more recent work has shown that this is not entirely true [*Keller & Reiners*, 1994]. From work conducted in the Venezuelan Amazon, *Jordan et al.* [1983] first postulated that if slash and burn practices continued unabated for a decade or longer nitrogen losses through leaching, denitrification and harvesting would seriously deplete soil reserves and thereby any process dependent on these nitrogen reserves. Tropical land tends to show a general slowing in the rate of soil nitrogen transformations with age and subsequent decline in soil nitrogen trace emissions [*Neill et al.*, 1995, 1997, 1999; *Piccolo et al.*, 1994, 1996]. This is evident on a range of soils in Amazonia (Table B1, cf. Appendix B) and has been observed in several studies of NO flux in relation to land age since deforestation. Despite a gradual decline in emissions in the long term, recent work has also shown that NO fluxes can remain elevated for a period of time after deforestation (sometimes for as long as 6 years) and thereafter decline to emission rates well below those of the original forest [*Sanhueza,* 1997; *Keller et al.*, 1993; *Verchot et al.*, 1999, *Veldkamp et al.*, 1999]. Forest clearing and repeated burning cause an increase in soil NO emissions due to high soil inorganic N-availability, and/or N-cycle decoupling (such as during chemodenitrification) that occurs after deforestation [*Vitousek & Matson*, 1985; *Anderson, et al.*, 1988; *Levine et al.*, 1990, 1996; *Harris et al.*, 1996; *Poth et al.*, 1995; *Keller et al.*, 1993; *Keller & Reiners*, 1994; *Neff et al.*, 1995; *Weitz et al.*, 1998; *Verchot et al.*, 1999]. There exists therefore a strong relationship between land age (time elapsed since deforestation), land-use/agricultural practices, which govern soil nitrogen cycling, and soil NO emissions in the tropics.

2.1.3 Objectives

In this work a 1-D plant-soil ecosystem model, which simulates soil-plant C and N cycles in response to soil moisture, temperature and biomass input parameters, was modified for tropical conditions. The model was optimized with field measurements of soil NO emissions from a forest and then used to hindcast field measurements of soil NO emissions from a 22 year old pasture in the seasonally

dry south western Brazilian Amazon (Rondônia). By applying a documented chronology of land management practices typical for this region (deforestation, cropping and grazing) the modeled forest environment was transformed to a grassland cattle pasture over 22 model years. Results from these integrations were then used to study the effects of land-use change on intra- and inter-seasonal soil NO emissions.

2.2 Study Area and Measurements

Rondônia is situated on the fringe of the Amazon basin (Fig. 2.3) and comprises of seasonally dry (May to September), *terra firme* (upland) tropical rainforest and various ages of deforested land primarily under agriculture. It is also situated in a region of the Amazon undergoing rapid land conversion and is known for a characteristic fishbone pattern of deforestation [*Alves et al.*, 1999]. Measurements of soil NO fluxes and several soil and biomass parameters used for model construction, calibration and optimization were conducted during two measurement campaigns, LBA-EUSTACH-1 and -2[4], at two sites (ca. 80 km apart) (Fig. 2.3), from 30 April–17 May 1999 (wet–dry season), and 24 September–27 October 1999 (dry–wet season). The pasture measurements are described in detail chapter 1.

Measurements of NO soil emissions were conducted using a dynamic chamber system during the dry–wet transition season of 1999 at a pasture site [Chapter 1] and during the wet–dry and dry–wet transition seasons at a forest site [*Gut et al.*, submitted, 2001a]. Median NO fluxes for FNS were 0.55 ng N m^{-2} s^{-1} [Chapter 1], and 4.9 ng N m^{-2} s^{-1} at RBJ for both seasons [*Gut et al.*, submitted, 2001a]. Measured NO fluxes from the forest soils were approximately an order of magnitude higher than those from the pasture soils. This difference was also confirmed by laboratory measurements of soil uptake rate and production of NO by *van Dijk et al.* [submitted, 2001] according to *Conrad* [1994]. Gaseous diffusion in soil measurements were (^{222}R) conducted at both RBJ and FNS [Chapter 1; *Gut et al.*, submitted, 2001a].

2.2.1 Forest site (RBJ)

The forest site, which was ca. 90 km north of the town *Ji-Paranã* (Fig. 2.3), was situated in the *Reserva Biolõgica do Jaru* (RBJ) and is run by the Brazilian Environmental Protection Agency IBAMA (*Instituto Brasileiro de Meio Ambiente e Recursos Renovãveis*). The reserve, which borders the *Rio Machado* River, comprises

[4] European Studies on Trace gases and Atmospheric Chemistry within the Large Scale Biosphere-Atmosphere Experiment in Amazonia

of open upland forest, with a canopy height of ca. 33 m and an estimated GPP of 200 g C m^{-2} $month^{-1}$ [*Lloyd et al.*, 1995].

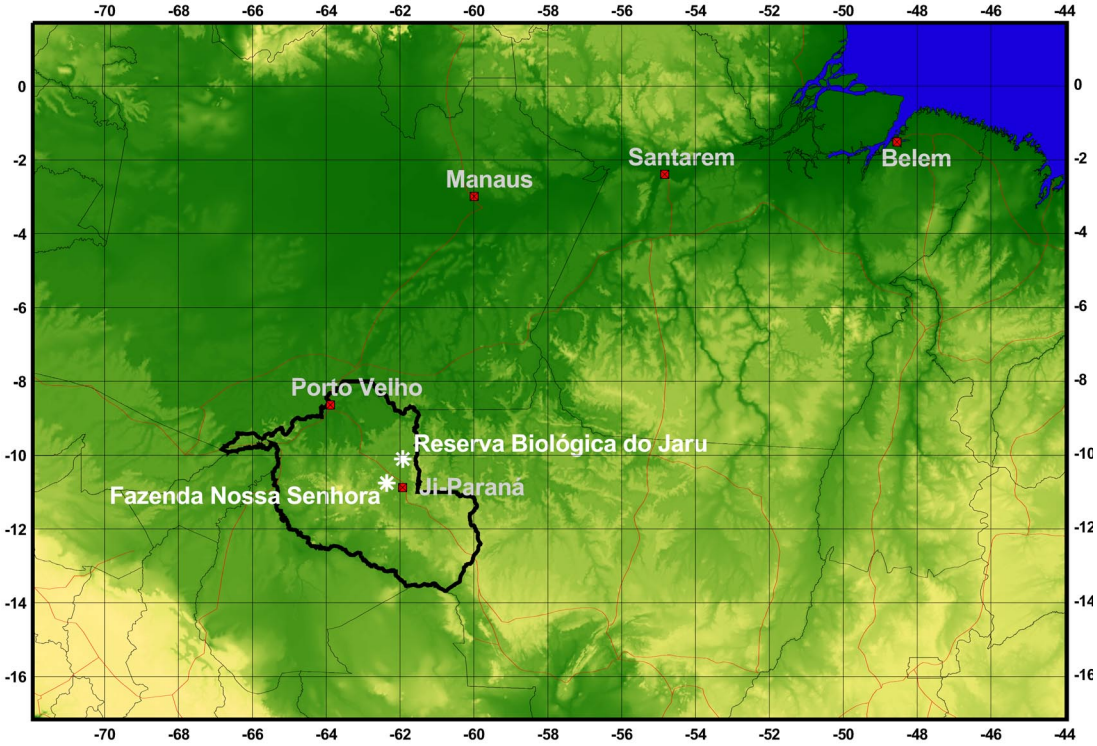

Figure 2.3 Location of the measurement sites *Fazendha Nossa Senhora da Aparecida* (FNS), and *Reserva Biológica do Jaru* (RBJ) in the state of Rondônia, over a 1 km DEM of Brazil.

2.2.2 Pasture site (FNS)

A 22-year-old pasture situated on a cattle ranch *Fazendha Nossa Senhora da Aperacida* (FNS), ca. 50 km west of *Ji-Paranã* (Fig. 2.3), was where measurements of soil NO fluxes and soil properties were conducted [Chapter 1]. The pasture was first deforested in 1977 and then cropped for 2 years, thereafter planted to grass, grazed and burnt on a two-year rotation for a following 12 years. The land was then ploughed (20 cm) and cropped for one year and then replanted to grass (*Bracharia brizantha*) and grazed for a further 8 years. At the time of measurement the pasture was under grazing. The soil was never fertilized. The grass sward at FNS had an average total above biomass of 3166 (± 682) kg ha^{-1} [*Waterloo, M.J.*, personal communication, 2000]. Assuming a leaf nitrogen content of ca. 0.67 %, as observed by *Davidson E.A.* [personal communication, 2000] at the *Fazenda*

Vitoria in Parã, the total above ground nitrogen in the live biomass was ca. 21 kg N ha^{-1}.

2.3 Original model description

Several models have been successfully used for soil nitrogen trace gas emission studies. These include a biome-based model by *Yienger & Levy* [1995], the CASA[5] model [*Potter et al.*, 1996, 1998], the DNDC[6] model [*Li et al.*, 2000], the NGAS model [*Parton et al.*, 1996], and the CENTURY (monthly) model [*Liu et al.*, 1999, 2000; *Raich et al.*, 2000]. Only three of these models have been used explicitly for tropical ecosystem studies [*Potter et al.*, 1998; *Liu et al.*, 2000; *Raich et al.*, 2000]. The *Yienger & Levy* [1995] model was the only model to include a scheme to simulate elevated soil NO emissions after biomass burning.

The DAYCENT plant-soil ecosystem model, which is based on the widely used CENTURY model (over 80 publications), was selected for its powerful ability to simulate the effects of agricultural management practices (cutting, fire, tillage, sowing, harvesting, fertilization, and grazing) on trace gas fluxes at a daily resolution over large timescales (centuries) [*Parton et al.*, 1998, *Kelly et al.*, 2000; *Parton et al.*, submitted, 2000]. The original submodels will be reviewed here only briefly in conjunction with figure 2.4. Changes to these submodels, which are specific to this work, are discussed in section 5.

The model simulates daily evaporation, plant production, terrestrial carbon, nitrogen transformation and NO, N_2O and N_2 gas emissions via a set of interlinking submodels for soil organic matter (SOM), land surface (soil moisture, soil temperature and plant productivity) and trace gas fluxes. These submodels are described in detail in *Parton et al.* [1998], *Parton et al.* [submitted, 2000] and *Del Grosso et al.* [2000].

[5] Carnegie Ames Stanford Approach Model

[6] Denitrification and Decomposition Model

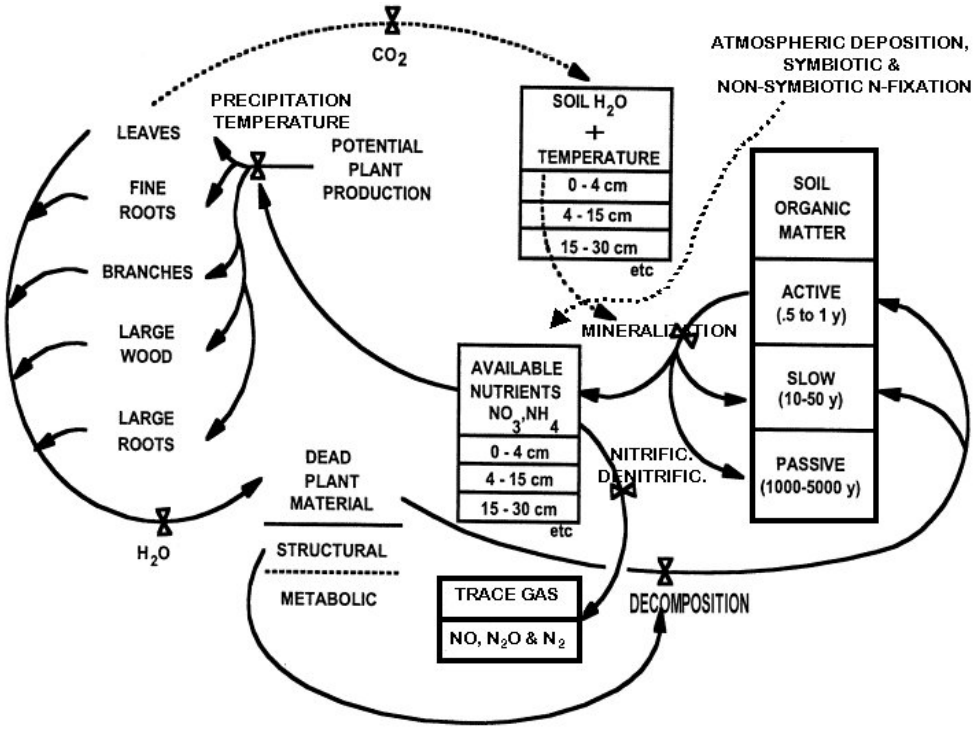

Figure 2.4 Schematic of the DAYCENT model.

2.3.1 Soil Organic Matter submodel

The SOM or carbon submodel, which runs on a monthly time step, comprises of three pools each with different turnover rates; active (0.5–1 yr.), slow (10–50 yr.) and passive (1000–5000 yr.). These comprise of above– and belowground litter (each with allowable ranges of C:N) and surface microbial biomass. Above– and belowground plant residues and organic animal excreta are further partitioned into structural (belowground plant residues) and metabolic (organic animal excreta) pools as a function of the lignin to nitrogen ratio found in the plant residues. Decomposition of dead plant material supplies the SOM pool and mineralization of SOM, N-fixation, and N-deposition supply the available nutrient pools (Fig. 2.4). The decomposition of both plant residues and SOM, which can be limited by anaerobic conditions (high soil water content), are assumed to be microbially mediated with an associated loss of CO_2 due to respiration. Soil physical properties, environmental variables, lignin and nitrogen concentrations of vegetation, litter and SOM all drive the flows of nutrients through these pools.

The submodel includes nitrogen inputs from symbiotic, non-symbiotic N-fixation and atmospheric deposition. Non-symbiotic N-fixation is carried out by all true free-living autotrophic or heterotrophic organisms within the plant canopy, and might include epiphytes, bryophytes, yeasts, lichens, cyanobacteria, and mosses not in direct symbioses with plants. Atmospheric (lightning & gas phase reactions) and non-symbiotic nitrogen fixation inputs are considered as wet deposition processes in the model, and are thus linearly controlled by the amount of rainfall per day (Fig. 2.4). All nitrogen deposition is assumed to be wet deposited, as no explicit scheme exists for dry deposition in the model. Symbiotic N-fixation, which represents legume and rhizobial based nitrogen fixation processes occurring in the soil-plant environment, is a linear function of net primary production (NPP) and only becomes effective when there is insufficient mineral nitrogen to satisfy plant requirements.

2.3.2 Land surface submodel

The soil water component of the land surface submodel runs on a daily time step and is based on work by *Parton et al.* [1998] and *Hillel* [1977], which simulates the transport of water through the plant canopy, litter, and a multi-layered soil system (0–1, 1–4, 4–15, 15–30 cm, etc.). A portion of the rainfall is intercepted and evaporated as a function of the amount of plant biomass and/or surface litter. Non-intercepted water enters the 11-layer soil profile and is infiltrated or redistributed, depending soil saturation conditions and then evaporated and transpired as a function of soil water potential and root biomass demand [*Parton et al.*, 1987]. Infiltration of water is governed by the hydraulic conductivity of each soil layer and progresses downward through the soil profile with excess water allowed to flow out as base flow.

Daily soil surface temperature is calculated using equations developed by *Parton* [1984] and *Eitzinger et al.* [2000], which calculate maximum soil temperature as a function of the maximum air temperature and the canopy biomass (lower for high biomass) and minimum soil temperature as a function of the minimum air temperature and canopy biomass (higher for higher biomass). The actual soil temperature used for decomposition, plant growth and nitrification is the average of these two soil temperatures.

The plant production submodel, which runs on a weekly time step, uses soil water content, temperature, and available nutrients to calculate plant growth and C is allocated among leafy, woody, and root biomass based on vegetation type.

2.3.3 Trace gas submodel

The nitrogen trace gas submodel of DAYCENT, which is described in detail in *Parton et al.* [submitted, 2000], is primarily based on the "*hole-in-the-pipe*" conceptual

scheme first proposed by *Firestone & Davidson* [1989]. This scheme describes the flow of inorganic nitrogen through an imaginary pipe as representing the rates of nitrification and denitrification in the soil, while the holes in the pipe or "leaks" describe the amount of nitrogen trace gas (NO, N_2O and N_2) that eventually escapes the soil surface [*Davidson, et al.*, 1993, 2000]. The submodel assumes that nitrification and denitrification contribute to the production of soil nitrogen trace gases. For this the submodel has two sub components *nitrify* and *denitrify* (denitrification). The *nitrify* component simulates nitrification, which is calculated as a function of soil NH_4^+ concentration, WFPS, soil– temperature, pH, and texture. The *denitrify* component simulates denitrification, which is calculated as a function of soil NO_3^- concentration, heterotrophic respiration (CO_2) and WFPS.

The original submodel assumes that N_2O trace gas is emitted at a rate equivalent to 2 % of nitrification (from *nitrify*). This 2 % proportionality constant was derived from observed N_2O flux data [*Mosier et al.*, 1996] and simulated model results [*Frolking et al.*, 1998] in recent work by *Parton et al.* [submitted, 2000]. The *denitrify* component produces an entirely gaseous product of N_2O and N_2 apportioned as a function of the ratio of soil NO_3^- concentration to CO_2 emission, corrected by WFPS [*Del Grosso et al.*, 2000]. The N_2O gas produced by *nitrify* and *denitrify* are combined to produce a total soil N_2O emission.

The amount of NO emitted from the soil is none other than the product of a $NO:N_2O$ ratio and the N_2O gas emitted (produced by *nitrify* and *denitrify*). The $NO:N_2O$ ratio is calculated as a function of soil parameters (bulk density, field capacity, WFPS) that influence gas diffusivity. Studies on concurrent NO and N_2O emissions have shown that the ratio $NO:N_2O$ correlates with soil water content with highest values for drier soils (< 60 % WFPS), decreasing as WFPS increases. [*Verchot et al.*, 1999; *Potter et al.*, 1996; *Davidson et al.*, 1991, 1993]. Soil diffusion was found to better represent the $NO:N_2O$ ratio than WFPS despite substantial unexplained variability with this approach [*Parton et al.*, submitted, 2000].

2.4 Model inputs

The DAYCENT model requires daily precipitation, air temperature and over 500 parameters relevant to climate, soil, biomass, nitrogen, carbon and agricultural land management. Model input parameters that were changed in this study are discussed below and are presented in tables B2 to B4 (cf. Appendix B). These input parameters were sourced from fieldwork conducted at RBJ and FNS and from studies conducted in Rondônia [*Guild et al.*, 1998; *Kauffman et al.*, 1995; *Hodnett et al.*, 1996, *Lloyd et al.*, 1995; *Waterloo M.J.*, personal communication, 2000; *Roberts J.M.*, personal communication, 2000]. Where no data were available, input

parameters were derived from previous CENTURY simulations of tropical forests [*Lui et al*, 2000; *Silver et al.*, 2000; *Raich et al.*, 1997; 2000].

2.4.1 Soil data

The model soil input parameters for the forest (Table B2, cf. Appendix B) were determined from both literature and soil samples taken from RBJ and FNS and analyzed for texture, pH, sand, clay, organic carbon, nitrogen (total, NH_4^+ and NO_3^-) and carbon content. Soils at RBJ were an acidic (pH 3.5), sandy (74 %) red yellow podzol (*Podzólica vermelho-amerolo A moderado textura média*) [*Hodnett et al.*, 1996]. Soil wilting point (WP) and FC were derived from measured soil clay and silt contents using the *Tomasella & Hodnett* [1998] pedo-tranfer functions for Brazilian soils. Soil saturated hydraulic conductivity (K_{sat}) was sourced from measurements of an Oxisol at *Fazenda Dimona* in Parã, Brazil [*Hodnett et al.*, 1996]. Chemical analyses of the soil samples showed approximately equal proportions of soil NH^+_4 (9.4 $\mu g\, NH_4^+\, g^{-1}$) and NO^-_3 (11.8 $\mu g\, NO_3^-\, g^{-1}$) concentrations for RBJ, while soil NH_4^+ concentrations (16.8 $\mu g\, NH_4^+\, g^{-1}$) prevailed over NO^-_3 (5.3 $\mu g\, NH_4^+\, g^{-1}$) at FNS (Table B2, cf. Appendix B).

2.4.2 Climate data

The model requires daily rainfall and surface air temperature data in order to simulate a particular ecosystem. A 10-year daily rainfall and air temperature data set was constructed from both pasture and forest ecosystems in Rondônia, encompassing the year's 1992-7 and 1999. These data represent the longest daily resolution meteorological data set currently available for Rondônia and were sourced from automated weather stations installed at RBJ and FNS (1999), from meteorological stations in Rondônia, manned during previous measurement campaigns (ABRACOS – *Anglo-Brazilian Climate Observation Study*), and archived by INPE (*Instituto Nacional de Pesquisas Espaciais*). Due to data paucity the weather data were separated into two five-year datasets. These were a predominantly forest weather data set (80 % measurements from forests, 20 % measurements from pastures) and a predominantly pasture meteorology (80 % from pastures and 20 % from forests). During model runs the weather data were supplied to the model and on a repetitive basis. This meant that if the model ran for 20 yrs. the weather dataset would be used four times over. The forest meteorology was used when the forest was growing (first 1000 model yrs.) and the pasture meteorology was used after deforestation, when pasture was installed (last 22 model yrs).

2.4.3 Biomass data

The model was initialized with observed biomass C fractions, C:N ratios, litterfall, and biomass fraction nitrogen content from several literature sources, details of which are listed in table B3 [*Lloyd et al.*, 1995; *Kauffman et al.*, 1995; *Guild et al.*,

1998; *Lui et al.*, 2000; etc.]. Leaf death rates and litter biomass were obtained from measurements conducted by *Roberts J.M.* [unpublished data, 2000], which revealed an estimated leaf turnover rate of 0.65 yr^{-1}, which is slightly less than that reported by *Klinge et al.* [1975] of 0.80 yr^{-1} for closed forests near Manaus.

2.4.4 Nitrogen fixation and deposition

Significant amounts of free nitrogen have been shown to be fixed by a variety of facultative micro-organisms in the stem/trunk and rootmat layer regions of the rainforest, supplying large quantities of nitrogen to the soil ecosystem either symbiotically or non-symbiotically [*Brinkman*, 1983]. Non-symbiotic N-fixation rates vary widely in the tropics and values of between 0.5–60 kg N ha^{-1} yr^{-1} have been reported by *Chestnut et al.* [1999], *Edmisten* [1970], *Forman* [1975] and *Goosem & Lamb* [1986]. N-fixation in the rootmat layer may range from between 2–20 kg N ha^{-1} yr^{-1} [*Sylvester-Bradley et al.*, 1980]. This value is extremely difficult to quantify and was therefore used as an adjustment parameter during model optimization (cf. Section 2.6). A value of 40 kg N ha^{-1} yr^{-1} was chosen, which lies between the minimum (2 kg N ha^{-1} yr^{-1}) and maximum (60 kg N ha^{-1} yr^{-1}) range reported by *Cleveland et al.* [1999] for the tropics.

Rates of symbiotic N-fixation in tropical forests range from 2–200 kg N ha^{-1} yr^{-1} and are primarily dependant on the quantity of below ground biomass [*Salati et al.*, 1982; *Sylvester-Bradley et al.*, 1980]. Recent work has shown that this source may be smaller in the tropics due to high temperatures, seasonal drought and soil acidity, which constrain legume root-nodule formation and therefore limit rhizobial growth and survival in the soil [*Hungria & Vargas*, 2000]. Symbiotic N-fixation, which varies linearly with NPP in the model, was set to a maximum of 100 kg N ha^{-1} yr^{-1} for the forest and 2 kg N ha^{-1} yr^{-1} for the pasture, reflecting the difference in total aboveground biomass between the two ecosystems (forest – 17150 g C m^{-2}; pasture – 296 g C m^{-2}) [*Cleveland et al*, 1999, *Guild et al.,* 1998, *Waterloo, M.J.*, personal communication, 2000].

Nitrogen deposition (g m^{-2}) from atmospheric sources (wet-deposition) was linearly scaled by annual rainfall for Rondônia (19679.7 mm). This was sourced from measurements made in the *Rio Madeira* river basin (eastern border of Rondônia) [*Lewis, et al.*, 1999] and corresponded to 4.63 kg N ha^{-1} yr^{-1}.

2.5 Model modifications

DAYCENT and its forbearer CENTURY have been applied in the past to simulate carbon and nitrogen fluxes and trace gas emissions for various ecosystems, however some inconsistencies have been observed in its application to tropical ecosystems [*Vitousek et al.*, 1994; *Motavalli et al.*, 1994, 1995]. Several

adjustments were therefore made to the model in order to better simulate Amazonian tropical conditions and thereby soil NO emissions. Changes implemented for each submodel are presented in the following sub sections.

2.5.1 Land surface sub-model

The algorithms governing soil water potential, which govern the bi-directional flow of soil water under saturated and unsaturated conditions, were changed by replacing the original *Gupta & Larson* [1979] soil texture pedo-transfer functions with those of *Tomasella & Hodnett* [1998] based on Brazilian soils. This scheme offered a better representation of the macro-pore structure found in Brazilian soils and facilitated faster drainage of excess water under conditions of high precipitation. In addition the multiplier used to compute the fraction of inorganic nitrogen leached from one soil layer to another during profile saturation was also reduced from 75 % to 35 % for the soils at RBJ so as to better represent the nitrogen conservation mechanisms found in tropical rainforests ecosystems [*Williams et al.,* 1997].

2.5.2 Temperature submodel

Due to constraints in the original soil surface temperature algorithm, which did not allow for biomass loads over 600 gm^{-2} [*Parton*, 1984; *Metherell et al.*, 1993], linear adjustments to the weights used to calculate the contribution of maximum and minimum air temperature on soil temperature were made using measured data from RBJ.

2.5.3 Nitrogen trace gas submodel

The modified nitrogen trace gas sub-model was, as in the original model (cf. Section 2.3.3.), based on the *"hole-in-the-pipe"* conceptual scheme [*Firestone & Davidson*, 1989]. The modified model, which is represented schematically in figure 2.5, assumes that soil organic nitrogen is mineralized to inorganic nitrogen (NH_4^+). A prescribed amount (80 %) of NH_4 is nitrified to produce NO_3^-, which is then denitrified to produce nitrous oxide or dinitrogen (N_2^-). The remaining 20 % of NH_4^+ is denitrified directly reflecting the heterotrophic nitrification pathway predominant in acidic and forest soils (C in Fig. 2.1) [*Schimel et al.*, 1984].

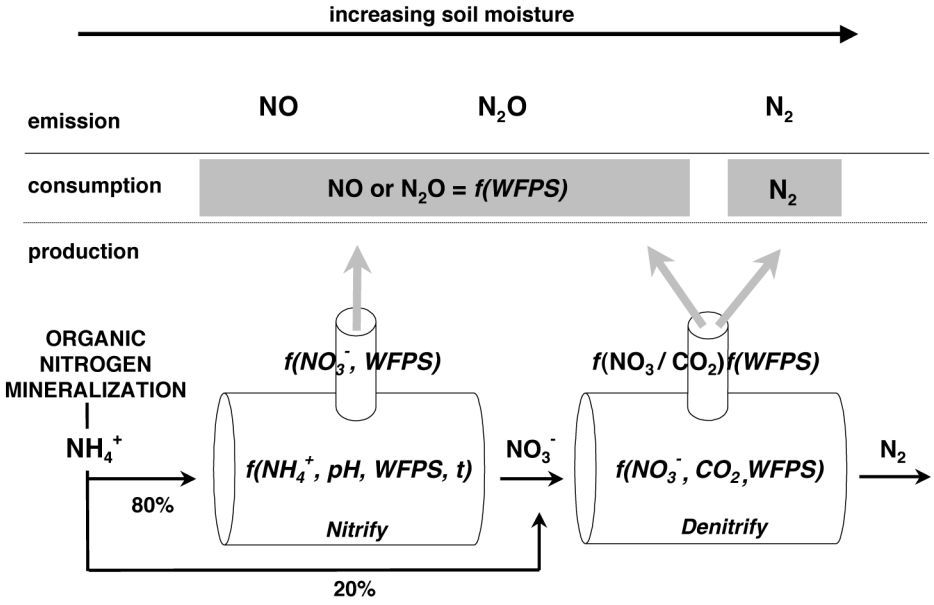

Figure 2.5 Schematic of the modified trace gas model based on the "*hole-in-the-pipe*" conceptual model of *Firestone & Davidson* [1989].

The modified trace gas model was based on the concept that NO production and consumption processes occur simultaneously in the soil such that when NO production exceeds consumption a net emission of NO from the soil to the atmosphere occurs [*Galbally & Johansson*, 1989]. Further, nitrification and denitrification are both responsible for the production of NO and N_2O, such that under drier soil conditions (< 60 % WFPS) both processes are important and under reducing soil conditions (> 60% WFPS) denitrification becomes more dominant.

A significant difference between the original and modified trace gas sub-models is the shift from an approach which assumed that nitrification and denitrification produced only N_2O gas to one in which both NO and N_2O are produced by nitrification and denitrification (Fig. 2.5). This facilitates the explicit simulation of NO production, doing away with the nitrification proportionality constant (2 % of nitrification, cf. Section 2.3.3.), which was empirically derived from N_2O data on soils which are generally to wet (Fig. 2.1) to produce significant amounts of NO. It also allows for the introduction of a soil NO consumption term, where the consumption of NO is proportional to the emission of N_2O [*Conrad*, 1966a]. This is achieved with an improved NO:N_2O ratio as a function of WFPS (Fig. 2.5) (cf. below).

The proportionality constant (2 % of inorganic nitrogen, cf. section 3.3) has been widely quoted in model literature as universal for gas production [*Frolking et al.*, 1998; *Potter et al.*, 1996, 1998], but was found to be unsatisfactory for the simulation of NO production in this study. The constant has also been previously applied in several models to describe gas emissions as either a function of mineralization as is the case for the CASA model [*Potter et al.*, 1996] or nitrification as is the case for the DNDC model, [*Li et al.*, 2000], NGAS model [*Parton et al.*, 1996], and the CENTURY model [*Liu et al.*, 2000]. Recent studies have confirmed that the product of soil mineralization (NH_4^+) is least related to soil NO and N_2O emissions in the tropics [*Davidson et al.*, 2000; *Erickson et al.*, 2001]. In this study the 2 % proportionality constant for nitrification was replaced with a function describing the fraction of nitrogen trace gas produced as a function of the amount of NO_3^- produced by *nitrify* (nitrification),

$$\textit{Gas fraction of nitrification} = 10^{\,0.943 \log N + 0.686} \qquad (2.1)$$

where N is daily NO_3^- produced from nitrification (*nitrify*). This modification is in line with the "*hole in the pipe*" conceptual model and recent tropical trace gas research findings, which suggests that much smaller proportions of total nitrification are responsible for NO production [*Davidson et al.*, 2000; *Erickson et al.*, 2001]. The function (eq. 2.1) was obtained from a review of studies where the measured soil nitrogen availability index *potential nitrification* and soil NO and N_2O fluxes were measured in the tropics [*Davidson et al.*, 2000]. The *potential nitrification* index has been shown to be most appropriate for studies in Brazil ($r^2 = 0.85$) [*Verchot et al.*, 1999], and global tropical soils ($r^2 = 0.47$) [*Davidson et al.*, 2000]. This index reflects the capacity of soil nitrifying bacteria to convert supplemented NH_4^+, under laboratory conditions, to NO_3^- [*Hart et al.*, 1994]. The revised *nitrify* production component produced values in line with estimates of NO production by *Davidson et al.* [1993] of less than 0.1 %.

After nitrification the remaining daily NO_3^- undergoes denitrification (*denitrify*) (Fig. 2.5) producing an entirely gaseous output apportioned into N_2O and N_2 as per the original model scheme [*Del Grosso et al.*, 2000; cf. Section 2.3.3]. The difference being that the N_2O portion of *denitrify* was made to represent the production of both NO and N_2O instead of the emission of N_2O only. The NO and N_2O produced from *denitrify* and *nitrify* was then combined to represent the total nitrogen oxide trace gas production within the soil.

The factor governing the quantity of NO and N_2O trace gas, which eventually escapes the soil surface is soil consumption. This is reflected in the improved submodel as the NO:N_2O ratio as a function of WFPS. The original sub-model portrayed the NO:N_2O ratio as a function of soil gas diffusion based on work

conducted by *Potter et al.* [1996]. This soil gas diffusion scheme was found to be unsuitable for this study as it could not reproduce measurements in the field made at RBJ and FNS [Chapter 1; *Gut et al.*, submitted, 2001a]. Several alternative NO:N_2O ratios were investigated during model design [*Keller & Reiners*, 1994; *Parton, et al.*, submitted, 2000; *Verchot et al.*, 1999; *Lui et al.*, 2000; *Davidson et al.*, 2000] and a scheme based on WFPS, derived from measurements exclusively on tropical soils by *Davidson et al.* [2000] was selected,

$$NO{:}N_2O = 10^{-0.026\ WFPS\ -\ 1.66} \tag{2.2}$$

The total emission of NO and N_2O from the soil was therefore the product of soil nitrogen trace gas production processes (*nitrify* and *denitrify*) and soil consumption (eq. 2.2) per day.

The original DAYCENT gas submodel also made use of a daily rainfall NO pulsing scheme, which simulated elevated NO emissions following precipitation events according to *Yienger & Levy* [1995]. This was found to be excessive as *nitrify* and *denitrify* were able to simulate rainfall-induced peaks in emissions sufficiently for RBJ.

2.6 Modeling strategy

The improved DAYCENT model was used in a hindcast fashion to predict field NO flux measurements at FNS (old pasture) from conditions at RBJ after deforestation and 22 years of agriculture. In other words the model was initialized with soil, plant and atmospheric conditions at RBJ (primary rainforest), optimized to reproduce the NO fluxes measured at this site, and then by application of a set of land-use management practices the model was used to predict the effects of deforestation, cropping, pasture installation and grazing on NO fluxes over 22 years.

After an initial model equilibration period of 1000 yrs., the simulated RBJ rainforest was subject to fire and a tree harvest event in the eighth month of the first model year, which removed a significant amount the canopy overstory (Table B4, cf. Appendix B). Thereafter land-use management practices were applied in accordance with the land-use chronology documented for FNS (cf. Section 2.2.2). This consisted of two years of beans, maize and sorghum harvested on a 4-month rotation, culminating with a fire event to burn off the remaining forest regrowth and crop residue. Followed by 12 years of tropical pasture grass under grazing with a burn every second year and a plough event followed by cropping for one year. The remaining years up to model year 22 simulated tropical grassland under grazing without fire.

It was impractical to validate the model in a true iterative sense [*Oreskes et al.*, 1994] due to the large model run time (ca. 10 minutes per 1000 model yrs.) and the numerous input parameters (> 500). Therefore an approach used in previous CENTURY model simulations was adopted [*Lui et al.*, 2000; *Silver et al.*, 2000; *Raich et al.*, 1997; 2000]. Where *a priori* knowledge of the measurement site, supported by a comprehensive literature survey, served as an empirical reference, against which a set of model parameters were compared with field measurements. The model was optimized by comparing the following observed (measured) data with model simulations: (a) observed soil water (15 cm), (b) observed soil surface temperature, (c) literature sourced above ground live biomass and (d) measured NO gas fluxes for the field measurements periods (cf. Section 2.2). No attempt was made to optimize simulations with observations on a day-by-day basis, instead observed and simulated data periods were compared and optimized using the root mean square error (RMSE) and unbiased correlation coefficient (r^2) statistics as measures of goodness of fit [*Wilks*, 1995]. For model optimization the following parameters were used: (a) initial active SOM pool C:N ratios, (b) non-symbiotic soil N-fixation, (c) symbiotic N-fixation, (d) WP, (e) FC, (f) K_{sat}, and (g) minimum soil water content fractions for the first three soil layers (0–15 cm).

Although DAYCENT was designed to simulate NO and N_2O emissions in response to soil-plant-climate dynamics, paucity of combined NO and N_2O flux measurements in Rondônia prevented model optimization for N_2O. However, laboratory N_2O flux investigations on soil samples from RBJ and FNS, for a range of soil moistures, revealed that model simulations of N_2O were within the measured ranges [*Lehmann & Kirkman*, unpublished data, 2001]. Hence, model simulations of NO fluxes only are discussed and presented in the next section.

2.7 Results

The modified DAYCENT model, which was optimized to reproduce overall NO flux magnitudes, captured the trend of daily measured fluxes at RBJ reasonably well. Results showed good agreement with measured rates during both the wet–dry ($r^2 = 0.88$, RMSE = 1.7 ng N m^{-2} s^{-1}) and dry–wet ($r^2 = 0.86$, RMSE = 2.0 ng N m^{-2} s^{-1}) transitions seasons (Fig. 2.6(a), Table B5). The model performed acceptably in hindcasting the NO fluxes ($r^2 = 0.43$, RMSE = 0.8 ng N m^{-2} s^{-1}) at FNS (Fig. 2.6(b), Table B5) via the application of land-use and agricultural management practices in accordance with the chronology at FNS. General agreement between observed and expected soil water content was also achieved at a soil depth of 15 cm ($r^2 = 0.86$, RMSE = 3.5 % vol.), and soil temperature at 2 cm ($r^2 = 0.88$, RMSE = 1.5 °C). Observed [*Waterloo, M.J.*, unpublished data, 2000] and expected total above ground nitrogen in the live biomass at FNS were within 30 % of each other (Table B5, cf. Appendix B).

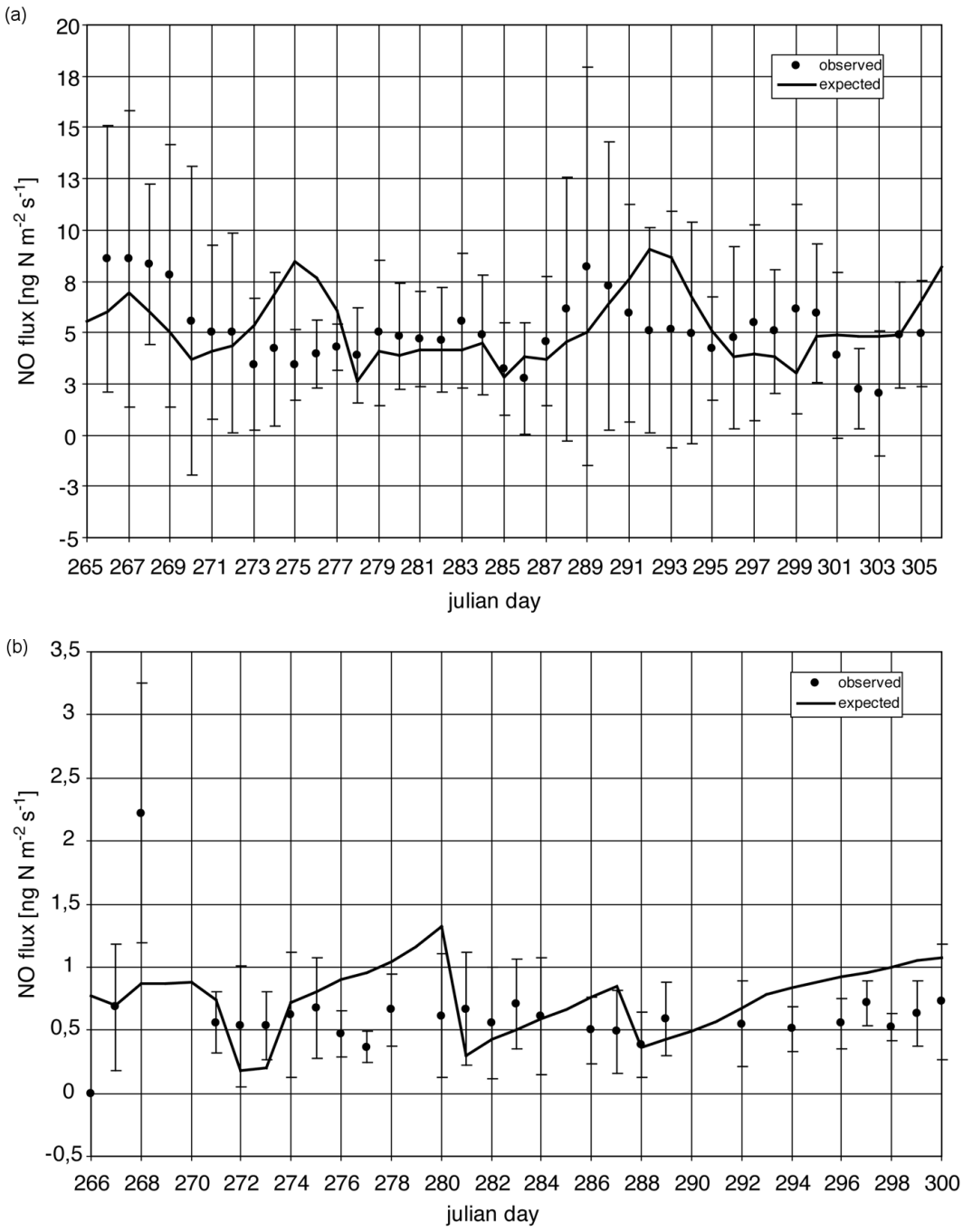

Figure 2.6 Daily measured (observed) and modeled (expected) NO fluxes (ng N m^{-2} s^{-1}) for (a) RBJ and (b) FNS during the dry–wet transition seasons of 1999.

2.7.1 Seasonality

Simulated soil properties at both sites revealed relatively stable annual temperatures at the soil surface, but showed noteworthy differences in WFPS, of up to a factor two between the dry (May–September) and wet seasons (Fig. 2.7 & 2.8). Simulations of NO emissions for RBJ showed 30 % higher fluxes during the wet season (October–April) as opposed to the dry season. Similar seasonal patterns of NO emissions were observed for simulations of Costa Rican forest soils by *Lui et al.* [1999] and measurements in Mexican tropical forests [*Davidson, et al.*, 1993]. However, model results contradict monthly measurements from closed forests in Parã [*Verchot et al.*, 1999] and Manaus [*Bakwin et al.*, 1990a], which indicated higher NO emissions during the dry season (Table B1, cf. Appendix B). Rather model NO fluxes show a pattern of higher fluxes during the wet–dry and (April) and dry–wet (September–November) transition seasons. During these periods model soil gross mineralization (production) and WFPS (consumption) conditions were optimal for NO emissions at both RBJ and FNS (Fig. 2.7 & 2.8). The simulated optimal WFPS for NO emissions occurred at between 20 and 30 % WFPS for both sites, which agreed reasonably well with optimums measured in the field and laboratory (20–28 % WFPS) [*van Dijk & Meixner*, submitted, 2000a, 2000b; *van Dijk et al.,* submitted, 2001; *Gut, A.*, personal communication, 2000].

Simulated soil gross mineralization and NO emissions were a factor 3 and 6 respectively lower at FNS than those at RBJ (Fig. 2.7 & 2.8). Results also showed no difference between dry and wet seasonal NO fluxes for FNS, but did exhibit a similar transition season pattern to RBJ. NO emissions at FNS were higher during the transition seasons (April and September) when soil moisture and gross mineralization made for optimal soil NO production and emission conditions. After a period of low precipitation during April and May 1999, NO fluxes were elevated three fold with the onset of rains in September. Thereafter, although gross mineralization increased slightly in the latter half of the year (Fig. 2.8(a)), NO emissions declined due to wetter soil conditions with the resumption of rains at FNS (Fig. 2.8(b)).

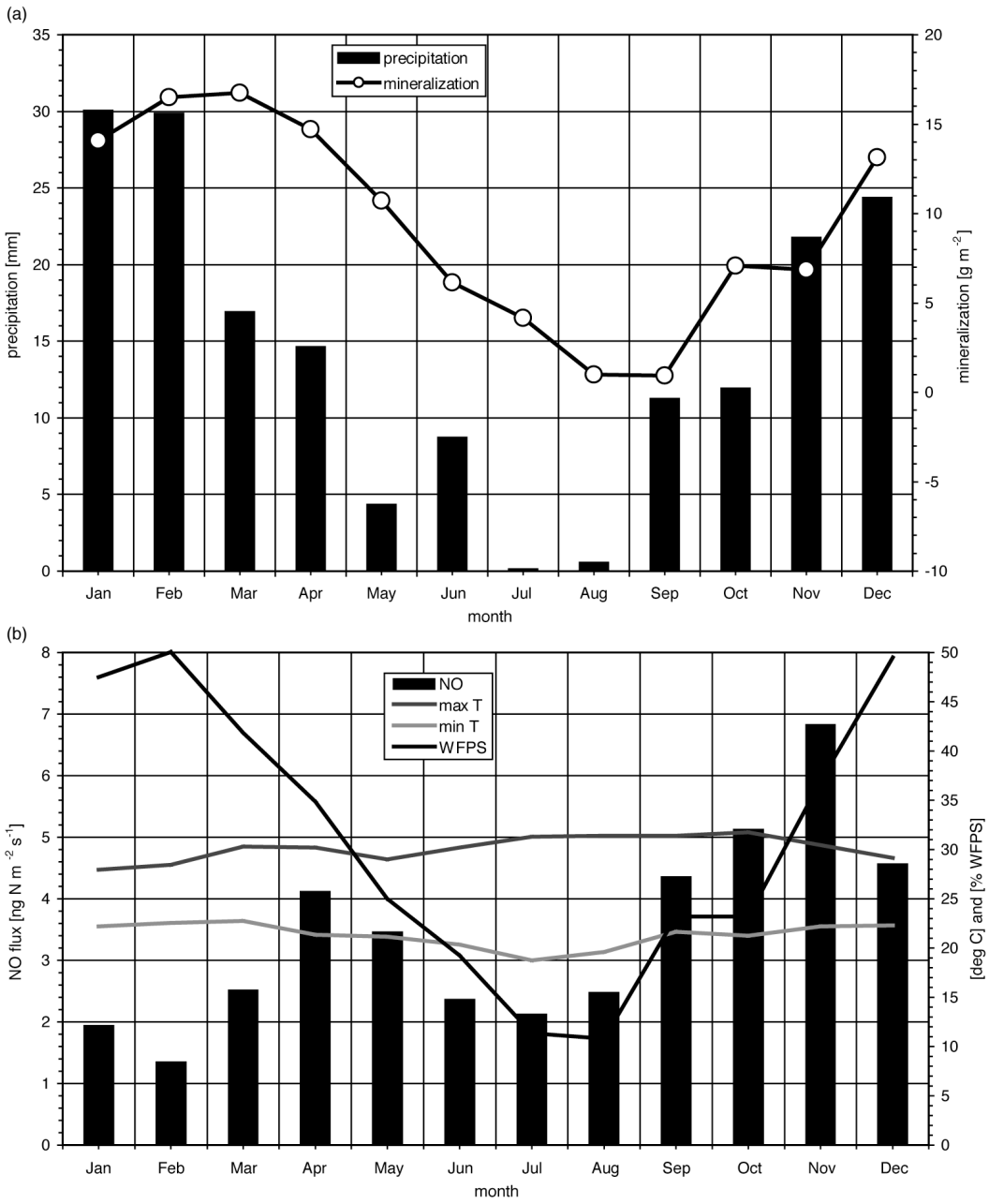

Figure 2.7 Mean monthly (a) precipitation for 1999 (mm), gross mineralization (g m^{-2}), (b) NO flux (ng N m^{-2} s^{-1}), soil minimum/maximum temperature (°C) and WFPS (%) for RBJ.

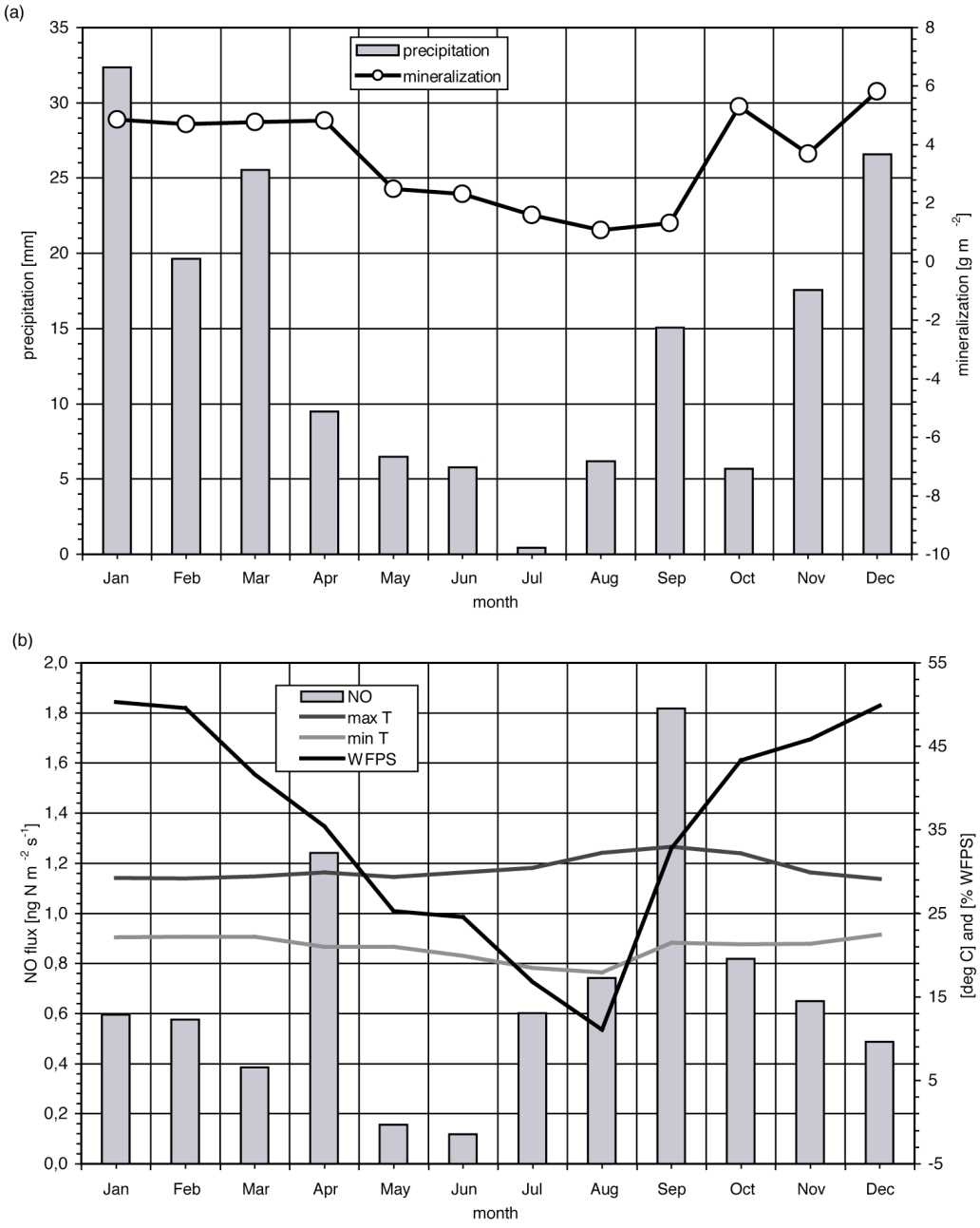

Figure 2.8 Mean monthly (a) precipitation for 1999 (mm), gross mineralization (g m^{-2}), (b) NO flux (ng N m^{-2} s^{-1}), soil minimum/maximum temperature (°C) and WFPS (%) for FNS.

2.7.2 Land-use change

Figure 2.9 illustrates the course of land-use events from rainforest (RBJ) to pasture (FNS) over a 27 year period. The figure 2.9(a) shows the simulated effect of primary forest, a slash and burn event, two years of cropping and fire, 12 years of grazed pasture and biannual burn, one plough and crop year, and then 8 years of grazed pasture on annual mean NO flux rates (ng N m^{-2} s^{-1}). Figure 2.9(b) includes a similar representation of these effects on soil inorganic nitrogen concentrations (μg g^{-1} d^{-1}) for the same period.

Results show that the change in biomass cover (land-use), which effectively reduced above ground annual C and N stocks to 1% and 2 % of the initial forest, respectively and below ground stocks to 13 %, was sufficient to affect a factor 6 reduction in mean annual soil NO flux rates from 4.2 ng N m^{-2} s^{-1} for the forest to 0.68 ng N m^{-2} s^{-1} for the pasture (Fig. 2.9(a)). The soil inorganic nitrogen concentrations (NO_3^- and NH_4^+) (Fig. 2.9(b)) first showed a sharp increase soon after deforestation and then declined during the initial period of cropping to gain somewhat during the first grazing period. It then declined steadily, after the plough event, to year 22 and beyond. The eventual decline in simulated soil inorganic nitrogen concentrations and consequently NO fluxes was the compound effect of the decline in nitrogen inputs from grass litterfall, the removal of nitrogen due to harvesting and grazing (Table. B4, Appendix B), and the gradual depletion of the original forest passive and labile soil nitrogen stocks. Clearly land-use and age since deforestation, which governs soil nitrogen, plays a determining role in the magnitude of NO fluxes. Results also show a notable increase soil NO_3^- concentrations and NO emissions for a short period soon after deforestation.

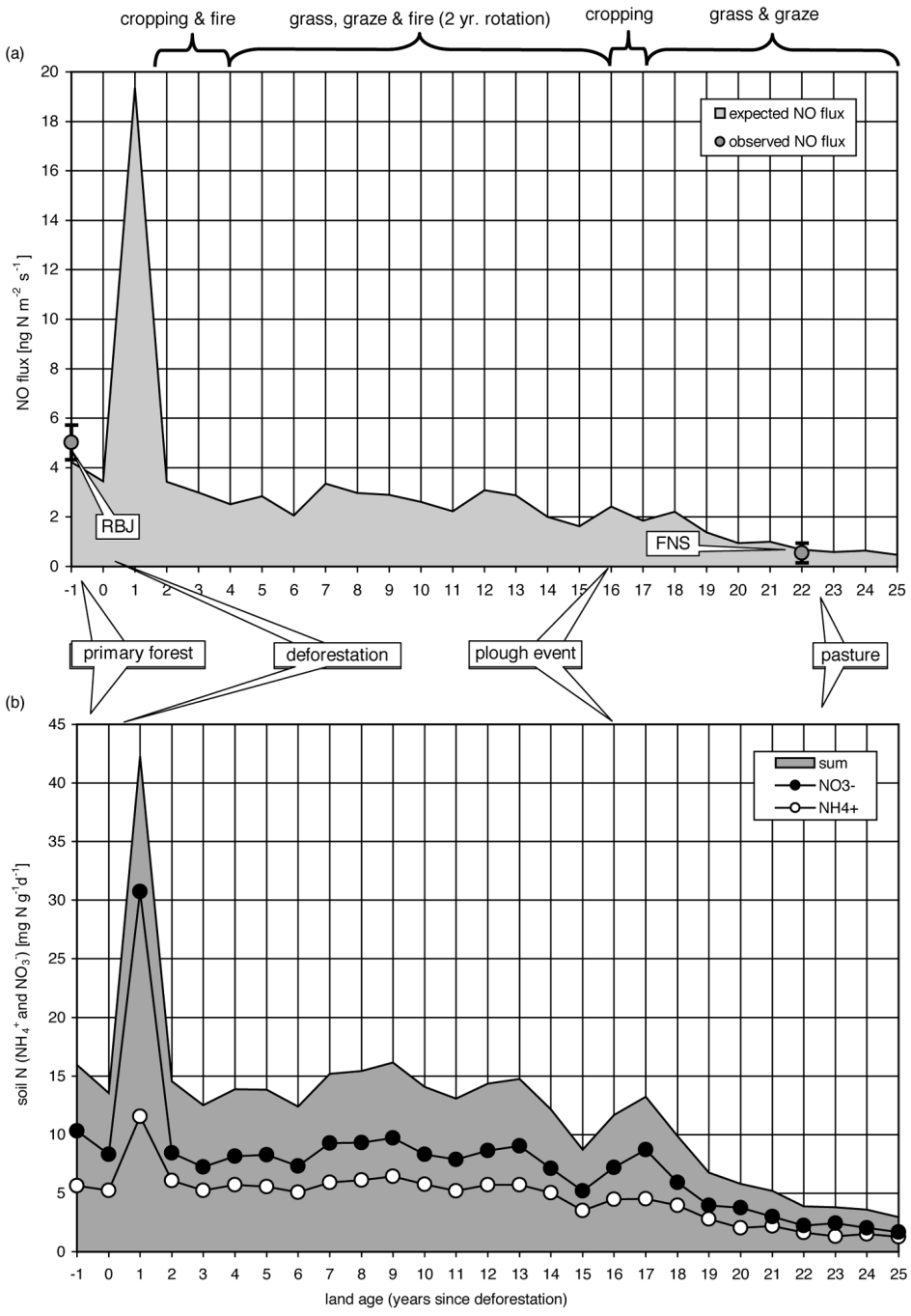

Figure 2.9 The modeled (a) mean annual NO flux (ng N m^{-2} s^{-1}) according to the FNS land use chronology, (b) mean annual soil nitrogen (NO_3^- and NH_4^+ and sum) concentration (μg g^{-1} d^{-1}).

2.7.3 Slash and burn pulse

Studies in Rondônia have shown that soil inorganic nitrogen (NO_3^- and NH_4^+) concentrations remain elevated after deforestation, and persist for as long as it takes for vegetation to re-establish and function as a nitrogen sink again [*Neill et al.*, 1997, 1999]. In tropical forest ecosystems this period has been shown to range from a few months [*Weitz et al.*, 1998] to several years [*Matson & Vitousek*, 1987; *Uhl & Jordan*, 1984]. These elevated soil nitrogen concentrations are only evident sometime after the burn (±1.5 months), and are probably due to the fire sterilization of the top horizon the soil [*Kauffman et al.*, 1995; *Lessa et al.*, 1996; *Neill et al.*, 1999]. This phenomenon may be responsible for elevated NO fluxes that have been observed after fire events [*Weitz et al.*, 1998; *Poth et al.*, 1995] sometimes lasting for between 4–6 months and resulting in up to a six fold increase in NO emissions [*Verchot et al.*, 1999].

Model results indicated a similar pattern due to forest slash and burning, with a four-fold increase in total soil nitrogen and significant changes in soil NO_3^-, lasting approximately one month, at which time soil organic matter mineralization and nitrification was enhanced (Fig. 2.9(b)). This resulted in NO fluxes, which were 19 fold greater than an equivalent non-burn year, lasting for a period of 2.5 months. It is evident that N-flow through the *"pipe"* was accelerated after the slash and burn event. The elevated soil NO_3^- concentrations were due to the sudden and dramatic disappearance of the plant biomass N-sink, resulting in a temporary accumulation of soil NO_3^- complemented by nitrogen additions from the ash (1.7 % N returned to the soil, cf. Table B4, cf. Appendix B). Ash additions have been shown to increase pH, available nitrogen as well as P, K, Ca, Mg and decrease exchangeable Al in soils [*Seubert et al.*, 1977; *Sanchez et al.*, 1983].

Elevated NO emissions soon after deforestation, similar to those above, have been reported by *Liu et al.*, [1999] in simulations of Costa Rican forest soils. Immediately after burning short term peaks of NO were observed in field measurements in Costa Rica [*Weitz et al.*, 1998] and Parã (Brazil) [*Verchot et al.*, 1999] and were attributed by to the decomposition of high concentrations of NO_2^- in the ashes [*Neff et al.*, 1995] and chemodenitrification [*Verchot et al.*, 1999]. At present no work exists on the explicit cause of these pulses (cf. Future model improvements, Section 2.9). The short-term effect of slash and burning on soil NO emissions is assumed to stem from purely enhanced biotic soil processes (nitrification and denitrification) in this model study and has been termed the "slash-and-burn-pulse" (S+B-pulse).

2.8 Discussion

The DAYCENT plant-soil ecosystem model was modified and successfully used to simulate a tropical ecosystem in order to study the effects of land-use change on soil NO emissions in Rondônia, Brazil. The model was initialized with soil, plant and climatic conditions from a previously studied primary rainforest and optimized to reproduce measured soil NO fluxes at this site. By supplying the model with a land-use practice chronology it was also successfully applied to predict soil NO fluxes measured at a 22-year-old pasture in Rondônia. The combined effect of forest cutting and burning, two years of cropping and fire, 12 years grazed pasture and a biannual burn, one plough and crop year, and then eight years of grazed pasture was to significantly reduce original forest C and N stocks and cycling. These changes resulted in a reduction in mean annual soil NO fluxes from the forest to the 22 year old pasture by a factor 6. In addition the cutting and burning of the forest biomass resulted in a 19 fold increase in emissions for a 2.5-month period after slash and burning. Model NO flux simulations also revealed increased fluxes during the transition seasons (from dry to wet), when soil moisture conditions were optimum for NO gas emissions for both the forest and the pasture.

As first suggested by *Keller et al.* [1993], *Neill et al.* [1997], and observed in recent work in the tropics by *Erickson et al.* [2001], land-use, which governs the magnitude and turnover of soil N-stocks and cycling and therefore NO emissions may be more important as predictors in the tropics than those conventionally used in temperate environments such as soil- physics and climate [*Yienger & Levy*, 1995, *Ludwig et al.*, 2001]. Model optimization revealed that land-use change, soil moisture, and nitrogen fixation/deposition, in that order, were the largest determinants of soil NO fluxes for both the RBJ and FNS ecosystems. Firstly (a) land-use change was responsible for the magnitude change in soil NO flux between the primary forest and the pasture, (b) soil moisture produced a measure of seasonality with differences between transition seasons, and (c) symbiotic, non-symbiotic N-fixation and atmospheric N-deposition determined the intra-seasonal variance in the fluxes.

As agriculture comes to dominate deforested regions of the Amazon, such as in the case of Rondônia, soil nitrogen inputs and transformation rates are expected to decline and thereby decrease overall soil NO emissions. The low annual NO emissions observed on old Amazonian pastures [Chapter 1, this Chapter] on a single point (1-D) basis, adds weight to the claim that the conversion of tropical forest to agriculture may not cause a significant increase in the contribution of nitrogen trace gases from tropical soils to the troposphere in the long term [*Keller et al.*, 1993]. Model simulations do however suggest that in the short to medium term, as land undergoes conversion to agriculture, episodes of high NO

emissions soon after deforestation (S+B pulses) may contribute significantly to annual soil emitted NO. This may have important implications for tropical tropospheric chemistry at the regional scale. In addition, emissions at regional scales are governed by the combined influences of land-use change, land age and the effects of canopy reduction on NO for many thousands of points at various stages of evolution. This effect is spatio-temporally investigated further in Chapter 3.

2.9 Future model improvements

Several studies have indicated the importance of the non-symbiotic contributions from faunae biomass such as termites, ants, and earthworms, which have been shown to produce casts with NH_4^+ levels an order of magnitude higher than the surrounding soil [*Decaens et al.*, 1999]. Future improvements to the model might include an improved non-symbiotic and atmospheric N-fixation scheme, which is not dependent on rainfall and takes account of sources other than canopy flora or wet deposition. [*Cleveland et al.*, 1999].

The significance of dry deposition of nitrogen species (HNO_3, NH_4, PAN and NO_x) either through the plant stomata/cuticle, onto the soil surface or via aqueous phase surface chemistry has been highlighted in chapter 1. These sources are presently not accounted for in the model. The model also requires an improved representation of wet and dry deposition such that during prolonged precipitation events (wet season) nutrient dilution can occur or during dry spells nitrogen dry deposition can continue to take place.

Recently suggestions that a partial decoupling of nitrogen cycling occurs in the soil after slash and burning (e.g. due to microbial sterilization) has been proposed as the cause for the S+B NO pulse observed in field measurements [*Neff et al.*, 1995; *Verchot et al.*, 1999; *Weitz, et al.*, 1998; *Keller, M.*, personal communication, 2000] (cf. Section 2.7.3). The decoupling of the nitrogen cycle would indicate an abiotic (chemodenitrification) NO production process rather than the obligatory biotic nitrification or denitrification processes used in the model. Chemodenitrification is also well known to be more prevalent under acid soil conditions [*Conrad*, 1995], but very few measurements exist at present in order to improve model concepts.

Preliminary work in this field has been undertaken by *Trebs & Kirkman* [unpublished data, 2001]. Where soils from RBJ were Gamma irradiated at 50 kGy day^{-1} in order to kill all microbial life (as confirmed by a lack of CO_2 production for 3 weeks after irradiation). Laboratory incubations at various soil moisture contents revealed that abiotic NO production accounted for up to 50 % of the total NO produced by these soils [*Trebs & Kirkman*, unpublished data,

2001]. These initial results suggest that a significant portion of the NO production is due to chemodenitrification. If in the natural environment, these soils are temporarily sterilized (e.g. after burning) and available soil nitrogen increases due to the removal of the plant nitrogen sink, this could result in significant abiotic soil NO emissions.

C h a p t e r 3

REGIONAL UP SCALING OF SOIL NO EMISSIONS IN RONDÔNIA

The quantification of soil NO emissions from a tropical forest-nonforest region is essentially a spatio-temporal problem requiring a knowledge of the emissions from forests, pastures and secondary growth, as well as the magnitude and duration of NO emissions that occur in the period immediately following forest clearing. An ecosystem model and satellite data were used in an up scaling scheme to estimate soil NO emissions for a 26,455 km^2 area of Rondônia for 1999. In order to account for the inherent spatio-temporality of soil NO emissions the scheme used the "time elapsed since primary forest deforestation" (or land age) as a link between NO emissions that occur at small temporal scales and land-use at the spatial scale. Results showed that this nested hierarchical approach to up scaling corresponded well with flux inventory-based estimates of regional soil NO emissions. Net soil NO emissions for the region in Rondônia contributed approximately 1.3 Gg N-NO to the regional tropospheric NO budget during 1999. A significant portion of these soil emissions came from pastures (0.71 Gg N-NO) and the period immediately following forest clearing (23 %). These first tropical spatio-temporal NO emission estimates indicated that the soils of this region remain a significant source of NO and have increased since development in the region first started. The soil source of NO is expected to continue to play an important role in tropospheric NO_x chemistry as long as primary forests continue to be cleared.

3.1 Background

The regional estimation of the soil emitted trace gas nitric oxide (NO) is complicated. Variations in soil atmosphere fluxes brought about by differences in climate, soil conditions and land-use change result in perturbations in local and regional atmospheric concentrations at a range of spatial and temporal scales. These scales range from soil microbial processes, which vary within a few centimeters at the soil surface, to seasonal and annual changes in climate and land-use. Therefore regional estimates of soil NO emissions are only possible by resorting to some form of spatial extrapolation [*Stewart et al.*, 1989]. The simplest approach would be to sample an area randomly and then compute the product of the sample mean and area. An improvement on this might be to sample strategically, based on a particular stratification system, such as land-use or soil type. Because trace gas fluxes are highly variable in time and space, stratification becomes complex and the number of samples required to achieve an estimate

with an acceptable level of error becomes prohibitively large [*Folorunso & Rolston*, 1984]. In addition, field sampling experiments are expensive and time consuming; hence, alternative approaches are required to provide reasonable estimates of regional soil NO fluxes. One such alternative is the use of a hierarchical up scaling framework, which estimates regional NO emissions using parameters that control soil NO emissions at the small scale, nested within a regional scale land-use database [*Matson et al.*, 1989].

The primary objective of this study was to estimate soil NO contributions to the regional tropospheric NO budget from a 26,455 km^2 area in the Brazilian state of Rondônia (Fig. 3.1) during 1999. Time elapsed since deforestation (land age) was used as a common denominator, combining both spatial and temporal soil NO emission predictors at different scales, to accomplish this. Comparisons were made between the relative contributions of the three predominant land-use classes (forest, pasture and secondary growth) and several land age classes (0–22 yrs.) in the region. These up scaled estimates were also compared against existing soil NO flux source inventories for the tropics [*Davidson & Kingerlee*, 1997]. These objectives were achieved using simulated NO flux data from an ecosystem model [Chapter 2] in combination with satellite data acquired over Rondônia.

3.2 Approach

In areas where land-use change is prevalent and occurs with devastating effect, due consideration of current and past land-use is essential for spatial NO emission extrapolation studies. Significant evidence exists to suggest that land-use in the tropics influences climate, biomass composition, soil properties and, thereby, the soil emission of NO [*Erickson et al.*, 2001]. This was demonstrated in chapter 2, where a 1-D ecosystem model was used to simulate the effects of land-use change on soil NO fluxes in Rondônia. The model was also used to generate an annual time series of NO emission estimates for a primary forest through to a 22 year old pasture, based on only two field measurements conducted during the LBA-EUSTACH campaigns [Chapter 2].

Model results [Chapter 2], corroborated by the literature, showed that at annual time scales, soil NO emissions are positively related to the time elapsed since deforestation (land age), with older lands producing less NO than forests and recently deforested areas [*Neill et al.*, 1995; 1997; 1999; *Verchot et al*, 1999; *Veldkamp et al.*, 1999]. Land age (yrs.) offers a useful means of spatially extrapolating NO flux measurements and, therefore, formed the basis of the up scaling approach used in this study.

Figure 3.1 Land-use age (0-22 years) based on ten LANDSAT TM scenes of path 231, row 067 (WRSII) in the state of Rondônia, Brazil [*Roberts et al.*, submitted, 2001].

Quantifying the contribution of soil NO emissions to the regional tropospheric NO budget also requires a top-of-canopy approach, as (bulk) soil NO emissions may be chemically converted to NO_2 by reaction with O_3 and deposited onto/into leaf surfaces within a forest canopy [*Jacob & Bakwin*, 1991; *Ammann et al.*, submitted, 2001]. As a result, not all NO emitted from soils may be considered a source to the atmosphere. This effect is termed the "canopy reduction factor" (CRF) and has been shown to be significant in reducing soil derived NO emissions from tropical forest ecosystems. Estimates of the CRF range from a value of 80 % proposed by *Bakwin et al.* [1990a, 1990b], 75 % estimated by *Jacob & Wofsy* [1990] and *Jacob & Bakwin* [1991], to 60 % calculated by *Yienger & Levy*, [1995] and *Davidson & Kingerlee* [1997]. Similar results have

been observed at RBJ during the dry-wet season by *Ammann et al.* [submitted, 2001] and *Rummel et al.*, [submitted, 2001].

3.2.1 Regional emissions

A nested hierarchical up scaling approach was adopted for the study area in Rondônia, which was equivalent to the area of a LANDSAT TM scene (26,455 km^2). This approach made use of mean annual model-generated soil NO emissions (encompassing parameters that control trace gas fluxes, cf. Chapter 2), a map of land age (spanning 23 yrs.) derived from 30 m (pixel) resolution satellite data [*Roberts et al.*, submitted, 2001] and CRF data derived from satellite-based leaf area index data (LAI) (cf. Section 3.3). The net annual soil NO emission estimate (Gg N-NO) for the 26,455 km^2 study area for the year 1999 was, therefore, the sum product of bulk NO emissions and CRF for pixels $i = 1$ to n such that,

$$F_{net} = \sum_{i=1}^{n} (F_{bulk,i}\, A_i\, CRF) \tag{3.1}$$

where A_i is the pixel area (900 m^2) and the bulk NO emission (ng N m^{-2} s^{-1}) per pixel i is equivalent to,

$$F_{bulk,i} = 4.3175\ e^{\,-0.0657\ t_i} \qquad (r^2 = 0.9) \tag{3.2}$$

where t_i represents the age of pixel i from 0 (forest) to 22 yrs (established pasture). $F_{bulk,i}$ was obtained by fitting an exponential function to a total of 52 years of simulated forest and non-forest data using the model in chapter 2. Equation (3.2) was obtained by running the model with the land-use chronology of the pasture *Fazenda Nossa Senhora* (FNS) in Rondônia [cf. Chapter 2]. This chronology, comprised of a forested period, deforestation followed by cropping, and then ploughing and grazing of permanent pasture, was assumed to be a typical land-use sequence for the study region.

Finally, an ecosystem dependent CRF algorithm from *Yienger & Levy*, [1995] was used to approximate the reduction of soil NO emissions within the canopy due to chemical and deposition processes. The algorithm, used to produce a set of CRF values between 0 and 1 is described by,

$$CRF = [\ e^{\,-(8.75\ SAI)}\ ] + [\ e^{\,(0.24\,LAI)}\ ] \,/\, 2 \tag{3.3}$$

where SAI is the stomatal area index representing the relative area of stomata to the leaf area (m^2 m^{-2}), and LAI is the leaf area index (m^2 m^{-2}) for three land-use classes—pasture, forest and secondary growth (2^{nd} growth).

3.2.2 Emissions by land class

In addition, soil NO emission estimates based on the three most predominant land-use classes in Rondônia (pasture, forest and 2nd growth) were derived. The most prevalent style of land-use type in Rondônia has been shown to be pasture [*Browder*, 1994], which comprised 37.2 % of the non-urban study area in 1999. This land-use class included all areas dominated by grass species (*Brachiaria brizantha* and *Panicum maximum*) and ranged in quality from highly degraded to well-managed pastures. The most dominant natural vegetation type was primary upland forest, which comprised 55.1 % of the study area. The third and smallest class was 2nd growth (7.8 %), comprising vegetation of low species diversity and biomass relative to the primary forest. Secondary growth typically occurs on pastures after abandonment, or primary forest after anthropogenic or natural disturbance if abandoned.

The mean annual bulk soil NO emissions for the three land-use classes were calculated according to the equation,

$$F_{class} = \sum_{i=1}^{n} \left(F_{bulk,i} A_i \delta_{l_i\, class} \right) \qquad \delta_{l_i\, class} = \begin{cases} 0 \text{ for } l_i \neq class \\ 1 \text{ for } l_i = class \end{cases} \tag{3.4}$$

where $F_{bulk,j}$ follows from eq. (3.2), A_j is the pixel area (900 m^2) of l_i, which is the land-use of pixel *i* belonging to the *class* forest, pasture or 2nd growth from a satellite-based land-use class map (cf. Section 3.3).

3.3 Data

In order to up scale simulated soil NO emissions in Rondônia to a regional net NO emissions estimate covering 26,455 km^2 (Fig. 3.1), four datasets were used. These were:

a) A land age map describing time elapsed from 0 (forest) to 22 years since deforestation, which was based on a multi-stage linear mixture analysis (sub-pixel classification) of ten years (1978, 1986–1990, 1992, 1993 and 1996–1999) of LANDSAT scene path 231, row 067 [*Roberts et al.*, 1998; *Roberts et al.*, submitted, 2001] (Fig. 3.1).

b) A land-use map comprising the land classes forest, pasture and 2nd growth from a LANDSAT scene acquired on 8 June 1999 and classified (cf. above) by *Roberts et al.* [submitted, 2001].

c) A leaf area index (LAI) ($m^2\ m^{-2}$) map, which was sourced from the MODIS (Moderate Resolution Imaging Spectrometer) instrument on board the NASA *Terra* platform [*Myneni et al.*, 2000]. Due to the paucity of cloud-free data from this source, an average LAI map was created from four 1 km resolution MODIS scenes recorded during July and August 2000. The LAI map was verified against field measurements of LAI conducted during 1999 [*Kirkman*, *G.A.*, unpublished data, 1999] and found to be acceptable (<10 % difference).

d) Mean stomatal area index (SAI) values for forest (0.030 $m^2\ m^{-2}$), pasture (0.006 $m^2\ m^{-2}$) and 2nd growth (0.012 $m^2\ m^{-2}$) were sourced from *Larcher* [1994].

3.4 Method

This section outlines the creation of the map datasets required to generate the up scaled soil NO emission estimates.

3.4.1 Bulk emissions

A bulk NO emissions map was generated by utilizing the land age map (a) (cf. Section 3.3) in eq. (3.2) using the ARC/INFO® GRID geographic information system (ESRI Inc., Redlands, USA). In order to appraise the impact of elevated emissions that occur on recently deforested land (cf. Chapter 2) on regional soil NO emissions, two emission scenarios were investigated. The first scenario (1) assumed that all recently deforested land (1-year old) exhibited a period of elevated NO emissions for 2 months of the year in accordance with the slash-and-burn pulse (S+B pulse) simulated by the model [Chapter 2]. This equated to approximately a 4 fold annual increase in NO flux for the 1-year old lands, which was more than twice as large as first proposed by *Yienger & Levy* [1995]. The second scenario (2) excluded the S+B-pulse and represented the case where this effect on regional NO emissions during 1999 was negligible. In addition these scenarios were run with and without the inclusion of a CRF in order to facilitate comparison with other methods that do not take CRF into account.

3.4.2 Canopy reduction factor (CRF)

The CRF for 1999 was created by implementing eq. (3.3) within ARC/INFO® GRID and making use of the SAI data (cf. Section 3.3 (d)) for the three land-use classes and the LAI map data (cf. Section 3.3 (c)), which was averaged by land class using the land-use map (cf. Section 3.3 (b)). This generated CRF´s of 0.227, 0.744 and 0.554 for the forest, pasture and 2nd growth land-use classes,

respectively. These factors were then used to adjust the bulk NO flux map based on land class to a net ecosystem, or top-of-canopy, NO flux map for 1999.

3.5 Results

The 26,455 km^2 study area in Rondônia had been subject to an average deforestation rate of ca. 2.35 % between 1978 and 1999 and in June 1999 approximately 54.2 % of the area was covered by primary rainforest, with 36 % pasture and 8 % covered by 2nd growth [*Roberts et al.*, submitted, 2001]. Results of NO emissions up scaling are presented in the section below.

3.5.1 NO emissions by land age class

The total and relative contributions of each land age class (0–22 yrs.) to net soil NO emissions (incl. S+B pulse) from the 26,455 km^2 study region of Rondônia are presented in figure 3.2(a) as a pie chart and values are listed in table C1. Despite a high CRF and a declining spatial coverage, the primary forest soils produced 0.42 Gg of NO, the highest of all land age classes, during 1999. The second most significant age class for this region was the 1-year old lands contributing a total of 0.32 Gg N-NO. This was followed by 4-year old (0.14 Gg N-NO) and 14-year old lands (0.12 Gg N-NO). Clearing of the forest (S+B pulse) contributed ca. 23 % to regional soil NO emissions during 1999 (Table C1). The S+B pulse signifies a potentially important short term source of soil-emitted NO, which has been overlooked in previous studies of the tropics.

3.5.2 NO emissions by regional land-use class

The entire study area contributed a total of 1.3 Gg of soil-emitted NO to the regional troposphere during 1999 (0.49 kg N $ha^{-1}yr^{-1}$). The largest proportion (68 %) of this flux came from non-forested lands (1–22 yrs.), totaling 0.88 Gg N-NO, with the balance from forests (Table C2, cf. Appendix C). Within the non-forested land group, the largest land class contribution, of 0.71 Gg N-NO, was from the pastures (Table C2; Fig 3.2(b)), at a mean flux rate of 0.72 kg N $ha^{-1}yr^{-1}$. Secondary growth, which contributed the least to soil NO from the study area, exhibited the highest emission rate (0.85 kg N $ha^{-1}yr^{-1}$) of all three land-use classes with (Table C2, cf. Appendix C). This was due to the large amount of 2nd growth clearing that took place in 1999, resulting in S+B pulse emission contributions from this land-use class [*Roberts et al.*, submitted, 2001].

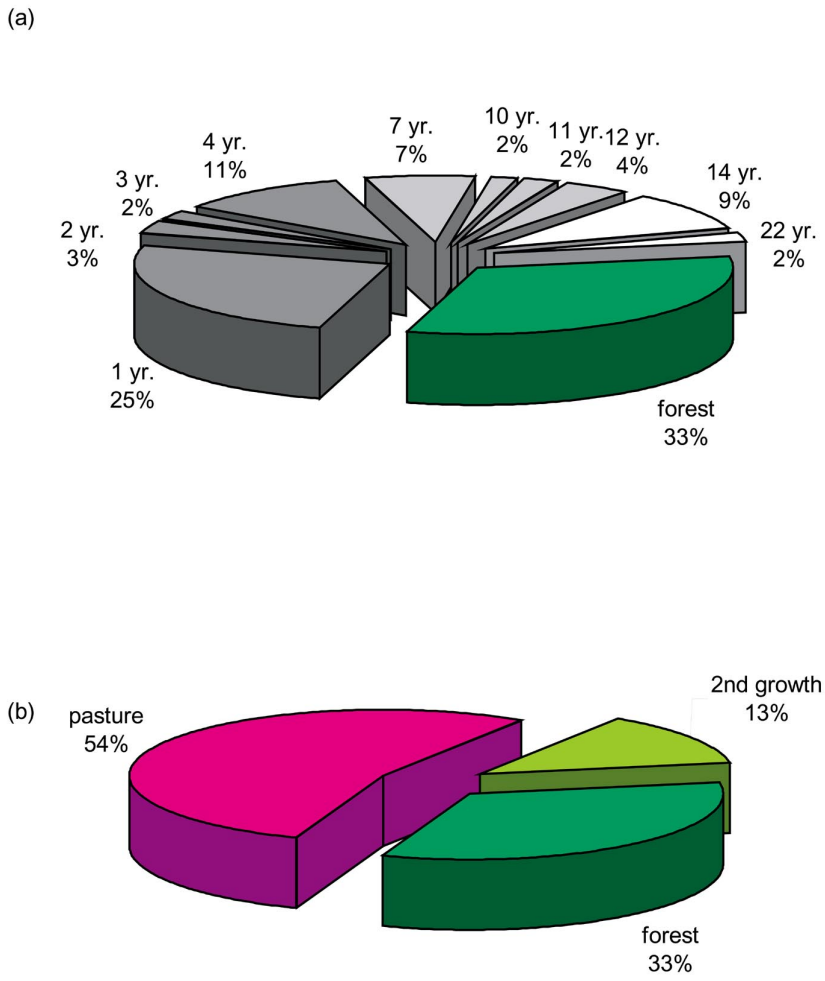

Figure 3.2 The percentage contribution per (a) land age class (forest–22 yrs.) and (b) land-use class to total regional soil NO emissions from a 26,455 km^2 area of Rondônia for 1999.

The forest land class exhibited the lowest net emission rate of all land-use classes at 0.3 kg N ha^{-1}yr^{-1} for 1999. It seems reasonable to assume that at one point in history before human settlement ca. 100 % of the study area was covered with forest. Assuming climatic and biomass conditions similar to present, this would mean that ca. 0.82 Gg of net soil NO would have been emitted per year according to this study. The soil NO emission estimate for 1999 therefore indicates a 60 % increase in NO emissions from the region since pre-anthropogenic time. If the S+B pulse is excluded, a 30 % increase is estimated.

3.5.3 NO emissions by global land-use class

In order to make comparisons with an inventory-based spatial extrapolation method [*Davidson & Kingerlee*, 1997], soil NO emission rates (excluding CRF) were scaled up to the areas described by three global tropical ecosystems in *Davidson & Kingerlee* [1997] and compared with their bulk emission estimates. This assumed that land-use and emissions in Rondônia during 1999 were representative for the entire tropical globe. Global NO emission rates [Tg N yr^{-1}] for forest, pasture and 2nd growth are presented in table C3. Emission rates for the land-use class "tropical fields/2° forests" in *Davidson & Kingerlee* [1997] were assumed to represent pastures and 2nd growth and their emission rates were assumed identical and global areas proportional.

The forest estimates (1.34 Tg N yr^{-1}) agreed reasonably with the inventory estimates (1.10 Tg N yr^{-1}), but the pasture land class showed a factor of two difference between the scaled (0.15 Tg N yr^{-1}) and inventory estimates (0.27 Tg N yr^{-1}). This can be attributed to the predominance of field measurements on fertilized fields used by *Davidson & Kingerlee* [1997] in their inventory estimate for pastures (tropical fields), which results in higher average soil NO emissions. The model [Chapter 2] and this study did not consider agricultural soil N-fertilization, due to the paucity of data on fertilizer rates and usage in Rondônia. Total global tropical ecosystem bulk soil NO emissions derived from the up scaling (1.71 Tg N yr^{-1}) and inventory (1.64 Tg N yr^{-1}) methods showed reasonable agreement.

3.6 Summary and Conclusion

Reliable prediction of regional net soil NO emissions requires a detailed knowledge of current and previous land-use patterns, plant-soil ecosystem interactions and in-canopy processes at reasonable spatial scales. This study has indicated that even with a limited number of field measurements, this approach can be used to produce estimates of soil NO emissions that agree reasonably with previous assessments of tropical regions [*Davidson & Kingerlee*, 1997]. The interplay between factors governing soil NO emissions at disparate scales was resolved by linking a proven ecosystem model [Chapter 2], reflecting current knowledge on NO soil emission processes, and a high resolution satellite database of land age by a common denominator—"time elapsed since deforestation". This common denominator has been shown to be a useful predictor of soil NO emissions in the tropics as old lands generally produce less soil NO than forests. This nested hierarchal approach to up scaling provided a first estimate of ecosystem-wide soil NO emissions based on land-use and land-use history for a 26,455 km^2 area of Rondônia.

Soils of the study area contributed a total of 1.3 Gg N-NO to the regional tropospheric NO budget. The largest contribution to net soil NO emissions came from the non-forested areas, which produced 0.88 Gg N-NO. Of this, approximately 80 %, or 0.71 Gg N-NO, were from pastures and 0.42 Gg N-NO were from forests within the study area. The 2nd growth land class contributed the least (0.17 Gg N-NO) to the regional NO budget, but exhibited the highest emission rate (0.85 kg N $ha^{-1}yr^{-1}$) of all three land classes. The slash and burning of 2nd growth was the highest in ten years during 1999 [*Roberts et al.*, submitted, 2001]. The clearing of land results in a temporary pulse of NO known as the S+B pulse, which is observed soon after deforestation [Chapter 2]. This effect contributed ca. 23 % to annual regional tropospheric NO concentrations and was the reason for the high emission rates observed for the 2nd growth land class.

It may be expected that as increasingly more areas of the tropics are deforested and put to agriculture, the combined effects of slower soil nitrogen cycling [cf. Chapter 2] on aged soils and, thereby, lower soil NO emissions might cause the combined contribution of NO from tropical soils to decline over time [*Keller et al.*, 1993]. This first attempt to combine the spatio-temporal effects of land age, land-use and CRF suggests that this may not be the case for a 26,455 km^2 area of Rondônia. Annual net soil NO emissions have been shown to be larger than when pristine forests covered the entire study region. This is a departure from the premise that soil in tropical regions might be a gradually declining source of nitrogen trace gases [*Keller et al.*, 1993]. Indicating instead that they may remain a significant source as they undergo anthropogenic change [*Johansson et al.*, 1988]. Further work is required in this region to substantiate this claim through studies based on a thorough appraisal of land-use and land-use history.

C h a p t e r 4

SOIL NO EMISSIONS OF ZIMBABWE

A mechanistic up scaling scheme was developed to estimate temporal nitric oxide (NO) emissions from soils for three distinct land-use classes by spatial extrapolation of laboratory measurements for Zimbabwe (383 667 km^2). Laboratory measurements on miombo woodland, grassland and agricultural Zimbabwean soils were used to derive moisture- and temperature-dependent NO emission algorithms. By combining monthly fields of modeled soil moisture and temperature (based on climate means, vegetation indices, soil and terrain elevation data), a mean monthly soil NO flux, including rainfall induced elevated flux events (pulsing), was obtained. Countrywide emission rates ranged from 0.1–0.4 ng N m^{-2} s^{-1} for the dry season to wet season mean fluxes of 3.7–9.4 ng N m^{-2} s^{-1} for miombo, 4.4–7.0 ng N m^{-2} s^{-1} for grassland and 4.6–10.9 ng N m^{-2} s^{-1} for agriculture. Annual net soil NO emissions (less canopy reduction) for Zimbabwe were 32.9 Gg N yr^{-1} with miombo woodlands (66 % of Zimbabwe) contributing 63 % to the regional NO budget. Rainfall induced NO pulsing contributed an additional 14 % to countrywide annual bulk NO emissions. The majority of these pulses occurred during the first half of the rainy season (November–December) with agricultural soils contributing the most and grassland soils the least to pulsing. The up scaling approach provided a first countrywide estimate of spatio-temporal soil NO emissions for a hitherto largely unresolved source—the soil moisture limited African subtropical savannas.

4.1 Background

Nitric oxide and nitrogen dioxide (NO_x) controls and regulates a set of tropospheric trace gas chemistry reactions involving the hydroxyl radical (OH), ozone (O_3) and hydrocarbons [*Crutzen*, 1974, 1979; *Singh*, 1987] and is fundamental to the photochemical formation of nitric acid (HNO_3), a component of acid deposition [*Crutzen*, 1979].

Broad sources of NO_x from southern Africa include pyrogenic (bush/wildfires), anthropogenic (traffic, industry, domestic biomass burning), and soil biogenic (microbial) emissions. The annual flux rates of soil NO_x from tropical and subtropical savannas have been estimated to be approximately 10 ng N m^{-2} s^{-1} [*Johansson et al.*, 1988; *Levine et al.*, 1996; *Parsons et al.*, 1996; *Serça et al.*, 1998; *Yienger & Levy*, 1995; *Otter et al.*, 1999]. However emissions from soils have been shown to exhibit extreme spatial and temporal variability, even among replicates from

the same site, making estimates of their contribution to global NO_x budgets difficult [*Davidson & Kingerlee*, 1997]. On a countrywide scale, biogenic NO_x sources have been estimated for Zimbabwe at approximately 8.5 Gg N yr^{-1} by *Meixner et al.* [1997]. In contrast, pyrogenic sources for Zimbabwe are estimated to be around 19 Gg N yr^{-1} [*Scholes et al.*, 1996], while anthropogenic sources for Zimbabwe (which include domestic and fossil fuel consumption) are approximately 40 Gg N yr^{-1} [*Marufu*, 1999].

Microorganisms are responsible for most NO production and NO consumption processes in soils, which in turn determine the exchange of NO between soils and atmosphere. Control over these processes is predominantly exerted on the microscopic level, i.e. the level of microorganism metabolism [*Conrad*, 1996a]. However, in the context of areal NO emission estimates, higher levels of controls must be considered [*Meixner & Eugster*, 1999]. Soil moisture, temperature and nutrients are well-known controllers for microbial nitrification and denitrification; the most important processes of biogenic NO emission [*Williams et al.*, 1992b; *Remde et al.*, 1993; *Parsons et al.*, 1996; *Conrad*, 1996b]. These environmental variables are accessible for Zimbabwe and can be used for scaling up laboratory and field measurements of biogenic NO emission from African savanna soils.

To relate laboratory studies of soil biogenic NO emission to field NO flux measurements a conceptual model (G&J model) was first presented by *Galbally & Johansson* [1989]. This model, which does not consider any dependencies on environmental variables, was also used by *Remde et al.* [1993] to compare laboratory NO emission measurements with field measurements on identical soil samples, yielding results that agreed to within a factor of two. *Rudolph & Conrad* [1996] studied NO release rates in the laboratory using a model soil core and a layered soil profile and concluded that it is feasible to predict NO emission from soils using the G&J model.

Galbally & Johansson [1989], *Remde et al.* [1993], *Rudolph & Conrad* [1996] as well as *Yang & Meixner* [1997] have shown that the soil layer, which contributes to the production and consumption of NO, is limited to layers very close to the soil surface (max. 0–5 cm). Recent laboratory studies have further shown that NO emission rates (a) exhibit a consistent nonlinear relationship to soil moisture with a maximum around 15–20 % water-filled pore space (WFPS) and (b) increase exponentially with increasing soil temperature provided soil moisture is not limiting [*Johansson*, 1984; *Williams et al.*, 1987, 1988, 1992b; *Yang & Meixner*, 1997; *Otter et al.*, 1999] modified the G&J model for soil moisture and soil temperature dependencies. Furthermore, they showed that within the range of soil temperature and moisture conditions observed under Zimbabwean field conditions, NO laboratory fluxes of these soils reproduced the field NO fluxes to within 10–80 %. More recently, *Otter et al.* [1999] used this modified G&J model

to estimate NO emissions for a southern African savanna ecosystem using data from laboratory analyzed soil samples under varying environmental soil moisture and temperature conditions. Their field measurements showed significant agreement ($r^2 = 0.74$) with modeled values.

Previous regional estimates of NO_x have simply expanded measured or mean exchange rates by ecosystem area, thereby ignoring distal environmental control heterogeneity [*Williams, et al.*, 1992b]. Estimates have been further improved with the inclusion of various forms of biome stratification [*Matson & Vitousek*, 1990; *Yienger & Levy*, 1995]. More elaborate process based schemes—which include soil substrate, temperature, moisture and microbial turnover interactions at global ecosystem scales—offer the most representative approach to date [*Potter et al.*, 1996]. While complex schemes are useful on a global scale, a more simplified mechanistic approach, like the modified G&J model, is required to bridge the gap between the spatial and temporal scales of field measurements and the scales necessary for regional NO flux quantification. A mechanistic model is used in this study to provide an *ab initio* mean monthly approximation of biogenic NO flux for three land-use types (miombo, grassland and agriculture) comprising 98 % of Zimbabwe (383 667 km^2).

Zimbabwe consists of savanna and open woodland ecosystems with mixed agriculture and can be considered typical for subtropical savanna NO flux studies and estimation (Fig. 4.1). A NO scaling scheme was developed using a geo-database (grid based) of a mean monthly probability index of soil moisture and temperature for Zimbabwe based on satellite and weather station data. These data surfaces were then used to drive an empirically improved G&J model [*Yang & Meixner*, 1997] using laboratory NO emission parameters for Zimbabwean soils.

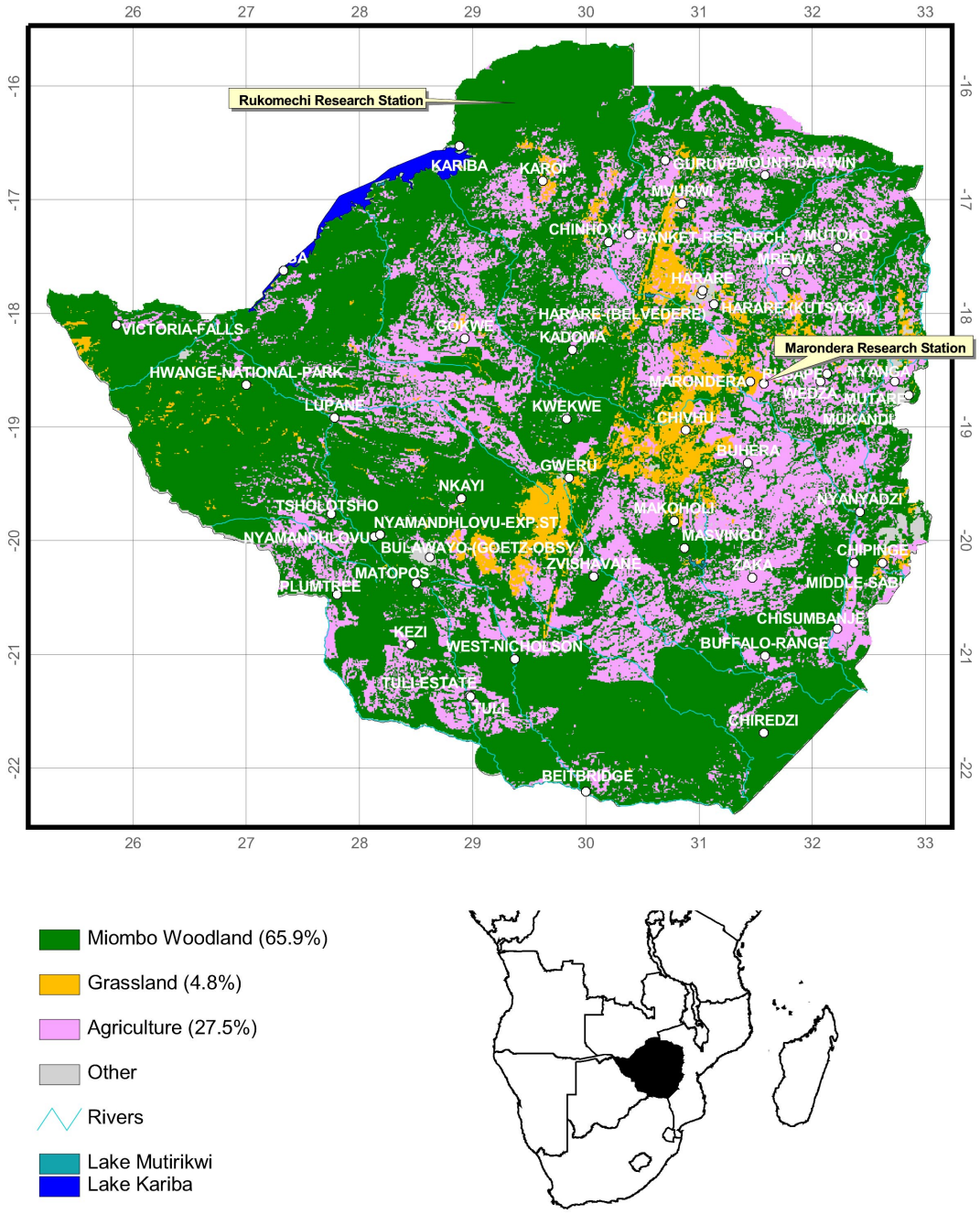

Figure 4.1 Location of meteorological stations, the two validation sites and land-use classification for Zimbabwe based on the VEGRIS database, courtesy of *RRSP*, Harare, Zimbabwe

4.2 Design and Methodology

The up scaling from laboratory measurements for Zimbabwe soils to mean monthly fields of NO flux at 1-km^2 resolution based on land-use type is based on the hypothesis that soil temperature and moisture are the primary large-scale controls on microbial production and consumption of NO in the subtropical savannas. Of these factors it is believed that topography, previously neglected in NO modeling efforts to date [*Meixner & Eugster*, 1999], is important in controlling NO emissions. Lower emissions are associated with shoulder or hilltops as compared with the footslope complex where the influence of topographically influenced water distribution and different textural content provides wetter average soil conditions and consequently higher soil emissions.

Like *Potter et al.* [1996] a probability index of WFPS is used in this study as a measure of soil moisture. WFPS defined, as the ratio of volumetric soil moisture to total soil porosity is useful for comparing soil moisture for soils of different texture. Soil moisture surfaces (a probability index of WFPS based on water storage capacity, discussed below) were produced using a modified version of the water budget module (WBM) of the CENTURY model [*Pulliam & Parton*, submitted, 1998] and a soil wetness index based on a digital elevation model (DEM, discussed below). Input data to the WBM comprised climate mean surfaces of minimum and maximum temperature, rainfall and potential evapotranspiration (PET) derived from 29 years of data from 50 meteorological stations of Zimbabwe (Fig. 4.1). In addition mean monthly leaf area indices (LAI) maps based on 10 years of dekad vegetative indices were generated and a generalized Zimbabwean soil map comprising soil texture for the upper 30 cm were used as model input.

The use of mean monthly model input data at a 1-km^2 resolution was dictated by data availability and offered the most appropriate consolidation of the various spatial and temporal scales present for the limited data available for Zimbabwe.

4.2.1 NO model

The determination of the NO flux by laboratory methods is described in detail by *Remde et al.* [1993] and *Yang et al.* [submitted, 1998]. In summary soil samples of the surface layer (0–5 cm) were taken from the Grassland Research Station Marondera (Zimbabwe) from the sites where NO emission field measurements were previously performed by a dynamic chamber technique [*Meixner et al.*, 1997]. Only two samples per ecosystem underwent laboratory analysis and the results were assumed to represent mean soil conditions for the entire country. This assumption was made for logistical reasons and it is not known if more extensive sampling (different ecosystems or more soil groups) would improve the pragmatic approach adopted in this study. The effects of nitrogen based fertilizers

on agricultural soils were assumed to be negligible as more than half of the maize (corn) production (dominant crop) is grown by the small-scale commercial farmers (SSCF) [*Commercial Farmers Union of Zimbabwe*, *CFU*, personal communication, 1998], who are limited in their financially ability to utilize fertilizer (on average less than 50 kg per farmer per yr.) [*FAO-Fertilizer Strategy for Zimbabwe*, 1999]. The expansion of commercial farming operations, although politically suppressed at present (2000) in Zimbabwe, may alter this scenario in the future. In addition the up scaling process encompassed no specific relationship between soil nutrients (NH_4^+, NO_3^- and NO_2^-) and NO emissions. The laboratory measurements examined the dependence of soil NO emissions on soil nutrients only in a qualitative sense (fertilized / not fertilized) rather than in response to specific nutrient concentrations.

Laboratory incubations were performed on the soil samples to derive NO net release rate J (mass per mass per time), emission rates F (mass per area per time), NO production rate P, NO consumption rate constant k and NO compensation mixing ratio m_c. Soil NO diffusion (D_e) was calculated using measured quantities, namely the soil bulk density (ρ = 1.3 g m^{-3}) and the gravimetric soil water content (θ), after *Millington* [1959]. Parameterizations of P and k as independent functions of soil moisture and temperature were not explicitly performed, instead an approach was adopted where incubations were performed at two specific soil moisture conditions (dry weight and 10 % dry weight) for each ecosystem soil, which approximated the standard NO emission flux for lower (<1 % WFPS) and the optimum (15–20 % WFPS) soil moistures. Thereafter independent soil moisture and temperature response incubations were performed to derive input parameters for the soil moisture and temperature NO flux dependency functions.

In order to relate laboratory NO emission rates to those of field measurements, *Galbally & Johansson* [1989] developed a conceptual model (G&J model) to estimate net NO flux from laboratory measurements of turnover and gas transport of NO within the soil as follows:

$$F = (D_e\, k\, \rho)^{0.5}\, (m_c - m_a)\, (M_N / V_m) \tag{4.1}$$

where F is the standard NO flux (ng N m^{-2} s^{-1}) for dry and wet soils, m_a is the ambient NO mixing ratio (ppb), M_N is the atomic weight of nitrogen, V_m is the molar gas volume and

$$m_c = (P / k)\, (V_m / M_N) \tag{4.2}$$

is the compensation mixing ratio [*Conrad*, 1994].

To consider the effects of soil temperature (with soil moisture constant) and soil moisture, *Yang et al.* [1996] and *Yang & Meixner* [1997], introduced two additional functions to the G&J model to account for soil temperature (T) and soil moisture (θ) such that,

$$F_T = F f(T) f(\theta) f_{pulse} \tag{4.3}$$

where F_T is the modified flux according to soil moisture, temperature and f_{pulse} is the pulsing factor (cf. Section 4.2.2).

The exponential relationship between net NO flux and soil temperature is well documented by *Williams et al.* [1992a] and *Yienger & Levy* [1995]. Setting $T_s = 25$ ºC as standard conditions for Zimbabwe (29-year country-wide mean of $T_s = (26.1 \pm 2.1)$ ºC, and setting B dependent on soil moisture for dry and wet soils, separately (Table D1, cf. Appendix D), the flux at any soil temperature can be expressed as the following function:

$$f(T_s) = F \exp(B_\theta \ (T_s - T)) \tag{4.4}$$

A meaningful NO emissions and soil water (WFPS) response function must consider (a) the optimum soil moisture conditions for emissions, (b) the effect of soil water on diffusion (D_e) and hence emissions and (c) a substrate diffusion limit at low soil moisture contents for most microbial processes [*Skopp et al.*, 1990]. For a given (constant) soil temperature ($T_s = 25$ ºC), the relation between net NO flux and soil moisture (θ) is described by a first-order empirical parameterization according to *Grundmann et al.* [1995],

$$f(\theta) = F \ \exp\left(\frac{(a\,\theta_2 - \theta_{opt})\ (\theta - \theta_{opt})}{(\theta_{opt} - \theta_1)\ (\theta - a\,\theta_2)}\right) \ \frac{(\theta - \theta_1)}{(\theta_{opt} - \theta_1)} \tag{4.5}$$

where a is a curve fitting parameter, θ_{opt} is the optimum soil water content, i.e. $\theta_{opt} = \theta(f(\theta) = f_{max})$, and θ_1 and θ_2 are defined by $\theta_1 = \theta_2 = \theta(f(\theta) \cong 0)$ for $\theta < \theta_{opt}$ and $\theta > \theta_{opt}$, respectively. For practical reasons, θ_1 is approximated by 0 % WFPS and θ_2 by the saturation soil moisture content. For the Zimbabwean soil samples studied, θ_{opt}, θ_1 and θ_2 were found to be hardly dependent on soil temperature. Similarly soil diffusion is assumed to be predominantly controlled by soil water content, which in turn is soil texture dependent as has been observed in recent incubations [*Kirkman G.A.*, unpublished data, 2000]. However, there is no evidence to suggest that this independence is globally applicable.

The parameters D_e, k, m_c, ρ, T_s and θ_{opt} derived from laboratory measurements were used to develop one dry season and one wet season (soils wetted to 10 % dry weight) algorithm for the three land-use types—miombo, agriculture and grassland. The soil moisture and temperature models were fitted using non-linear least-squares optimization with a and B as fitting parameters (Table D1, cf. Appendix D). The dry season algorithm was used when soil moisture was equal to or lower than the countrywide dry season mean soil moisture (July, mean WFPS < 9 %, for approximately seven months of the year) [*Torrance*, 1981], while the wet season algorithm was used for the remaining five months. The combined NO model took on a form similar to that illustrated for July in Figure 4.2, where NO fluxes were co-dependant on soil moisture and temperature.

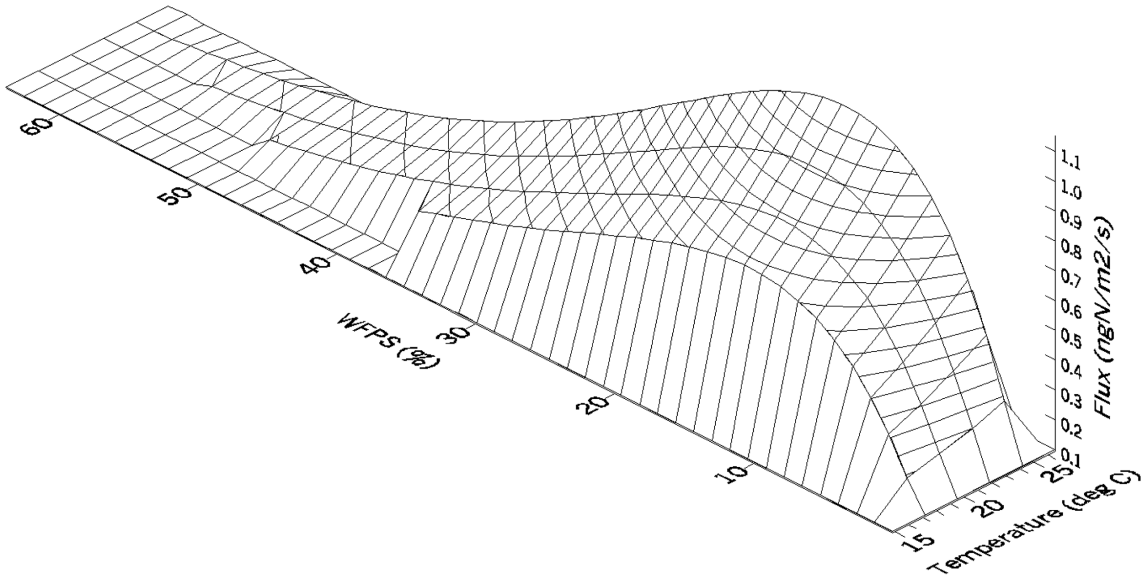

Figure 4.2 Modeled NO flux rates (ng N m^{-2} s^{-1}) against WFPS and soil temperature (°C) for the miombo land-use class of Zimbabwe (July).

4.2.2 Pulsing

In savanna ecosystems, following a period of drying, the onset of the first rains results in a relatively short-lived but extreme NO emission event termed a pulse. This phenomenon has been observed to be initiated by changes in soil temperature, soil substrate (dry period accumulation of NH_4^+ and NO_3^-), and soil moisture [*Johansson et al.*, 1988; *Johansson & Sanhueza*, 1988; *Meixner et al.*, 1997; *Scholes et al.*, 1997; *Otter et al.*, 1999]. The magnitude of the pulse is a nonlinear

combination of the above controls, with soil substrate accumulation positively related to the time between rain events [*Davidson*, 1992].

Attempts have been made to account for pulsing using empirically derived "pulsing factors" based on soil moisture and daily and monthly exponential decay functions [*Yienger & Levy*, 1995; *Otter et al.*, 1999] or excess soil water (greater than field capacity) distributed equally throughout the year [*Potter et al.*, 1996]. These approaches fail to incorporate the interdependencies governing the magnitude and duration of a pulse; the length of the *drying-out* period (or time between rain events), the amount of *moisture* added to the soil and the *frequency* at which the above occur.

In order to model pulse events on a monthly scale, a modified version of this "factor increase in nominal flux" approach was empirically derived from data on Colorado grassland soils [*Hutchinson, G.L.*, personal communication, 1999]. Individual pulses were treated as single cumulative events comprising a fixed number of equally spaced pulses per wet season month (i.e. 1, 3 and 9). The nine-pulse scenario (approximately 1 pulse per 3 days) represents a conservative estimate of monthly rain events for the wet season in accordance with a 30-year mean monthly rain day frequency for Zimbabwe. Rainy days per month were found to range from between 20 in *Manicaland West* to 8 in *Matabeleland South* [*Torrance*, 1981]. A 3-day drying-out period represents the minimum time required for soil to dry sufficiently so as to produce a significant pulse [*Otter et al.*, 1999]. Three soil moisture (rainfall induced) regimes were used, namely, 15%, 30% and 60% increases in WFPS from month n–1. A pulse therefore becomes a factor increase of NO flux for month n as a function of the soil moisture conditions for month n–1. This factor increase in NO flux is described by a linear equation,

$$f_{\text{pulse}} = -0.7485\, r^2 + 3.8527\, r - 1.2569 \qquad (4.6)$$

where r is the absolute change in soil moisture (WFPS) from month n–1 and f_{pulse} describes a nine pulse per month factor increase in NO.

The method is idealized in that it assumes pulses occur at fixed intervals interspersed by drying-out periods sufficient to allow subsequent pulses. In addition, augmenting fluxes by a factor is biased towards areas with a nonzero flux at the start of the rainy season, whereas in reality the reverse is more likely to occur. It is acknowledged that this approach is based on assumptions not fully representative of real processes and on relationships derived from unrepresentative soils under controlled laboratory conditions. It is likely that pulses are overestimated in the wet to dry transition months, while underestimated during dry to wet months. Nevertheless it offers a first-order estimate of a seasonal-dependent phenomenon at a mean temporal scale.

4.2.3 Canopy reduction factor

Quantifying biogenic NO emissions from an ecosystem requires a top-of-canopy approach, as the bulk emission from soils undergoes exchange within the canopy [*Jacob & Bakwin*, 1991]. NO is highly reactive in the atmosphere and converts (by reaction with ozone) rapidly to NO_2, which in turn is photolyzed back to NO at similar time scales under daylight conditions [*Kramm et al.*, 1991]. Since these chemical reaction times are in the same order as characteristic turbulent transport times of the atmospheric surface layer, oxides of nitrogen cannot be considered as passive tracers in turbulent surface exchange regimes [*Kramm et al.*, 1991]. Within vegetation canopies, turbulent transport generally diminishes allowing sufficient conversion of biogenic NO from soil with ambient ozone to NO_2. Furthermore, shadowing by vegetation will more or less suppress the back reaction (NO_2 photolysis) to NO. Uptake of NO_2 by vegetation is small but still an order of magnitude larger than that for NO [*Meixner*, 1994]. As a result, not all of the NO emitted from soils may escape to the atmospheric surface layer above the vegetation canopy. Vegetative scavenging of NO_x has been shown to be a significant NO sink and can limit biogenic emissions by as much as 75 % [*Jacob & Bakwin*, 1991]. The canopy reduction factor (CRF) is a function of dynamical features ranging from temporal changes in radiation and turbulence to surface characteristics, leaf area index (LAI) and canopy height. *Yienger & Levy* [1995] developed an empirical method to determine CRF using LAI. This approach has been adopted to estimate the CRF based on NDVI (Normalized Difference Vegetation Index) (cf. Section 4.3.7) derived monthly LAI values for Zimbabwe (Table D2, cf. Appendix D) and stomatal area indices for the three land-use classes from Table 6 in *Yienger & Levy* [1995].

4.2.4 Soil water and temperature model

Countrywide monthly soil moisture and temperature data surfaces for Zimbabwe were required as input in the NO model. A combination of topography based soil wetness index (a function of slope and flow accumulation, cf. Section 4.3.2), and a subcomponent of the CENTURY biosphere model was used to generate these data. The use of a topographic index introduced an element of relief, which is ordinarily not present in two dimensional modeled fields of soil moisture, and thereby improved the overall agreement between observed and modeled ranges of soil moisture for the selected validation sites. Despite numerous uncertainties associated with using monthly tipping-bucket soil water models, as found in CENTURY, many researchers have applied them with success to problems ranging from catchment scale studies to global water balance and climate change scenarios [*Thornthwaite*, 1948; *Manabe*, 1969; *Mather*, 1972; *Alley*, 1984; *Mintz & Serafini*, 1992; *Mintz & Walker*, 1993]. The monthly approach requires a minimal of input data, a prerequisite for studying this area, namely precipitation, temperature, potential evapotranspiration, biomass fractions, and soil water

holding capacity. However the lack of soil moisture validation data prevents a more quantitative appraisal of model uncertainty, which is assumed to be ca. 100 %.

The combined topographic and modeled soil moisture scheme drew from basic hydrological theory. Throughflow (Q) can be described as a function of area,

$$Q = (R - E - I - D)\, A \tag{4.7}$$

where the term in parenthesis is rainfall R less evapotranspiration E, interception I, and vertical discharge D, and A is the upslope contributing area per unit length of contour or flow accumulation [*Speight*, 1980].

Further, throughflow can be described as function of water storage,

$$Q = K\, H\, S \tag{4.8}$$

where K is lateral hydraulic conductivity, H is soil water storage and S is the tangent of the slope. Therefore soil water storage can be expressed as

$$H = [(R - E - I - D)\, A] \,/\, (K\, S) \tag{4.9}$$

Assuming uniform lateral hydraulic conductivity, the soil wetness index is therefore (A/S) [*Jones*, 1986].

In order to produce the ($R - E - I - D$) term, the CENTURY tipping-bucket soil water balance model (WBM) was used to estimate mean monthly water storage. A detailed comparative review of the WBM model and validation for several ecosystems is presented in *Pulliam & Parton* [submitted, 1998]. The strength of the WBM is its ability to link ecosystem processes such as rates of evaporation, transpiration water loss, vegetation canopy structure, and litter accumulation (cf. Sections 4.3.5 & 4.3.6) to soil hydrology. The WBM was modified to reflect subtropical climate conditions by removing the snow parameterization and by replacement of the *Linacre* [1977] PET formulations with monthly normal potential evapotranspiration surfaces [*FAO/SADC/RRSP*, 1998], which caused inconsistencies in the original version. The soil water holding capacity routines [*Gupta & Larson*, 1979] were replaced with those of *Saxton et al.* [1986], which are based on soil textures. These were found to be superior when validated against soil profile data of selected Zimbabwean soils. Further the model parameters for bare soil evaporation and canopy interception were optimized by non-linear least-squares fitting to 15 years of evaporation data from 20 meteorological stations [*Torrance*, 1981].

The water storage index of WFPS is arrived at by normalizing H with saturated soil water holding capacity in a similar method to *Potter et al.* [1996] where saturated soil water holding capacity describes interstitial-pore space such that,

$$\text{WFPS} = H / \theta_s \tag{4.10}$$

where θ_s is the saturated water content of the soil after eq. 7 reported in *Saxton et al.* [1986].

The temperature regime of any soil is profoundly modified by the growth of vegetation, as the surface becomes increasingly shaded owing to canopy development. The presence of shade reduces the maximum and increases the minimum temperature at surface depths, and there is usually a small decrease in average temperature. The empirical relationships described in detail by *Parton* [1984] and implemented in the CENTURY model were used to generate the monthly fields of soil temperature using a mean monthly biomass estimate for Zimbabwe (cf. Section 4.3.5).

Validation of the modeled mean monthly soil temperature and moisture with observed values for Zimbabwe was hindered due to a lack extensive field data. The soil moisture model was brought into agreement with the range of values for stations listed in the Climate Handbook of Zimbabwe [*Torrance*, 1981] for expected percentage soil moisture for Inyanga, Harare and Sabi Valley. In addition, data from two locations, Grasslands Research Station, Marondera and Tsetse Research Station, Rukomechi (Fig. 4.1) were used to validate three months of the model.

4.3 Data Surface Generation

Input data to the soil moisture, temperature and CRF schemes were sourced from published data, purchased from regional data projects or measured in the field. In order to run the upscale process, spatial data were converted into 2-dimensional or interpolated data surfaces. The following describes the data and data generation methods for achieving this.

4.3.1 Climate surfaces

Climate mean data surfaces were provided by the *Food and Agriculture Organization/Southern African Development Community Regional Remote Sensing Project* (FAO/SADC RRSP), Harare, Zimbabwe [1998]. Average monthly precipitation, minimum/maximum temperature and potential evapotranspiration for the 1961–1990 period from the *FAOCLIM 1.2 database* [1995] using approximately 50 stations were fitted to a 0.1-degree Digital Elevation Model of Zimbabwe. A co-kriging procedure was used, where the correlation matrix between the

dependent and independent variables was used to generate second power inverse distance weights, which were in turn used to interpolate missing data. A full description of data and methodologies can be found on '*The RRSP CD*' [1998] available from the *Regional Remote Sensing Project*, Harare.

4.3.2 Digital elevation model (DEM)

A 30 arc second DEM (United States Geological Survey (USGS) in Sioux Falls, USA) was used to generate the slope (S) and upslope contributing area per unit length of contour (A) for eqs. (4.7 to 4.9) using the routines SLOPE and FLOWACCUMULATION in ARC/GRID (ESRI, Inc., Redlands, USA).

4.3.3 Land-use classification

Three specific land-use classes for Zimbabwe were selected for this study, namely, "miombo" comprising woodland (53.2 %) and bushland (12.7 %); "grassland" comprising wooded grassland (3 %), and grassland (1.8 %); and "agriculture" comprising agricultural land (27.5 %) (Fig. 4.1). These classes coincide with the soils that underwent laboratory analysis. Miombo woodland (25,7470.33 km^2) is the largest land-use type in Zimbabwe comprising ecosystems dominated by trees of the genera *Brachystegia, Julbernardia* and *Isoberlinia*. The grassland land-use type (18,904.07 km^2) comprises the smallest area of the three land-use classes. Maize is the most extensive agricultural crop grown in Zimbabwe with approximately 1.397 million ha $year^{-1}$ [*CFU*, personal communication, 1998] or approximately 13% of land classified as agriculture (10,7292.32 km^2) in this study. It is assumed that 50% of land within this group is or was under maize or similar mono-cultivation within the last 10 years.

A 1-km^2 rasterized land classification was kindly donated by SADC, Harare, Zimbabwe comprising a subset of the 1:1000,000 Vegetation Resources Information System (VEGRIS) Woody Cover map [*ForMat*, 1998]. This database comprises the most up-to-date record of land cover as derived from LANDSAT TM imagery produced by the *Zimbabwe Forestry Commission, Forest Research Centre*, Harare.

4.3.4 Soil property surfaces

A soil map combining texture; percentage sand, silt and clay; bulk density; and organic matter was constructed and gridded to a 10-km^2 scale. The soil groups were sourced from the *FAO-UNESCO Digital Soil Map of the World* [*FAO-UNESCO*, 1995] with data supplemented by pedon attributes from soil profiles of major groups as selected by *Chemistry and Soil Research Institute*, Harare and published sources [*Thompson & Purves*, 1978; *Nyamapfene*, 1991]. The soils groups and properties used in this study are presented in table D3.

4.3.5 Leaf area index measurements (LAI)

LAI measurements were taken during the month of December 1998 with a LI-COR LAI-2000 Plant Canopy Analyzer (LI-COR, LAI-2000, Lincoln, NE, USA) at selected sites throughout Zimbabwe. The LAI-2000 uses measurements of above and below canopy radiation to obtain an estimate of the canopy gap fraction, which is then inverted to infer canopy structure. The LAI-2000 has been shown to estimate LAI to within an error of 15 % [*Welles & Norman*, 1991]. Over 40 determinations of LAI (comprising > 1000 measurements) were taken from several ecosystems, covering most of Zimbabwe. Values ranged from 4.2 $m^2 m^{-2}$ for rainforest to 0.62 $m^2 m^{-2}$ for Mopane-Acacia woodlands. To our knowledge these measurements comprise the first nationwide LAI data set for Zimbabwe; therefore all data are presented in table D2.

4.3.6 Leaf biomass surfaces

The LAI and biomass data surfaces were used as input parameters to the soil moisture, temperature and Canopy Reduction Factor (CRF) models. There exists considerable empirical evidence to suggest that the fraction of incident photosynthetically active radiation (FPAR) absorbed by photosynthesizing tissue of a canopy is related to the top-of-canopy spectral vegetation index [*Asrar et al.*, 1984; *Weigand et al.*, 1991]. *Sellers et al.* [1994] describes a method to derive LAI from remotely sensed AVHRR land-cover data in the Simple Biosphere Model (*SiB2*). In order to derive LAI surfaces for Zimbabwe, field measurements were used to invert the *SiB2* algorithms for December to produce the parameters for the remaining months. The agreement was satisfactory with a root mean square error between modeled and observed LAI of approximately 15% for December.

LAI is therefore given as,

$$L_{t,I} = L_s + L_d + L_g \tag{4.11}$$

where L_t is the total leaf area index; L_s is the stem area index taken as 0.076 for clustered and 0.2 for uniform vegetation [*Dorman & Sellers*, 1989]; L_d is the dead leaf area index such that,

$$L_d = L_{g-1} - L_g \tag{4.12}$$

where L_g is the green leaf area index per month for uniform and clustered vegetation.

The general relationships between FPAR and LAI for uniform and clustered green leaf area index per cell (i) are exponential

$$L_{g,\,I} = L_{g,\,max} \log(1–\text{FPAR}) \,/\, \log(1–\text{FPAR}_{max,\,i}) \tag{4.13}$$

and linear relationship

$$L_{g\,I} = L_{g\,max}\,\text{FPAR} \,/\, \text{FPAR}_{max\,i} \tag{4.14}$$

respectively. FPAR_{max} is the NDVI 95th percentile, and $L_{g\,max}$ is the maximum green leaf area index per month. [*Monteith*, 1973; *Huemmrich & Goward*, 1992].

The LAI field measurements were least-squares fitted to corresponding NDVI derived FPAR indices for December using nonlinear optimizations to arrive at $L_{g,\,max}$ for December. Biomass has been shown to peak in March or April in *Brachystegia/Julbernardia* woodlands in nearby Zambia [*Chidumayo*, 1990]. Therefore, December values of $L_{g,\,max}$ are an underestimate of maximum values. Thus, the remaining months were linearly scaled with the relative difference of monthly and December values of NDVI reflectance such that

$$L_{g,\,max} = L_{g,\,\text{December}}\,(1 + \text{NDVI}_n – \text{NDVI}_{\,\text{December}})\ \{n < 12\} \tag{4.15}$$

where $L_{g,\,max}$ is the maximum LAI for January to November and $L_{g,\,\text{December}}$ is the LAI for December. With this scheme the yearly maximum LAI (April) is on average 8 % higher than the December $L_{g,\,max}$ and the minimum LAI (September) is on average 26 % lower.

To determine FPAR from NDVI, two approaches were considered, (a) a linear relationship between NDVI and FPAR, which describes a typical or average canopy including ground cover, leaf area, leaf orientation and optical properties [*Myneni & Williams*, 1994],

$$\text{FPAR} = 1.1638\,\text{NDVI} – 0.142\ (r^2 = 0.919,\ N = 252) \tag{4.16}$$

and (b) the *SiB2* approach [*Sellers et al.*, 1994]. This approach uses a simple ratio (SR) (near infrared/visible wavelength) to arrive at FPAR. The use of *SiB2* was tested and found to be slightly inferior to (a) when cross-validated with measured LAI. This is possibly due to the lower SR limit (0.001) allowing for a greater degree of soil reflectance interference in the equation. The *SiB2* FPAR values were consistently 1.3-fold higher than those derived from eq. (4.16).

FPAR fields underwent a classification into uniform or clustered vegetation type by means of cell-by-cell (0.1-degree) assignment to a vegetation classification based on the VEGRIS map. Natural moist forest, woodland, bushland and the wooded grassland classes were considered clustered vegetation. Uniform

vegetation comprised of forest plantation, grassland and cultivation land-use classes.

Three key assumptions were made in using FPAR and field measurements to calculate LAI surfaces in this study. Firstly, field LAI measurements are assumed to be green leaf area index. This certainly is not the case as field measurements include all three forms of vegetation. However given the large variances in LAI within a relatively small area this is not unreasonable. Secondly, December 1998 is assumed to represent a mean December LAI indicative of the entire country, a logistical constraint not easily resolved. Thirdly, LAI is assumed to remain static throughout the month and to vary between months.

Biomass as a function of LAI is commonly presented as a linear relationship where a ratio is used to relate LAI to biomass ($g\ m^{-2}$) [*Luedeke et al.*, 1994; *Bossel*, 1994; *Pulliam & Parton*, submitted, 1998]. A similar linear approach was used in this study to relate LAI to biomass per month for use in the soil water and temperature model. For this, a map of the maximum potential aboveground biomass for 1980 [*Brown & Gaston*, 1997] was used such that

$$\mathrm{BIO}(t) = [\mathrm{BIOMAX} / \mathrm{LAIMAX}(t)]\ \mathrm{LAI}(t) \qquad (4.17)$$

where LAIMAX is the maximum LAI for month *t*. Biomass was then apportioned into three distinct classes—, namely, *LITTER*, *LIVE* and *STANDING DEAD* classes ($g\ m^{-2}$) —using a monthly scaling factor based on a review of literature estimates for the dominant land-cover class (miombo) [*Guy*, 1981; *Stromgaard*, 1985; *Campbell et al.*, 1988; *Chidumayo*, 1990, 1997; *Fuller & Prince*, 1996].

4.3.7 Normalized difference vegetation index

Monthly mean NDVI datasets for Zimbabwe were constructed from ten years (1983–1994) of 8-km^2 resolution, 10-day composite data (three per month). The daily data were sourced from the NOAA AVHRR Global Area Coverage (GAC) 1-B database, available from NOAA's Satellite Active Archive. The calculation of the long-term averages excluded 1983/84 and 1991/92, which were affected by the *Pinatubo* and *El Chichon* eruptions and data after 1995 owing to differences with the current NOAA14 satellite.

4.4 Results and Discussion

Results are presented in four sections, (a) mean biogenic NO emission flux rates ($ng\ N\ m^{-2}\ s^{-1}$), including nine pulses per wet season, providing an overview of the relative contributions of each of the three land-use classes, (b) comparison

between measured and modeled flux rates for an area surrounding Marondera indicating a measure of model validity, (c) bulk and net NO emissions (Gg N yr^{-1}) estimates and (d) spatial distribution of flux rates. Figure 4.3 provides a graphic overview of soil temperature, WFPS, and LAI for March (month of highest LAI) and the middle of season months of July and December used in the calculation of the NO fluxes.

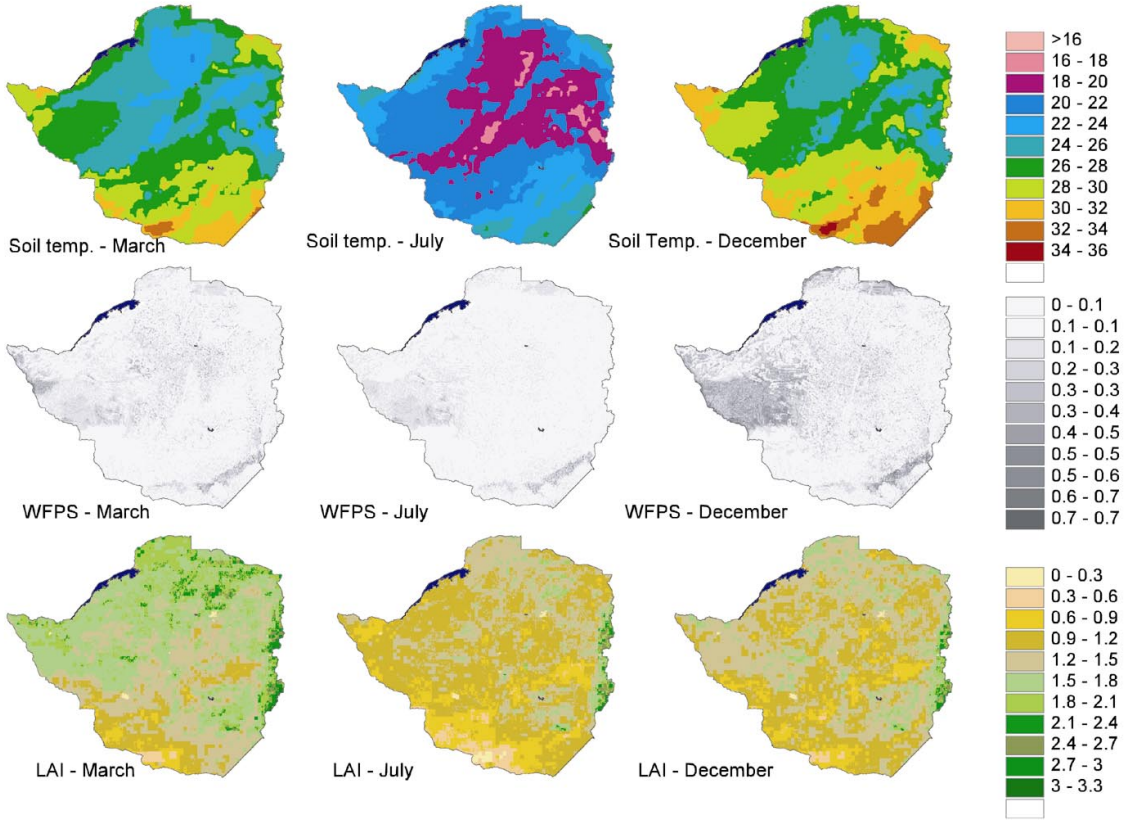

Figure 4.3 Mean soil temperature, WFPS, and LAI for March, July and December.

4.4.1 NO flux by land-use

The countrywide data distributions of monthly NO emissions from miombo soils are approximately normal with 53 % of the country showing fluxes below monthly mean values and 88 % within 1 standard deviation. The grassland NO soil emissions follows a similar pattern with 54 % and 80 %, while data distributions of NO emissions from agricultural soil are slightly positively skewed with 56 % and 72 %, respectively, for the entire year. Figures 4.4 show the

seasonal variance in mean, maximum and standard deviation of the countrywide NO flux rate over a mean 12-month period for the three land-uses. Extreme flux rates or those > 3 standard deviations above the mean or larger than 8 ng N m^{-2} s^{-1} for all land-use classes are limited to < 0.7 % of the total area of the country.

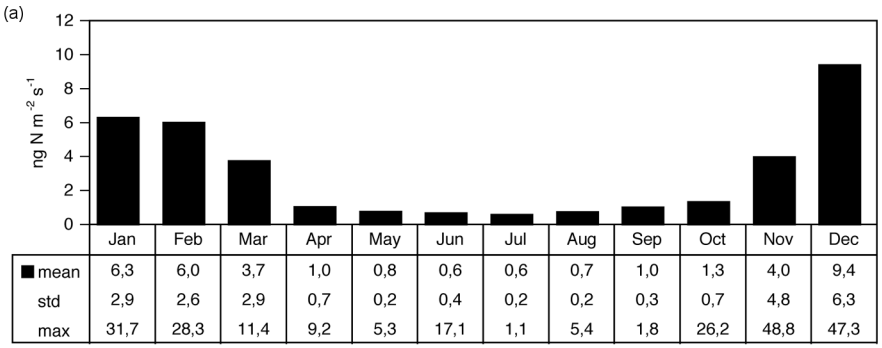

	Jan	Feb	Mar	Apr	May	Jun	Jul	Aug	Sep	Oct	Nov	Dec
mean	6,3	6,0	3,7	1,0	0,8	0,6	0,6	0,7	1,0	1,3	4,0	9,4
std	2,9	2,6	2,9	0,7	0,2	0,4	0,2	0,2	0,3	0,7	4,8	6,3
max	31,7	28,3	11,4	9,2	5,3	17,1	1,1	5,4	1,8	26,2	48,8	47,3

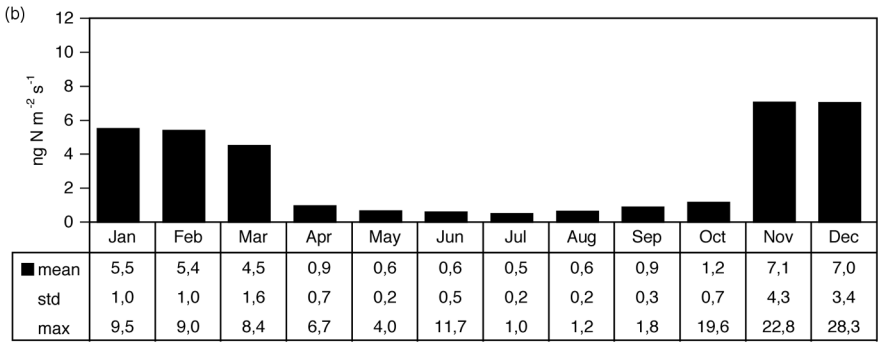

	Jan	Feb	Mar	Apr	May	Jun	Jul	Aug	Sep	Oct	Nov	Dec
mean	5,5	5,4	4,5	0,9	0,6	0,6	0,5	0,6	0,9	1,2	7,1	7,0
std	1,0	1,0	1,6	0,7	0,2	0,5	0,2	0,2	0,3	0,7	4,3	3,4
max	9,5	9,0	8,4	6,7	4,0	11,7	1,0	1,2	1,8	19,6	22,8	28,3

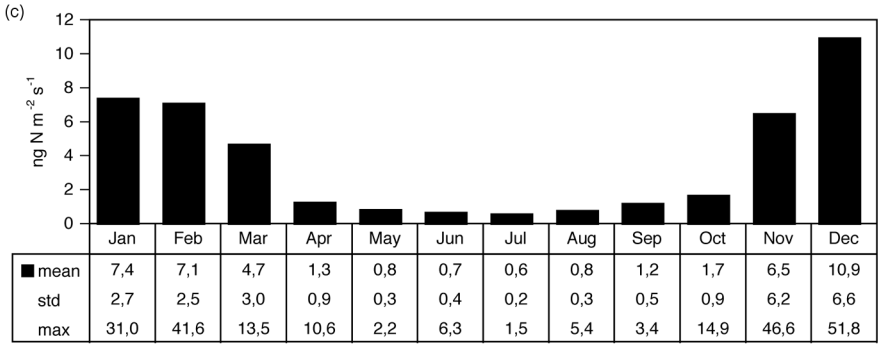

	Jan	Feb	Mar	Apr	May	Jun	Jul	Aug	Sep	Oct	Nov	Dec
mean	7,4	7,1	4,7	1,3	0,8	0,7	0,6	0,8	1,2	1,7	6,5	10,9
std	2,7	2,5	3,0	0,9	0,3	0,4	0,2	0,3	0,5	0,9	6,2	6,6
max	31,0	41,6	13,5	10,6	2,2	6,3	1,5	5,4	3,4	14,9	46,6	51,8

Figures 4.4 Mean, standard deviation and maximum monthly NO flux rates for (a) miombo, (b) grassland and (c) agriculture soils in ng N m^{-2} s^{-1}.

The highest fluxes occur during December for all land types: (9.4 ± 6.3) ng N m^{-2} s^{-1} for miombo, (7.0 ± 3.4) ng N m^{-2} s^{-1} for grassland and (10.9 ± 6.6) for agriculture with an average countrywide soil moisture of 17 % (WFPS) and soil temperature of 28 ºC. Average NO fluxes for the entire country for the dry season range from 0.1–0.4 ng N m^{-2} s^{-1}, and average soil moisture and temperature seldom exceed 9 % WFPS and 24.9 ºC, respectively. Wet season fluxes range from 3.7–9.4 ng N m^{-2} s^{-1} for miombo, 4.4–7.0 ng N m^{-2} s^{-1} for grassland and 4.6–10.9 ng N m^{-2} s^{-1} for agriculture; and soil moisture is on average 15 % WFPS and soil temperature 27.7 ºC.

A comparison of countrywide mean NO flux rates for all three land-use classes shows that agricultural fluxes are consistently higher than those of the other classes for all months except November. The population growth rate of Zimbabwe is currently approximately 3 % per annum, with 70 % of this growth taking place in the rural areas. It is therefore anticipated that the demand for rural land for agricultural land will increase [*FAO–A Fertilizer Strategy for Zimbabwe*, 1999]. Future scenario model runs were conducted by expanding the area under unfertilized agriculture by one neighboring cell in all directions (with no increase in fertilizer use). Using this crude approximation, which assumes that only current agricultural areas will grow in all directions, suggests that a doubling of the area under agriculture results in an 81 % increase in agricultural net NO emissions and resultant nationwide annual net increase of 5 %.

Pulsing is generally restricted to the start of the wet season and occurs predominantly during November and December with the onset of the first rains. The pulse constitutes between a 7 % (1 pulse per wet season month) and 14 % (nine pulses per wet season month) increase in countrywide annual emissions. Agricultural soils are the highest (16 %) and grasslands (13 %) the lowest contributors to pulsing. This indicates that soil moisture related pulsing could be a significant contributor to annual NO emissions in Zimbabwe and hence the eutrophic soils of the subtropical African savannas.

4.4.2 Model verification

The ability of the model to extrapolate laboratory measured flux rates to a regional scale was tested against field measurements for a range of model points within a 5-km radius of the location of the field-based measurements (Grassland Research Station, Marondera; cf. *Meixner et al.* [1997]). Table D4 compares revised mean flux estimates (corrected with VEGRIS land-use areas) from *Meixner et al.* [1997] against those for this study and fluxes from South African soils [*Levine et al.*, 1996; *Otter et al.*, 1999]. Modeled bulk fluxes are used for comparison since the field measurements were not able to account for CRF [*Meixner et al.*, 1997]. Model verification for the months October, November and December at selected sites

were found to be in good agreement with field measured data for the same period ($p = 0.05$, $df = 3$) and observed and modeled monthly variances were satisfactorily emulated ($r^2 = 0.82$). However, modeled average miombo flux rates (7.2 ng N m^{-2} s^{-1}) were higher than observed rates (1.2 ng N $m^{-2}s^{-1}$) owing to large differences in modeled and field measured soil moisture for 79 km^2 area around Marondera and possible overestimation of pulsing in the wet to dry transition months. The model results are within the range found in South African soils.

4.4.3 Annual net and bulk NO emissions estimates

Several postulations have been put forward as annual estimates for savanna ecosystem contributions towards global NO emissions. *Scholes et al.* [1997] provides a rough estimate of 0.15 g N-NO m^{-2} for nutrient deprived South African soils moist enough to support emissions for 25 % of the year. Using this emission rate and the area of Zimbabwe, an annual emission of 57.6 Gg N yr^{-1} for 98% of Zimbabwe could be estimated. *Meixner et al.* [1997] using only the product of area and flux rate arrived at an estimate of approximately 22.4 Gg N yr^{-1} (revised estimate) for the same area. These approaches (a) do not attempt to resolve terrain effects on soil moisture, (b) they use no specific land-use classification system, (c) nor employ a form of pulse parameterization, (d) no vegetation based canopy reduction scheme is used (e) and they do not drive their flux estimates by climate mean environmental conditions.

Global modeling studies, which include these and more detailed parameterizations include those of *Potter et al.* [1996] (based on soil mineralization rates and water content) and *Yienger & Levy* [1995] (based on a set of biome related fitting parameters). Flux rates from these two studies were scaled to the area of Zimbabwe (Table D5 (a), cf. Appendix D). These calculations indicate a bulk NO emission of 48.8 Gg N yr^{-1} for *Potter et al.* [1996], a bulk and net NO emission estimate of 38.5 Gg N yr^{-1} and 27.8 Gg N yr^{-1} respectively for *Yienger & Levy* [1995].

In this study regional estimates first proposed by *Meixner et al.* [1997] using a limited dynamic chamber measured dataset are revised by using laboratory derived empirical relationships (which agree acceptably with the measured data) on soils and land surface data from the region. Table D5 (b) shows countrywide annual bulk (excluding CRF) and net NO emissions in Gg N yr^{-1} for the three land-use classes including an estimate derived from the *Meixner et al.* [1997] estimates (without CRF losses). On average CRF accounts for a 25 % reduction (countrywide) in soil surface emissions (miombo 28 %, grasslands 21 % and agriculture 26 %). The effects of CRF on net NO emissions per month are presented in figure 4.5 for each land-use class. Although this crude estimate based

on the *Yienger & Levy* [1995] approach is based on measurements in the Brazilian rain forest, which fails to account for ozone titration, the nonlinear relationship with soil emissions and canopy residence time it offers an upper limit estimate for what is essentially a sparse canopy ecosystem.

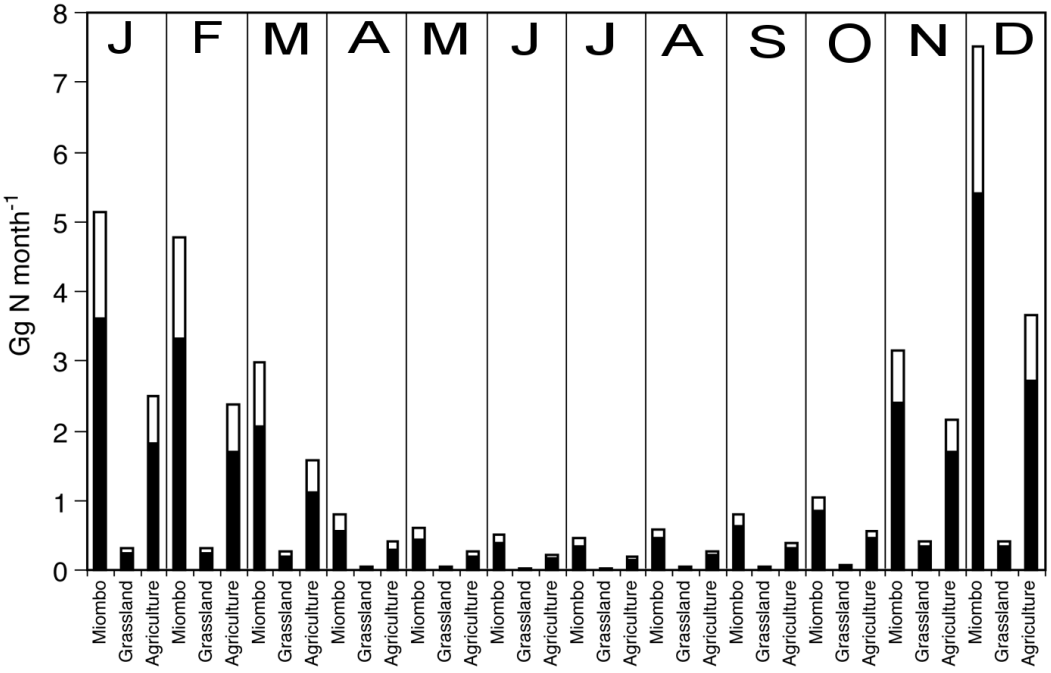

Figure 4.5 Net NO emissions (including pulsing, less canopy reduction) per land-use class per month (Gg N month^{-1}). The unshaded bars indicate the portion of bulk emissions reduced by the canopy (CRF).

Total annual modeled net NO emissions from soils for Zimbabwe are 32.9 Gg N yr^{-1} (Table D5 (b), cf. Appendix D), which are slightly higher than first estimated by *Yienger & Levy* [1995]. Bulk emissions (45.1 Gg N yr^{-1}) are somewhat lower than the annual estimate (57.6 Gg N yr^{-1}) first postulated by *Scholes et al.* [1997] and further qualified by *Otter et al.* [1999] based on field measurements of South African savannas. The bulk NO emissions estimate lies between the schemes based on soil mineralization and moisture (48.8 Gg N yr^{-1}) [*Potter et al.*, 1996] and that based on biome specific emission factors (38.5 Gg N yr^{-1}) [*Yienger & Levy*, 1995].

Miombo woodlands comprise 66 % of Zimbabwe and contribute 63 % to the regional NO budget. Modeled miombo woodland bulk emissions are a factor of six (28.4 Gg N yr^{-1}) higher than the field-based estimates as first estimated by *Meixner et al.* [1997] (5.1 Gg N yr^{-1}) (Table D4, cf. Appendix D). The modeled grassland estimates (2.1 Gg N yr^{-1}) are twice a large as field-based estimates (1.0 Gg N yr^{-1}), while bulk modeled (14.6 Gg N yr^{-1}) and field based (16.4 Gg N yr^{-1}) estimates for agricultural soils are reasonably similar. These differences could also be ascribed to the large variability generally found between field and laboratory measurements (10–80 %). Despite these apparent shortcomings these data are appropriate as a revised NO soil emission estimate for Zimbabwe.

4.4.4 Spatial distribution of NO

The distribution of biogenic NO across Zimbabwe for miombo, grassland and agriculture land-use groups is influenced by the spatial mean distribution of soil moisture, temperature and biomass for each month. This is well represented in the model (Fig. 4.2) with peak fluxes occurring between 15 and 20 % WFPS and temperatures ranging from 15 to 25 ºC.

Figure 4.6 shows the spatial variability of the monthly average estimate of biogenic NO emission rate for Zimbabwe as determined by soil moisture and temperature. For most of the country during the dry season (April–October) fluxes are spatially indistinguishable for all land-use classes and are generally <5 ng N m^{-2} s^{-1} with a mean of (0.89 ± 0.35) ng N m^{-2} s^{-1}. Some enhanced emissions are evident from the wetter Eastern Highlands at the start (October) and end (April) of the wet seasons. The wet season maps of January to March, November and December show the onset of NO emissions during November in the central provinces and then a tailing off for the entire country in March. The mean flux rate of all land classes for the wet season is (6.27 ± 2.5) ng N m^{-2} s^{-1} with mean minimum and maximum rates of 0.05 ng N m^{-2} s^{-1} and 19.5 ng N m^{-2} s^{-1}, respectively.

The largest extent of elevated values (5–31 ng N m^{-2} s^{-1}) is found predominantly in the southwestern and central *Mashonaland* and in an extensive area to the west of Bulawayo during December. This area is covered predominately by miombo woodland, and flux values range between 22 and 32 ng N m^{-2} s^{-1}. The combination of warm soil temperatures (25–30 ºC), optimal WFPS (15–20 %) and rainfall preceded by extreme drying make this area an obvious source.

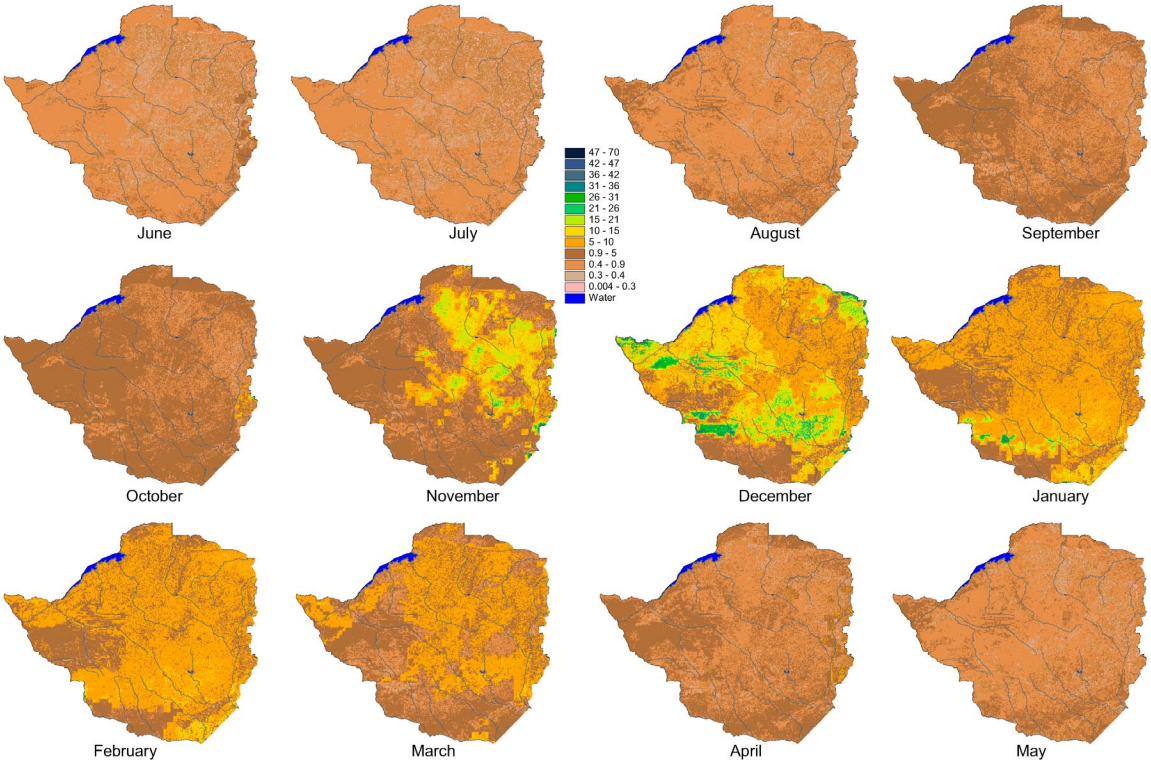

Figure 4.6 Spatial distribution of miombo NO flux rates (ng N m^{-2} s^{-1}) per month for Zimbabwe.

4.5 Conclusions

This study has shown that with available models, laboratory-based emission parameters, satellite and observation derived geo-databases of land-use, and climate factors, an estimate of total NO flux contribution from several ecosystems is possible. Despite known problems with laboratory NO flux measurements [*Hutchinson et al.* 1997], model limitations, the lack extensive validation data and errors introduced in estimating soil properties, the approach provides a first countrywide estimate of spatio-temporal NO flux for a hitherto largely unresolved source, subtropical savannas. This scheme (a) offers an enhancement to the product (area by flux rate) approach to up scaling by including explicit laboratory derived NO flux dependencies, (b) distal parameters such soil water, temperature and land-use, and (c) provides ecosystem derived estimates of two important flux regulators: pulsing and canopy reduction.

Biogenic NO emissions in Zimbabwe are linked to seasonal climatology and are sensitive to the onset of rainfall at the end of the dry and dry-to-wet transition

periods. By December soil moisture had recovered sufficiently to produce an increase in NO flux of up to 14 %, due to pulsing in some areas.

Miombo is the largest source of NO in this region owing to the spatial extent of this land class; however, emissions rates for agriculture are larger for most of the wet season. Consequently as more land is converted from miombo to agriculture (2.1 % annual population growth rate in rural areas), an approximate doubling of the current agricultural land would result in an addition of almost 2 Gg N yr^{-1} to the net NO emissions budget for Zimbabwe.

4.6 Future Approach and Considerations

Land-use ecosystem classification, soil moisture and temperature have been shown to be useful common denominators for scaling laboratory based NO fluxes for a moisture limited ecosystem [*Meixner et al.*, 1997; *Serça et al.*, 1998]. These three scaling parameters are sufficient predictors for the eutrophic African subtropical savanna soils, whereas they may not be as applicable to dystrophic wet tropical soils. However these alone are not sufficient and often impractical for up scaling at the larger scales, as land-use practices are difficult to document in areas where human cultivation have been present for extended periods of time (> 100 years) and soil moisture and temperature have to be largely modeled. Future improvements might include laboratory NO production and consumption responses to soil properties such as pH, matric potential and nitrogen indices (NH_4^+ and NO_3^-, net mineralization and potential nitrification rates), all of which are affected by anthropogenic activities (clearing and cultivation) and offer extended model validity. Although deriving databases of these soil properties would probably once again limit this approach to the landscape scale. Other improvements might be to resolve soil water and temperature on a daily basis (more suited to the landscape scale), an empirical scheme based on observations of selected ecosystem soils to improve the effects of pulsing and the inclusion of soil diffusion measurements (^{222}R) during field validation experiments. This will facilitate that the modeled NO diffusion, production and consumption rates reflect soil physical and chemical heterogeneity more precisely.

Chapter 5

SUMMARY

The primary objective of this work was to exploit the current wisdom governing the processes responsible for soil NO emission with the use of laboratory–, field measurements and models to provide up scaled regional estimate for two important biomes—savanna/woodlands and tropical forests/pastures. This was successfully achieved and in doing so it was shown that just a handful of field measurements could be used to produces regional soil NO emission estimates that adequately agreed with inventory and model based approximations. This was achieved by using environmental predictors that were particular to a region and thereby provided the most predictability. In addition this work has provided a significant contribution to the understanding of soil NO emissions, and plant/soil NO_2 and O_3 exchanges over aged dystrophic tropical soils.

In chapter 1 the measurement of NO_x and O_3 exchange over an old cattle pasture in Rondônia provided valuable new insights, which have implications for future NO_x and O_3 multi-resistance modeling in the tropics. The combined plant, soil and wet surface uptake of trace gases, accentuated by stomatal activity and aqueous phase chemistry on vegetative and soil surfaces at night are believed to result in a trace gas deposition diel pattern only previously observed by *Kaplan et al.*, [1988] near Manaus and *Andreae et al.*, [1992] in the Congo Basin. Their results could not be explained by changes in stomatal activity alone and where put to differences in aerodynamic resistance (R_a) between the dry and wet seasons. In this work we have demonstrated rather, that canopy resistances control the larger nighttime uptake of NO_2 and O_3.

The field experimental section of this work also produced the first NO_x budget for an old cattle pasture—an increasingly predominant land-use class in the tropical Amazon. In this section it was shown that the combination of conservative soil N–cycling and lower effective soil NO diffusion at an old pasture in Rondônia resulted in the lowest ever measured NO fluxes for this land type in the Amazon basin (a mean of 0.65 ng N m^{-2} s^{-1}). Approximately nine times lower than corresponding rainforest NO emissions. The surface of the pasture was also shown to remove seven times more NO_2 from the atmosphere as was emitted as NO, making it a net NO_x sink during 1999. These findings may

have implications for future tropical NO_x budgets as more land is converted to agriculture, and obliges further urgent study. Soil NO emissions results from this section facilitated the modeling and up scaling conducted in chapters 2 and 3.

In chapter 2 a process-oriented model (DAYCENT) was modified and used to analyze the dynamic role in which land-use change plays on soil nutrient dynamics and its subsequent effect on soil NO emissions. Initialized with forest biomass, soil and climatic parameters, the 1-D model was used to hindcast field NO flux measurements from a pasture (presented in chapter 1), with reasonable success. The most dominant NO emission-controlling factor in the region was soil nitrogen, which was directly dependent on land-use and land age since primary deforestation. It was shown that forest clearing could result in periods of extended elevated soil NO release, known as slash and burn pulses (S+B pulse), before soil NO emissions fell to levels 6 fold lower than those from primary forest soils.

The quantification of soil NO emissions from a tropical forest-nonforest region is essentially a spatio-temporal problem requiring a knowledge of the emissions from forests, pastures and secondary growth, as well as the magnitude and duration of NO emissions that occur in the period immediately following forest clearing. In chapter 3 this space time scale problem was solved by making use of the relationship that exists between NO flux and land age (time elapsed since deforestation), which was shown [Chapter 2] to be a reasonable predictor of soil NO emissions for the tropics. Mean annual soil NO fluxes from the model [Chapter 2] were used in conjunction with satellite imagery in a nested hierarchical up scaling scheme to produce an estimate of soil NO emissions per land-use class for a 26,455 km^2 area of Rondônia (Brazil). Results, which accounted for the canopy reduction of soil NO, showed that the largest producer of NO from the region were the non-forested areas (pasture and 2^{nd} growth) with significant contributions from the S+B pulse that occurs soon after deforestation. The up scaling exercise also showed that annual net soil NO emissions during 1999 were higher than when pristine forests covered the entire study area. This suggests that tropical regions undergoing anthropogenic change may be a more significant source of soil NO in the future than currently envisaged.

In chapter 4 the contribution of the subtropical savannas to the African savanna NO budget, based on two decades of mean meteorological conditions, were simulated. From this up scaling study it was shown that soil fluxes were produced in significant quantities in response to the transition from the dry to wet seasons with some differences in NO flux magnitudes between the three land-use classes (miombo, grassland and agriculture). In contrast to the dystrophic soils of the tropics, the combination of both land-use and soil moisture were shown to be useful environmental predictors controlling NO fluxes over the land-use complex

of Zimbabwe. Rainfall related increases in NO emissions (moisture pulsing) contributing ca. 14 % to regional fluxes. Up scaled estimates compared well with model and inventory soil NO emissions measured in Africa [*Serça et al.*, 1994, 1998]. In addition soil NO emissions for the savannas are reported to be largely comparable to emissions resulting from biomass burning [*Levine et al.*, 1997]. The superposition of these sources may result in periods of high O_3 production, and would therefore explain the seasonally high O_3 concentrations previously observed over southern Africa [*Levine, et al.*, 1996; *Kirkman, et al.*, 2000; *Scholes & Andreae*, 2000].

This work has unequivocally demonstrated that land-use change can contribute significantly to variations in the tropospheric concentrations of NO and exchanges of trace gases over the tropics and subtropical savannas. Land use practices in combination with climate, soil characteristics and ambient trace gas concentrations control the surface exchange of NO_x and O_3 in regionally specific ways. These regional effects are evident when comparing the soil NO emission rates for the two ecosystems examined in this study. Despite the rapid changes in land use, currently occurring in the tropics, annual soil NO emission rates for this region (0.49 kg N ha yr^{-1}) were approximately one half of those estimated for the subtropical savannas (0.86 kg N ha yr^{-1}). The tropics are expected to continue to play an important role in global tropospheric NO_x chemistry as long as primary forests continue to be cleared, but to a lesser extent than tropical savannas.

This work also suggests that classifying soil NO emissions, as natural sources may no longer be entirely correct. Soil-plant communities, particularly those in more remote areas of the globe, are not immune to the affects of mankind who is able to affect these ecosystems in spectacular ways and thereby the chemistry of the atmosphere that sustains him.

Appendix A

TABLES TO CHAPTER 1

Table A1. Trace gas detectors, micrometeorological instrumentation, and sensors used at *Fazendha Nossa Senhora da Aparecida* (FNS) during LBA-EUSTACH-2 (24 September to 27 October 1999) and LBA-EUSTACH-1 (30 April to 17 May 1999).

Quantity	Technique or Sensor	Model/Manufacturer	Limit†	Time (s)§
NO conc. (3.5 m above ground)	Gas phase chemiluminescence	Model 42C TL (trace level) Thermo Environment Instruments Inc., U.S.A.	0.025 ppb	300
NO_2 conc. (3.5 m above ground)	Catalytic conversion of NO_2 to NO by molybdenum converter (at 300°C) & gas phase chemiluminescence	Model 42C TL (trace level) Thermo Environment Instruments Inc., U.S.A.	0.025 ppb	300
O_3 conc. (3.5 m above ground)	UV absorption, symmetric dual cell design	Model 49C Thermo Environment Instruments Inc., U.S.A.	0.5 ppb	300
NO conc. (dynamic chambers)	Gas phase chemiluminescence	Model 42C TL (trace level) Thermo Environment Instruments Inc., U.S.A.	0.07 ppb	60 1800
NO_2 conc. (dynamic chambers)	Catalytic conversion of NO_2 to NO by molybdenum converter (at 300°C) & gas phase chemiluminescence	Model 42C TL (trace level) Thermo Environment Instruments Inc., U.S.A.	0.14 ppb	60 1800
O_3 conc. (dynamic chambers)	UV absorption, symmetric dual cell	Model 49C Thermo Environment Instruments Inc., U.S.A.	0.03 ppb	60 1800
^{220}Rn conc. (dynamic)	Alpha particle detection	Alphaguard PQ 2000 Pro, Genitron, Germany	2 Bq m^{-3} ± 10%	—

O_3 conc. (micromet. gradient)	UV absorption, symmetric dual cell, intakes switched at 0.53 and 4.5 m above ground	Model 49 Thermo Electron Inc., U.S.A.	0.5 ppb ± 0.56 ppb	2 1800
Soil temp. (dynamic chambers)	Thermistors at 0.05m below ground	Campbell Scientific Ltd., U.K	—	—
Volumetric soil moisture (dynamic chambers)	Time domain reflectrometry (TDL) sensors at 0.05m below ground	TRIME-ES P2M, IMKO GmbH, Germany	—	—
Surface wetness (dynamic chambers)	Surface wetness grids at soil surface inside and outside chambers	237 WSG Campbell Scientific Ltd., U.K.	—	—
Wind speed profile	3-cup-anemometers (optical switch) at 0.53, 1.02, 2.02, & 4.50 m above ground	A100ML, Vector Instruments, U.K.	0.25 m s^{-1} ± 0.10 m s^{-1}	10 1800
Wind direction	Potentiometric wind vane, at 4.5 m above ground	W200P Vector Instruments, U.K	± 5 deg	10 1800
Air temperature profile	Fine-wire (0.72μm), non-aspirated thermocouples, chrome-constantan (E-type) at 0.53, 1.02, 2.02, and 4.50 m above ground	Campbell Scientific Ltd., U.K	± 0.02 K	1 1800
Global radiation flux	Pyranometer sensor at 2.02 m above ground	LI200SZ LI-COR Inc., U.S.A	< ± 3 %	10 1800

† Detection or precision limit

§ Integration, execution or averaging time

Table A2. Net mineralization and nitrification rates for established pastures in Rondônia.

Pasture (older than 20 yrs.)	μg NH_4^+ g^{-1} d^{-1}	μg NO_3^- g^{-1} d^{-1}
Neill et al. 1997 (*Nova Vida*)	–0.023	–0.02
Neill et al. 1999 (*Nova Vida*)	0.03	0.16
Neill et al. 1997 (*Ouro Preto*)	–0.22	0.22

Table A3. Soil properties for FNS, determined during LBA-EUSTACH-2.

Soil parameter	Unit	Value
Organic Carbon	%	1.87
Total Phosphorus	%	0.021
Total Nitrogen	%	0.122
Total Carbon	%	2.58
Total Sulfur	%	0.008
Plant available Phosphorus	mg PO_4 100 g^{-1}	2.62
Plant available Potassium	mg K 100 g^{-1}	13.04
pH [$CaCl_2$]	—	5.2
Bulk soil density	Mg m^{-3}	1.56
Clay content	%	11.47
Silt content	%	11.73
Sand content	%	76.80
Wilting Point†	cm^3 cm^{-3}	6.69
Field Capacity†	cm^3 cm^{-3}	19.56
CEC (cation exchange capacity)	mmol $z^{-1}100g^{-1}$	16.77
Ammonium pool (NH_4^+)	μg NH_4^+ g^{-1}	16.81
Nitrate pool (NO_3^-)	μg NO_3^- g^{-1}	5.25
Nitrite pool (NO_2^-)	μg NO_2^- g^{-1}	0.27
Net mineralization rate	μg $NH4^+$ g^{-1} d^{-1}	–0.89
Net nitrification rate	μg NO_3^- g^{-1} d^{-1}	0.40
Potential nitrification rate	μg NO_3^- g^{-1} d^{-1}	1.69
C:N ratio	—	21.6

† Based on *Tomasella* & *Hodnett* [1998] pedo-transfer functions

Table A4. Median and inter-quartile-range (IQR) (s m^{-1}) of canopy resistances $R_c(NO_2)$ and $R_c(O_3)$, turbulent resistances R_a, molecular-turbulent boundary layer resistances R_b, $v_d(NO_2) = R_{tot}(NO_2)^{-1}$ and $v_d(O_3) = R_{tot}(O_3)^{-1}$ deposition velocities (mm s^{-1}) for (a) LBA-EUSTACH-1 and (b) EUSTACH-2 campaigns. Daily values fall between 06H00 – 18H00 local time. Values derived from substitution with values from the "dry–wet" period are in brackets.

(a) LBA-EUSTACH-1, 30 April to 17 May 1999, "wet–dry" transition period.

	R_a		R_b		$R_c(O_3)^{\dagger}$		$v_d(O_3)^{\dagger}$	
	day	night	day	night	day	night	day	night
median	20	79	22	54	100	(65)[§]	6	(5)[§]
IQR	*11*	*93*	*17*	*38*	*61*	*17*	*14*	*8*

[†] aerodynamic gradient method for values between 06H00–18H00 local time
[§] values derived from substitution with "dry–wet" nighttime data

(b) LBA-EUSTACH-2, 24 September to 27 October 1999, "dry–wet" transition period.

	R_a		R_b		R_c		v_d	
Gas	day	night	day	night	day	night	day	night
NO_2 (median)	23	51	23	33	209	229	4	3
NO_2 (IQR)	*13*	*76*	*16*	*41*	*182*	*149*	*6*	*6*
O_3 (median)	23	51	23	33	106	65	6	5
O_3 (IQR)	*13*	*76*	*17*	*41*	*101*	*50*	*8*	*7*
$O_3^{\dagger}$ (median)	23	51	23	33	141	—	5	—
$O_3^{\dagger}$ (IQR)	*13*	*76*	*17*	*41*	*130*	—	*6*	—

[†] aerodynamic gradient method for values between 06H00–18H00 local time

Table A5. (a) & (b). NO emission fluxes (ng N m^{-2} s^{-1}) and dry deposition fluxes of NO_2 (ng N m^{-2} s^{-1}) and O_3 (n mol m^{-2} s^{-1}) derived by the inferential method (cf. Section 1.2.4) for LBA-EUSTACH-1 and -2 campaigns: means, standard deviations, counts, medians and quartiles.

(a) LBA-EUSTACH-1, 30 April to 17 May 1999, "wet–dry transition period.

gas	mean	std dev.	count %	Q25	median	Q75
NO_2[†]	–0.91	0.89	46%	–1.05	–0.70	–0.46
O_3[§]	–3.39	2.78	46 %	–4.34	–2.75	–1.67

[†] values derived from a proxy $R_c(NO_2)$ (cf. Section 1.3.3)
[§] values derived from substitution with "dry–wet" nighttime data

(b) LBA-EUSTACH-2, 24 September to 27 October 1999, "dry–wet" transition period.

gas	mean	std dev.	count %	Q25	median	Q75
NO	0.65	0.39	9 %	0.43	0.55	0.75
NO_2	-4.60	2.91	12 %	-5.75	-3.93	-2.80
O_3	-6.76	4.07	19 %	-8.74	-6.11	-3.71

Appendix B

TABLES TO CHAPTER 2

Table B1. Average forest and pasture soil NO flux rates characterized by dry or wet season (ng N m^{-2} s^{-1}) for the Amazon basin.

Forest	ng N m^{-2} s^{-1}	Season	Source
Manaus, clay soils	11.9	dry	*Kaplan et al.* [1988]
Manaus, clay soils	2.1	wet	*Bakwin et al.* [1990a]
Manaus, sand soils	7.8	dry	*Bakwin et al.* [1990a]
Parã	4.1	dry	*Davidson & Kingl.* [1997]
Parã	2.7	wet	*Davidson & Kingl.* [1997]
Parã	2.9	dry	*Verchot et al.* [1999]
Parã	5.9	dry	*Verchot et al.* [1999]
Parã	3.3	wet	*Verchot et al.* [1999]
Rondônia	8.8	dry	*Garcia-M. et al.* [2001]
Rondônia	4.9†	dry/wet	*Gut et al.* [submitted]

Pasture	ng N m^{-2} s^{-1}	Season	Source
Parã (fert., active) §	2.5	dry	*Davidson & Kingl.* [1997]
Parã (fert., active)	27.7	wet	*Davidson & Kingl.* [1997]
Parã (fert., old)	1.4	dry	*Davidson & Kingl.* [1997]
Parã (31 yrs.)	1.5	dry	*Verchot et al.* [1999]
Parã (31 yrs.)	1.7	wet	*Verchot et al.* [1999]
Rondônia (22 yrs.)	0.55†	dry	cf. Chapter 1

† median NO flux value

§ previously fertilized and maintained

Table B2. Soil property model initialization parameters.

Soil parameter	Unit	Value
Organic Carbon	%	1.07
Total Phosphorus	%	0.01
Total Nitrogen	%	0.15
Total Carbon	%	1.41
Total Sulfur	%	0.01
Plant available Phosphorus	mg PO_4 100 g^{-1}	2.62
Plant available Potassium	mg K 100 g^{-1}	6.66
pH [$CaCl_2$]	—	3.6
Bulk soil density	Mg m^{-3}	1.31
Clay content	%	13.1
Silt content	%	12.9
Sand content	%	73.9
Wilting Point (WP)†	cm^3 cm^{-3}	7.5
Field Capacity (FC)†	cm^3 cm^{-3}	20.7
CEC (cation exchange capacity)	mmol $z^{-1}100g^{-1}$	17.75
Ammonium pool (NH_4^+)	μg NH_4^+ g^{-1}	9.4
Nitrate pool (NO_3^-)	μg NO_3^- g^{-1}	11.8
C:N ratio (soil upper 5 cm)	—	9.2
Saturated hyd. conductivity (K_{sat})	cm s^{-1}	0.00184
C surface OM (active)	g m^{-2}	40.5
C soil OM (active)	g m^{-2}	414.6
C soil OM (slow)	g m^{-2}	888.2
C soil OM (passive)	g m^{-2}	430.2
C:N ratio surface OM (active)	—	4.6
C:N ratio soil OM (active)	—	11
C:N ratio soil OM (slow)	—	12.5
C:N ratio soil OM (passive)	—	6.5
Surface plant C residue	g m^{-2}	144.2
C:N ratio of surface and soil litter	—	27.7

† Based on *Tomasella* & *Hodnett* [1998] pedo-transfer functions

Table B3. Forest and pasture biomass model initialization parameters.

Forest parameter	Value	Source
Aboveground live C	17150 g m^{-2}	*Guild et al.* [1998]
Aboveground live N	156.5 g m^{-2}	*Guild et al.* [1998]
Belowground live C	2805 g m^{-2}	*Liu et al.* [2000]
Belowground live N	33.8 g m^{-2}	*Metherell et al.* [1993]
C leaf	430 g m^{-2}	*Guild et al.* [1998]
N leaf	19.6 g m^{-2}	*Guild et al.* [1998]
C fine branch	3665 g m^{-2}	*Guild et al.* [1998]
N fine branch	45.5 g m^{-2}	*Guild et al.* [1998]
C large wood	13055 g m^{-2}	*Guild et al.* [1998]
N large wood	94.4 g m^{-2}	*Guild et al.* [1998]
C fine root	165 g m^{-2}	*Metherell et al.* [1993]
N fine root	8.6 g m^{-2}	*Guild et al.* [1998]
C coarse root	2640 g m^{-2}	*Liu et al.* [2000]
N coarse root	137.9 g m^{-2}	*Liu et al.* [2000]
C dead fine branch	113 g m^{-2}	*Liu et al.* [2000]
C dead large wood	1641 g m^{-2}	*Liu et al.* [2000]
C dead coarse root	528 g m^{-2}	*Liu et al.* [2000]
Theoretical maximum net biomass production	418 g C m^{-2} mo^{-1}	*Metherell et al.* [1993]
C:N ratio of leaves	21.9	*Guild et al.* [1998]
C:N ratio for fine roots	19.1	*Guild et al.* [1998]
C:N ratio for fine branches	86.2	*Guild et al.* [1998]
C:N ratio for large wood	138.4	*Guild et al.* [1998]
C:N ratio for coarse roots	19.1	*Guild et al.* [1998]
Decomposition dead fine branch	5 % yr^{-1}	*Liu et al.* [2000]
Decomposition dead large wood	0.1 % yr^{-1}	*Graça* [1999]
Decomposition dead coarse root	0.9 % yr^{-1}	*Liu et al.* [2000]
C allocation new leaves	0.46	*Liu et al.* [2000]
C allocation new fine roots	0.08	*Liu et al.* [2000]
C allocation new fine branches	0.16	*Liu et al.* [2000]
C allocation new large wood	0.17	*Liu et al.* [2000]
C allocation new coarse roots	0.13	*Liu et al.* [2000]
C allocation old leaves	0.46	*Liu et al.* [2000]
C allocation old fine roots	0.08	*Liu et al.* [2000]
C allocation old fine branches	0.16	*Liu et al.* [2000]
C allocation old large wood	0.17	*Liu et al.* [2000]
C allocation old coarse roots	0.13	*Liu et al.*, [2000]

Leaf death rate Jan	2 %	*Roberts* [pers. comm.]
Leaf death rate Feb	3 %	*Roberts* [pers. comm.]
Leaf death rate Mar	4 %	*Roberts* [pers. comm.]
Leaf death rate Apr	3 %	*Roberts* [pers. comm.]
Leaf death rate May	8 %	*Roberts* [pers. comm.]
Leaf death rate Jun	13 %	*Roberts* [pers. comm.]
Leaf death rate Jul	12 %	*Roberts* [pers. comm.]
Leaf death rate Aug	11 %	*Roberts* [pers. comm.]
Leaf death rate Sep	6 %	*Roberts* [pers. comm.]
Leaf death rate Oct	4 %	*Roberts* [pers. comm.]
Leaf death rate Nov	3 %	*Roberts* [pers. comm.]
Leaf death rate Dec	4 %	*Roberts* [pers. comm.]
Maximum LAI	7 m^{-2} m^{-2}	*Kirkman* [unpub. data]
N retranslocation at leaf death	81 %	*Kauffman et al.* [1995]
Death rate fine root	0.035 %	*Liu et al.* [2000]
Death rate fine branch	0.18 %	*Liu et al.* [2000]
Death rate large wood	0.12 %	*Liu et al.* [2000]
Death rate coarse root	0.32 %	*Liu et al.* [2000]

Pasture parameter	Value	Source
Potential aboveground biomass (grass)	317 g m^{-2} yr^{-1}	*Waterloo* [pers. comm.]
Potential aboveground biomass (soyabean)	400 g m^{-2} yr^{-1}	*Metherell et al.* [1993]
Potential aboveground biomass (maize)	600 g m^{-2} yr^{-1}	*Metherell et al.* [1993]
Potential aboveground biomass (sorghum)	620 g m^{-2} yr^{-1}	*Metherell et al.* [1993]

Table B4. Model land-use management parameters.

Fire parameter	Value	Source
Fraction of leaf live component removed	98 %	*Kauffman et al.* [1995]
Fraction of fine branch live component removed	88 %	*Kauffman et al.* [1995]
Fraction of large wood live component removed	37 %	*Kauffman et al.* [1995]
Fraction of dead fine branches component removed	89 %	*Kauffman et al.* [1995]
Fraction of large wood dead component removed	79 %	*Kauffman et al.* [1995]
Fraction of C that is returned in the live leaf	22 %	*Kauffman et al.* [1995]
Fraction of C that is returned in the fine branch	20 %	*Kauffman et al.* [1995]
Fraction of C that is returned in the large wood	8 %	*Kauffman et al.* [1995]
Fraction of N that is returned in the live leaf	18 %	*Kauffman et al.* [1995]
Fraction of N that is returned in the fine branch	16 %	*Kauffman et al.* [1995]
Fraction of N that is returned in the large wood	7 %	*Kauffman et al.* [1995]
Fraction of understory standing dead removed	97 %	*Kauffman et al.* [1995]
Fraction of understory litter removed	95 %	*Kauffman et al.* [1995]
Fraction of N in burnt understory returned to soil	2 %	*Kauffman et al.* [1995]

Tree removal parameter	Value	Source
Leaf live component removed	98 %	*Kauffman et al.* [1995]
Fine branch live component removed	88 %	*Kauffman et al.* [1995]
Large wood live component removed	37 %	*Kauffman et al.* [1995]
Dead fine branches component removed	89 %	*Kauffman et al.* [1995]
Large wood dead component removed	79 %	*Kauffman et al.* [1995]
C returned to live leaf	22 %	*Kauffman et al.* [1995]
N returned to live leaf	18 %	*Kauffman et al.* [1995]
C returned to fine branch	20 %	*Kauffman et al.* [1995]
N returned to fine branch	16 %	*Kauffman et al.* [1995]
C returned to large wood	8 %	*Kauffman et al.* [1995]
N returned to large wood	7 %	*Kauffman et al.* [1995]

Grazing parameter	Value	Source
N excreted in faeces and urine	20 %	*Davidson* [pers. comm.]
Live biomass removed by grazing	30 %	*Metherell et al.* [1993]

Harvesting parameter	Value	Source
Biomass removed by harvesting	95 %	*Metherell et al.* [1993]

Table B5. Observed and expected medians (std. dev.), root mean square error (RMSE) and correlation (r^2) estimates of goodness of fit for the parameters used for model optimization (NO fluxes are in units of ng N m^{-2} s^{-1}).

Model parameter for RBJ (forest)	Observed	Expected	RMSE †	r^2 §
Soil water content at 15 cm [% vol.]	15 (5)	9.8 (12)	3.5	0.86
Soil temperature at 2 cm [°C]	25.3 (1)	25.3 (1)	1.5	0.88
NO flux, wet–dry season (day 125-131)	4.8 (1)	3.6 (0.7)	1.7	0.88
NO flux, dry–wet season (day 265-305)	5.0 (2)	4.8 (1.6)	2	0.86

Model parameter for FNS (pasture)	Observed	Expected	RMSE †	r^2 §
NO flux, dry–wet season (day 266-300)	0.6 (0.3)	0.79 (0.3)	0.8	0.43
Above ground live biomass N [g m^{-2}]	2.1	2.7 (13)	—	—

† RMSE = $\sqrt{1/n \, \Sigma(y - x)^2}$

§ $r^2 = cov(x, y)/s_x \, s_y$

Appendix C

TABLES TO CHAPTER 3

Table C1 Land age contribution to net annual soil NO emissions (non urban areas) (Gg N–NO).

Age	Area [ha]	NO flux [Gg N–NO]	NO flux Std Dev
Forest	1.4×10^{6}	0.42	0.00
1 yr.	9.7×10^{4}	0.32 (0.08)†	0.04
2 yr.	6.4×10^{4}	0.04	0.02
3 yr.	4.4×10^{4}	0.03	0.01
4 yr.	2.0×10^{5}	0.14	0.02
7 yr.	1.5×10^{5}	0.09	0.02
10 yr.	4.8×10^{4}	0.02	0.01
11 yr.	6.6×10^{4}	0.03	0.01
12 yr.	1.3×10^{5}	0.05	0.01
14 yr.	3.1×10^{5}	0.12	0.02
22 yr.	1.3×10^{5}	0.03	0.00
Total		1.3 (1.06)†	

† excluding S+B pulse

Table C2 Net soil NO emission rates and regional contributions for different land-use classes.

Land-use	Area (ha)	Mean (kg N $ha^{-1}yr^{-1}$)	Range	Std Dev	Regional (Gg N yr^{-1})
Forest	1.4×10^6	0.30	0.07–0.3	0.03	0.42
Pasture	9.7×10^5	0.72	0.23–3.7	0.8	0.71
2^{nd} growth	2.0×10^5	0.85	0.18–2.8	0.9	0.17

Table C3 A comparison of bulk NO emissions (excl. CRF) by ecosystem for the tropical globe, from *Davidson & Kingerlee* [1997]† and the current up scaling study [Chapter 3].

Ecosystem	Area† (ha)	Inventory† (Tg N yr^{-1})	Up scale (Tg N yr^{-1})
Forest	1.0×10^9	1.10	1.34
Pasture	1.5×10^8	0.27	0.15
2^{nd} growth	1.5×10^8	0.27	0.23
Total	1.3×10^9	1.64	1.71

† after *Davidson & Kingerlee* [1997]

Appendix D

TABLES TO CHAPTER 4

Table D1. Mean ecosystem (dry/wet) NO model parameters where m_c (ppb) is compensation mixing ratio, *P* is NO production rate (ng N h^{-1} g^{-1} dry weight), *k* is consumption rate constant (cm^{-3} N h^{-1} g^{-1} d.w.) *De* is the soil NO diffusion coefficient (cm^2 s^{-1}), θ_{opt} is the optimum soil moisture for NO production (WFPS), and *a* and *B* are fitting parameters.

Ecosystem	m_c	*P*	*k*	*De*	θ_{opt}	*a*	*B*
Miombo (dry)	4.9	0.5	47.4	0.08	0.13±0.004	5.4±5.3	0.07±0.02
Miombo (wet)	47.4±2.0	1.5±0.3	53.8±7.4	0.03±0.001	0.13±0.004	5.4±5.3	0.07±0.002
Grassland (dry)	10.9±2.9	0.2±0.1	26.5±5.1	0.05±0.009	0.17	84.9	0.08
Grassland (wet)	84.6±1.6	2.2±0.04	45.4	0.01	0.17	84.9	0.07
Maize (dry)	9.3±0.1	0.2±0.1	35±2.5	0.06±0.003	0.18±0.007	1.5±0.59	0.01±0.03
Maize (wet)	73.8±33.6	1.4±0.2	36.7±12.4	0.03	0.18±0.007	1.5±0.59	0.08±0.001

± signifies one standard deviation at two degrees of freedom

Table D2. Leaf area index (LAI) and standard error (SE) ($m^2\ m^{-2}$) at various locations in Zimbabwe—December 1998.

Lat.	Long.	Vegetation type	Location	LAI	SE
–22.00	29.91	Sparse Mopane-Acacia woodland	Beitbridge	0.9	0.1
–22.00	29.91	Sparse Mopane-Acacia woodland	Beitbridge	0.9	0.2
–22.00	29.91	Sparse Mopane-Acacia woodland	Beitbridge	0.8	0.1
–21.42	29.69	Sparse Mopane-Acacia woodland	Beitbridge	0.7	0.1
–21.42	29.69	Sparse Mopane-Acacia woodland	Beitbridge	1.1	0.1
–20.49	29.04	Terminalia woodland	Bulawayo	1.0	0.1
–20.49	29.04	Terminalia woodland	Bulawayo	1.3	0.1
–19.69	28.40	Teak/Terminalia woodland	Bulawayo	1.7	0.2
–18.60	27.07	Msasa/Brachystegia woodland	Gwaai	1.4	0.1
–18.16	25.99	Teak/Terminalia woodland	Hwange	1.0	0.1
–17.93	25.85	Rain forest	Vic. Falls	4.2	0.3
–18.73	26.95	Teak/Terminalia woodland	Hwange	1.6	0.1
–18.79	26.98	Teak/Terminalia woodland	Hwange	0.6	0.1
–18.73	26.94	Teak/Terminalia woodland	Hwange	1.2	0.1
–18.73	26.94	Teak/Terminalia woodland	Hwange	1.1	0.1
–18.73	26.92	Teak woodland (low)	Hwange	1.2	0.1
–18.68	26.91	Teak woodland (high)	Hwange	1.0	0.1
–19.93	28.51	Acacia nilotica/Acacia bushland	Bulawayo	1.8	0.1
–19.93	29.01	Grassland on high ground	Bulawayo	0.8	0.1
–19.69	29.57	Grassland on high ground	Gweru	0.7	0.1
–19.30	29.79	Terminalia woodland	Gweru	0.6	0.0
–18.12	30.21	Msasa/Brachystegia woodland	Chegutu	1.3	0.0
–18.11	31.82	Tobacco (mature)	Macheke	3.8	0.4
–17.85	31.25	Msasa/Brachystegia woodland	Ruwa	1.2	0.1
–16.14	29.40	Mopane woodland (riverine)	Rukomechi	1.5	0.2
–16.14	29.40	Mopane/Terminalia woodland	Rukomechi	0.7	0.1
–16.15	29.40	Mopane woodland (escarpment)	Rukomechi	0.8	0.1
–16.17	29.20	Mopane/Teak woodland	Mana Pools	1.0	0.1
–17.49	30.55	Msasa/Brachystegia woodland	Chinoyo	1.3	0.1
–18.05	31.39	Maize	Bromley	2.4	0.1
–18.05	31.39	Paprika	Bromley	0.9	0.1
–18.05	31.39	Disturbed Msasa bushland	Bromley	1.1	0.1
–18.17	31.46	Maize (mature)	Marondera	2.4	0.1
–18.18	31.47	Bluegum (mature)	Marondera	2.7	0.1
–18.18	31.48	Pine (mature)	Marondera	1.5	0.2
–18.18	31.47	Miombo (unburned)	Marondera	1.9	0.1
–18.18	31.47	Miombo (burned every yearly)	Marondera	1.6	0.2
–18.18	31.47	Miombo (burned every 4 years)	Marondera	1.7	0.1
–18.18	31.47	Miombo (burned every 2 years)	Marondera	2.2	0.1

–18.18	31.47	Miombo (burned every 2 years)	Marondera	1.3	0.1
–18.11	31.82	Tobacco (mature, irrigated)	Macheke	3.4	0.3
–18.11	31.82	Brachystegia woodland	Macheke	1.8	0.1
–18.10	31.83	Tobacco (dryland)	Macheke	4.2	0.3
–18.10	31.83	Tobacco (irrigated)	Macheke	3.6	0.4
–20.24	30.96	Msasa/Brachystegia woodland	Masivingo	0.8	0.1

Table D3. Sand, silt, clay, bulk density (BD) and organic matter (OM) properties of the major soil groups in Zimbabwe, [*FAO-UNESCO*, 1995].

Soil group	Sand (%)	Silt (%)	Clay (%)	BD (g/cm^{-3})	OM (%)
Chromic Cambisols	40.1	21.5	38.4	0.8	1.44
Vertic Cambisols	23.3	26	50.7	1.7	1.1
Orthic Ferralsols	28.7	18.4	52.9	1	1.92
Rhodesian Ferralsols	40.4	14.8	44.6	1.2	1.52
Eutric Gleysols	42.8	20.4	36.8	1.2	1.3
Lithosols	58.9	16.2	24.9	1.01	0.97
Eutric Fluvisols	70.8	12.8	16.5	0.9	1.15
Chrom. Luvisols	64.3	12.2	23.5	1.4	0.63
Ferric Luvisols	74.6	9.6	15.9	1.5	0.39
Gleyic Luvisols	59.9	13.4	26.7	1.1	0.73
Calcic Luvisols	75.4	7.4	17.2	1.5	0.34
Orthic Luvisols	76	9.9	14.1	1.4	0.41
Plinthic Luvisols	69.9	10.5	19.5	1.8	0.73
Eutric Nitosols	68.4	10.5	21.2	1.3	0.6
Arenosols	91.9	3.2	5	1.5	0.23
Ferr. Arenosols	91.7	3.3	5.1	1.5	0.27
Luvic Arenosols	92.8	2.7	4.7	1.01	0.2
Vertisols	58.9	16.2	24.9	1.5	0.97
Pellic Vertisols	25.1	12.2	62.7	1.1	0.68
Calcic Xerosols	48.7	29.9	21.6	1.4	0.64

Table D4. Dry season, wet season measured and modeled NO flux rate (ng N m^{-2} s^{-1}) descriptive statistics for the validation site (a) Marondera, Zimbabwe and for (b) South Africa excluding CRF.

(a)

Land-use soil type	Dry	wet season				
	Mean	min.	mean	max.	std. dev	median	n
Measured fluxes [1]							
Grassland	0.1	0.2	3.7	28.9	6.08	1.4	34
Miombo	0.2	0.2	1.2	4.1	1.1	0.7	20
Agricultural[2]	0.2	6.3	11.3	14.7	3.79	12.2	4
Modeled fluxes [3]							
Grassland	0.6	0.4	5.5	10.1	2.6	4.4	7
Miombo	0.6	0.5	7.2	13.3	3.4	5.8	59
Agriculture	0.7	0.5	8.2	15.4	4.0	6.5	8

[1] revised flux values from *Meixner et al.* [1997]
[2] unfertilized maize
[3] 9 pulses per wet season month

(b)

Soil type	dry mean	wet season min.	mean	max
Measured fluxes [*Levine et al.,* 1996]				
Savanna soil	3.3	4.7	19.4	34.0
Measured fluxes [*Otter et al.,* 1999]				
Nutrient poor soil	1.3	1.3	7.9	13.9
Nutrient rich soil	0.9	0.9	5.5	12.2

Table D5 (a). Annual bulk and net nitric oxide emissions (Gg N yr^{-1}) for Zimbabwe inferred from global modeling results of *Yienger & Levy* [1995] and *Potter et al.* [1996]. The area of Zimbabwe is defined as a grid (419,820 km^2), bounded by 16°S–22°S and 27°E–33°E. "Lower" and "Upper" values correspond to the lower and upper ranges as indicated by the legends in Figure 1 (a) and Figure 3 of *Yienger & Levy* [1995] and Figure 6 (b) of *Potter et al.* [1996], respectively. Values in the text correspond to the values corrected for 98 % of the area of Zimbabwe.

	lower	upper	mean	mean[†]
Yienger & Levy [1995], incl. CRF	21.6	39.2	30.4	27.8
Yienger & Levy [1995], excl. CRF	33.3	50.9	42.1	38.5
Potter et al. [1996], excl. CRF	48.4	58.4	53.4	48.8

[†] corrected for 98 % of the area of Zimbabwe (383,667 km^2)

Table D5 (b). Dry (7 months), wet (5 months) season, bulk and net nitric oxide emissions (Gg N yr^{-1}) per land-use for Zimbabwe. Including a comparison with field measurement based bulk emissions after *Meixner et al.* [1997]. Modeled values include nine pulse events per wet season month.

Land Use	dry	wet	bulk	field[†]	net[§]
Grassland	0.3	1.8	2.1	1.0	1.6
Miombo	4.8	23.6	28.4	5.1	20.5
Agriculture	2.3	12.3	14.6	16.4	10.8
Total	7.5	37.6	45.1	22.4	32.9

[†] derived from revised *Meixner et al.* [1997] emission rates (cf. Table D4)

[§] net values are bulk values less CRF

BIBLIOGRAPHY

Alley, W.M., On the treatment of evapotranspiration, soil moisture accounting, and aquifer recharge in monthly water balance models, *Water Resources Research*, 20, 1137–1149, 1984.

Alves, D.S., Pereira, J.L.G., De Sousa, C.L., Soares, J.V., Yamaguchi, F., Characterizing landscape changes in central Rondônia using Landsat TM imagery, *International Journal of Remote Sensing*, 20, 2877–2882, 1999.

Ammann, C., On the applicability of relaxed eddy accumulation and common methods for measuring trace gas fluxes, ETH, *Züricher Geographische Schriften*, 73 pp., Zürich, 1999.

Ammann, C., U. Rummel, A. Gut, M. Scheibe, F. X. Meixner, and M. O. Andreae, Canopy reduction effect on nitric oxide emission from Amazonian rain forests, *J. Geophys. Res.*, submitted, 2001.

Anderson, I.C., Levine, J.A., M.A., Proth, M.A., Riggan, P.J., Enhanced biogenic emissions following surface biomass burning, *J. Geophys. Res.*, 93, 3893–3898, 1988.

Andreae, M.O., Chapuis, A., Cros, B., Fontan, J., Helas, G., Justice, C., Kaufman, Y.J., Minga, A., Nganga, D., Ozone and aitken nuclei over equatorial Africa: Airborne observations during DECAFE 88, *J. Geophys. Res.*, 97, 6137–6148, 1992.

Andreae, M.O., de Almeida, S.S., Artaxo, P., Brandao, C., Carswell, F. E., Ciccioli, P., Culf, A., Esteves, J. L., Gash, J. Grace, J., Kabat, P., Lelieveld, J., Malhi, Y., Manzi, A. O., Meixner, F.X., Nobre, A., Nobre, C., de Lourdes Ruivo, M. A., Silva-Dias, M. A., Stefani, P., Valentini, T., Waterloo, M., Towards an understanding of the biogeochemical cycling of carbon, water, energy, trace gases and aerosols in Amazonia: An overview of the LBA-EUSTACH experiments, *J. Geophys. Res.*, submitted, 2001.

Andreae, M.O., Merlet, P., Emission of trace gases and aerosols from biomass burning, *Global Biogeochemical Cycles*, submitted, 2001.

Asrar, G., Fuchs, M., Kanemasu, E.T., Hatfield, J.H., Estimating absorbed photosynthetic radiation and leaf area index from spectral reflectance in wheat, *Agronomy Journal*, 76, 300–306, 1984.

Aubert, G., Tavernier, R., Soil survey. Soils of the Humid Tropics. National Academy of Sciences, Washington, D.C., 17–44, 1972.

Bakwin, P.S., Wofsy, S.C., Fan, S,-M, Keller, M., Trumbore, S.E., da Costa, J.M., Emission of nitric oxide from tropical forest soils and exchange of NO between the forest canopy and atmospheric boundary layers, *J. Geophys. Res.*, 95, 16755–16764, 1990a.

Bakwin, P.S., Wofsy, S.C., Fan, S.-M., Measurements of reactive nitrogen oxides (NO_y) within and above a tropical forest canopy in the wet season, *J. Geophys. Res.*, 95, 16765–16772, 1990b

Baldocchi, D. D., Deposition of gaseous sulfur compounds to vegetation, in *Sulfur nutrition and assimilation and higher plants*, edited by L. J. De Kok et al., SPB Academic Publishing, The Hague, The Netherlands, 271–293, 1993.

Baumgartner M., Bock E., Conrad R., Processes involved in uptake and release of nitrogen-dioxide from soil and building stones into the atmosphere, *Chemosphere*, 24, 1943–1960, 1992.

Besler, L.W., Population ecology of nitrifying bacteria, *Annual Review of Microbiology*, 33, 309–333, 1979.

Blackmer, A.M., Cerrato, M.E., Soil properties affecting the formation of nitric oxide by chemical reaction of nitrite, *Soil Science Society of America Journal*, 50, 1215–1222, 1986.

Bossel, H., TREEDYN3 Forest Simulation Model - mathematical model, program documentation, and simulation results, Forschungszentrum Waldoekosysteme der Univ. Goettingen, Goettingen, ISBN 0939-1339, 1994

Brinkman, W.L.F., de Nascimento, J.C., The effect of slash and burn agriculture on plant nutrients in the tertiary region of central Amazonia, *Turrialba*, 23, 284–290, 1973.

Brinkman, W.L.F., Nutrient balances of a central Amazonian rainforest: comparison of natural and man-managed systems, Hydrology of Humid Tropical Regions, edited by Keller, R., International Association of Scientific Hydrologists, Publication No. 140, 153–163, 1983.

Browder, J.O., Surviving in Rondônia: The Dynamics of Colonist Farming Strategies in Brazil's Northwest Frontier, *Studies in Comparative Int. Development*, 29, 45–69, 1994

Browder, J.O., Godfrey, B.J., *Rainforest Cities*, Columbia University Press, New York, 429 pp., 1997.

Brown, S., Gaston, G., Tropical Africa: Land Use, Biomass, and Carbon Estimates for 1980, in The Miombo CD-ROM, LUCC International Project Office, Institut Cartografic de Catalunya (ICC), Parc de Montjuïc, s.n. E-08038 - Barcelona, Spain, 1997.

Campbell, B.M., Swift, M.J., Hatton. J., Frost, P.G.H., Small-scale vegetation pattern and nutrient cycling in miombo woodland in Verhoeven, J.T.A., Heil, G.W., Werger, M.J.A., eds., Vegetation structure in relation to carbon and nutrient economy, SPB Academic Publishing, The Hague, 69–85, 1988.

Cardenas, L., Rondon, A., Johansson, C., Sanhueza, E., Effects of soil moisture, temperature and inorganic nitrogen on nitric oxide emissions from acidic tropical savannah soils, *J. Geophys. Res.*, 98, 14783–14790, 1993.

CFU, Commercial Farmers Union of Zimbabwe, P.O. Box, WGT 390, Westgate, Harare, Zimbabwe, 1998.

Chalk, P.M., Smith, C.J., Chemodenitrification, *Development in Plant Soil Science*, 9, 65–89, 1983.
Chameides, W. L., Acid dew and the role of chemistry in the dry deposition of reactive gases to wetted surfaces, *J. Geophys. Res*., 92, 11895–11908, 1987.
Chameides, W.L., Kasibahtla, P.S., Yeinger, J., Levy, II.H., Growth of continental-scale metro agro-plexes, regional ozone production, and world food production, *Science*, 264, 74–77, 1994.
Chestnut TJ. Zarin DJ. McDowell WH. Keller M. A nitrogen budget for late-success ional hillslope tabonuco forest, Puerto Rico, *Biogeochemistry,* 46, 85–108, 1999.
Chidumayo, E.N., Aboveground woody biomass structure and productivity in a Zambezian woodland, *Forest Ecology Management,* 36, 33–46, 1990.
Chidumayo, E.N., Annual and spatial variation in herbaceous biomass production in a Zambian dry miombo woodland, *South African Journal of Botany,* 63, 74–81, 1997.
Cleveland, C.C, Townsend, A.R., Schimel, D.S., Fisher, H., Howarth, R.W., Hedin, L.O., Perakis, S.S., Latty, E.F., Von Fisher, J.C., Elseroad, A., Wasson, M.F., Global patterns of terrestrial biological nitrogen (N_2) fixation in natural ecosystems, *Global Biogeochemical Cycles*, 13, 623–645, 1999.
Conrad, Flux of NO_x between soil atmosphere: Importance and soil microbial metabolism, in Denitrification in Soil and Sediment, edited by Revsbech, N.P., Soerensen, J., Plenum Press, New York, 105–128, 1990.
Conrad, R., Compensation concentration as critical variable for regulating the flux of trace gases between soil and atmosphere, Biogeochemistry, 27, 155–179, 1994.
Conrad, R., Soil microbial processes involved in production and consumption of atmospheric trace gases, Advances in Microbial Ecology, 14, edited by Jones, J. G., Plenum Press New York, 1995
Conrad, R., Soil microorganisms as controllers of atmospheric trace gasses (H_2, CH_4, OCS, N_2O and NO), *Micro-biological Reviews*, 60, 609–40, 1996a.
Conrad, R., Metabolism of nitric oxide in soil and soil micro-organisms and regulation of flux into the atmosphere, in Microbiology of atmospheric trace gases, edited by Murrell, J.C., Kelly, D. P., Springer Verlag, Berlin, 167–203, 1996b.
Crutzen, P.J., Photochemical reaction initiated by and influencing ozone in unpolluted tropospheric air, *Tellus*, *26*, 45–55, 1974.
Crutzen, P.J., The role of NO and NO_2 in the chemistry of the troposphere and stratosphere, *Annual Reviews of Earth Planetary Science*, 7, 443–472, 1979.
Crutzen, P. J., Andreae, M. O., Biomass burning in the tropics: Impact on atmospheric chemistry and biogeochemical cycles, *Science*, 250, 1669–1678, 1990.

Crutzen, P.J., Ozone in the Troposphere, in *Composition, Chemistry, and Climate of the Atmosphere*, edited by Singh, H.B., Van Nostrand Reinhold, New York, 1995.

Davidson, E.A., Vitousek, P.M., Matson, P.A., Riley, R., García-Mendéz, G., Maas, JM., Soil emissions of nitric oxide in a seasonally dry tropical forest of Mexico, *J. Geophys. Res.*, 96, 15439–15445, 1991.

Davidson, E.A., Fluxes of nitrous oxide and nitric oxide from terrestrial ecosystems, Microbial Production and Consumption of Greenhouse Gases: Methane, Nitrogen Oxides, and Halomethanes, edited by Rogers, J.E., Whitman, W.B., American Society for Microbiology, Washington, 219–235, 1991.

Davidson, E.A., Pulses of nitric oxide and nitrous oxide flux following wetting of dry soil: an assessment of probable sources and importance relative to annual fluxes, *Ecological Bulletins*, 42, 149–155, 1992.

Davidson, E.A., Matson, P.A., Vitousek, P.M., Riley, R., Dunkin, K., Garcia-Mendez, G., Maass, J.K., Processes regulating soil emissions of NO and N_2O in a seasonally dry tropical forest, *Ecology*, 74, 130–139, 1993.

Davidson, E.A., Soil water content and the ratio of nitrous oxide to nitric oxide emitted from soil, in Biogeochemistry of Global Change: Radiatively Active Trace Gases, edited by R.S. Oremland, 369–386, Chapman & Hall, New York, 1993.

Davidson, E. A., Kingerlee, W., A global inventory of nitric oxide emissions from soils, *Nutrient Cycling in Agroecosystems*, 48 37–50, 1997.

Davidson, E.A., Keller, M., Erickson, H.E., Verchot, L.V., Veldkamp, E., Testing a conceptual model of soil emissions of nitrous and nitric oxides, *BioScience*, 50, 667–680, 2000.

Decaens, T., Rangel AF., Asakawa N., Thomas RJ., Carbon and nitrogen dynamics in ageing earthworm casts in grasslands of the eastern plains of Colombia, *Biology & Fertility of Soils,* 30, 20–28, 1999.

Del Grosso, S.J., Parton, W.J., Mosier, A.R., Ojima, D.S., Kulmala, A.E., Phongpan, S., General model for N_2O and N_2 gas emissions from soils due to denitrification, *Global Biogeochemical Cycles*, 14, 1045–1060, 2000.

Delany, A.C, Davies, T.D., Dry deposition of NO_x to grass in rural East Anglia, *Atmospheric Environment*, 17, 1391–1394, 1983

Delmas, R., Serça, D., Jambert, C., Global inventory of NO_x sources, *Nutrient Cycling in Agroecosystem*, 48, 51–60, 1997.

Dignon, J., NO_x and SO_x emissions from fossil fuels: a global distribution, *Atmospheric Environment*, 26, 1157–1163, 1992.

Dorman, J.L., Sellers, P.J., A global climatology of albedo, roughness length and stomatal resistance for atmospheric general circulation models as represented by the simple biosphere model (SiB), *Journal of Applied Meteorology*, 28, 833–855, 1989

Duyzer, J.H., Meyer, G.M., van Aalst, R.M., Measurement of dry deposition velocities of NO, NO_2 and O_3 and the influence of chemical reactions, *Atmospheric Environment*, 17, 2117–2120, 1983.
Edmisten, J., Preliminary studies on the nitrogen budget of a tropical rainforest, in A Tropical Rainforest, edited by H.T. Odum and R.F. Pigeon, Office of Info. Serv. U.S. At. Energy Comm. Springfield, VA, H211-H215, 1970.
Eitzinger, J., Parton, W.J., Hartman, M., Improvement and validation of a daily soil temperature submodel for freezing/thawing periods, *Soil Science*, 165, 525–534, 2000.
Emde, K., Szöcs, A., Geoökologische Arbeitsmethoden II, Johannes Gutenberg Universität Mainz, 2000.
Erickson, H., Keller, M., Davidson, E., Nitrogen oxide fluxes and nitrogen cycling during post-agricultural succession and forest fertilization in the humid tropics, *Ecosystems*, 4, 67–84, 2001.
FAOCLIM database Publication No. 11 of the FAO Agrometeorology Series Working Paper, FAOCLIM 1.2, A CD-ROM with worldwide agroclimatic data, 68 pp., 1995.
FAO-UNESCO, The digital soil map of the world, version 3.5, FAO, Rome, 1995.
FAO/SADC/RRSP, Southern African Development Community Regional Remote Sensing Project (FAO/SADC RRSP) CD-ROM, Merchant House, 43 Robson Manyika, P.O. Box 4046, Harare, Zimbabwe, 1998.
FAO-Fertilizer Strategy for Zimbabwe, FAO, Rome, 1999.
Feigl, B., Melillo, J., Cerri, C.C., Changes in the origin and quality of soil organic matter after pasture introduction in Rondônia (Brazil), *Plant and Soil*, 175, 212–29, 1995.
Firestone, M.K., Davidson, E.A., Microbial basis of NO and N_2O production and consumption in soils, in Exchange of Trace Gases between Terrestrial Ecosystems and the Atmosphere, edited by Andreae, M.O., Schimel, D.S., John Wiley & Sons, Chichester, 7–21, 1989.
Fishman, J.S., Ramanathan V., Crutzen, P.J. and Liu, S.C., Tropospheric Ozone and Climate, *Nature*, 282, 818–820, 1979.
Folorunso, O.A, Rolston, D.E., Spatial variability of field-measured denitrification gas fluxes, *Soil Science Society of America Journal*, 48, 1214–1219, 1984.
Forman, R.T., Canopy lichens with blue-green algae: A nitrogen source in a Columbian rain forest, *Ecology*, 56, 1176–1184, 1975.
ForMat, Vegetation mapping in Zimbabwe using satellite remote sensing and geographic information systems, 10/1, Newsletter of the Research and Development Division, Zimbabwe Forestry Commission, Forest Research Centre, Harare, 1998.
Frolking, S.E., Mosier, A.R., Ojima, D.S., Li, C., Parton, W.J., Potter, C.S., Priesack, E., Stenger, R., Haberbosch, C., Dorsch, P., Flessa, H., Smith, KA.,

Comparison of N_2O emissions from soils at three temperate agricultural sites - simulations of year-round measurements by four models. *Nutrient Cycling in Agroecosystems*, 52, 77–105, 1998.

Fuentes, J. D., Gillespie, T. J., den Hartog, G., Neumann, H. H., Ozone deposition onto a deciduous forest during dry and wet conditions, *Agricultural and Forest Meteorology*, 62, 1–18, 1992.

Fujisaka, S., White, D., Pasture or permanent crops after slash-and-burn cultivation? Land-use choice in three Amazon colonies, *Agroforestry Systems*, 42, 45–59, 1998.

Fuller, D.O., Prince, S.D., Rainfall and foliar dynamics in tropical Southern Africa: Potential impacts of global climatic change on savanna vegetation, *Climate Change,* 33, 69–96, 1996.

Galbally, I.E., Johansson, C., A model relating laboratory measurements of rates of nitric oxide production and field measurements of nitric oxide emission from soils, *J. Geophys. Res.*, 94, 6473–6480, 1989.

Galloway, J.N., Schlesinger, W.H., Levy, II.H., Micheals, A., Schnoor, J.L., Nitrogen fixation: Anthropogenic enhancement-environmental response, *Global Biogeochemical Cycles*, 9, 235–252, 1995.

Garcia-Montiel, D.C., Steudler, P.A., Melillo, J.M., Neill, C., Piccolo, M.C., Cerri, C., Patterns of NO, N_2O, CO_2 emissions from Brazilian Forest and pastures following a simulated rain event, Supplement to EOS, Transactions, AGU Volume 80, Number 46, November 16, 1999.

Gödde M., Conrad R., Influence of soil properties on the turnover of nitric oxide and nitrous oxide by nitrification and denitrification at constant temperature and moisture, *Biology and Fertility of Soils*, submitted, 2000.

Goosem, S., Lamb, D., Measurements of Phyllosphere nitrogen fixation in a tropical and two sub-tropical rainforests, *J. Tropical Ecology*, 2, 373–376, 1986.

Graça, P.M.L.A.G., Fearnside, P., Cerri, C.C., Burning of Amazonian forest in Areqemes, Rondônia, Brazil: biomass, charcoal formation and burning efficiency, *Forest Ecology and Management*, 120, 179–191, 1999.

Grundmann, G. L., Renault, P., Rosso, L., Bardin, R., Differential effects of soil water content and temperature on nitrification and aeration, *Soil Science Society of America Journal*, 59, 1342–1349, 1995.

Guild, L.S., Kauffman, J.B., Ellingson, L.J., Cummings, D.L., Castro, E.A., Dynamics associated with total aboveground biomass, C, nutrient pools, and biomass burning of primary forest and pasture in Rondônia, Brazil during SCAR-B, *J. Geophys. Res.*, 103, 32091–32100, 1998.

Gupta, S.C., Larson, W.E., Estimating soil water characteristics from particle size distribution, organic matter content and bulk density, *Water Resources Research*, 15, 1633–1635, 1979.

Gut, A., Blatter, A., Fahrni, M, Lehmann, B.E., Neftel, A., Staffenbach, T., A new membrane tube technique (METT) for continuous gas measurements in soils, *Plant and Soil*, 198, 97–87, 1998.

Gut, A., Neftel, A., Staffelbach, T., Riedo, M., Lehmann, B.E., Nitric oxide flux from soil during the growing season of wheat by continuous measurements of the NO soil-atmosphere concentration gradient: A process study, *Plant and Soil*, 216, 165–180, 1999.

Gut, A., van Dijk, S., Scheibe, M., Rummel, U., Kirkman, G.A., Welling, M., Meixner, F.X., Andreae, M.O., NO flux from an Amazonian rain forest soil: Continuous measurements of the flux and NO soil compensation concentration, *J. Geophys. Res.*, submitted, 2001a.

Gut, A., Scheibe, M., Rottenberger, S., Ammann, C., Kuhn, U., Kirkman, G.A., Meixner, F.X., Kesselmeier, J., Lehmann, B.E., Exchange fluxes of NO, NO_2, and O_3 at soil and leaf surfaces in an Amazonian rain forest, *J. Geophys. Res.*, submitted, 2001b.

Guy, P.R., Changes in the Biomass and Productivity of Woodlands in the Sengwa Wildlife Research Area, Zimbabwe, *Journal of Applied Ecology,* 18, 507–519, 1981.

Harris, G.W., Wienhold, F.G., Zenker, T., Airborne observations of strong biogenic NOx emissions from Namibian savanna at the end of the dry season, *J. Geophys. Res.*, 101, 23707–23711, 1996.

Hart, S.C. J.M. Stark, E.A. Davidson, and M.K. Firestone, Nitrogen mineralization, immobilization and nitrification, in Methods of Soil Analysis: Part2 Microbial and Biogeochemical Properties, edited by R.W. Weaver, et al., Soil Sci. Soc. of Am., Madison, Wis., 985-1018, 1994.

Hecht, S.B., Deforestation in the Amazon basin: magnitude, dynamics and soil resource effects, Studies of Third World Society, 13, 61–101, 1982.

Hicks, B.B., Baldocchi, D.D., Meyers, T.P., Hosker, R.P., Jr., Matt, D.R., A preliminary multiple resistance routine for deriving dry deposition velocities from measured quantities, *Water, Air, and Soil Pollution*, 36, 311–330, 1987.

Hicks, B.B., Matt, D.R., Combining biology, chemistry and meteorology in modeling and measuring dry deposition, *Journal of Atmospheric Chemistry*, 6, 117–131, 1988.

Hillel, D., Computer Simulation of Soil-Water Dynamics: A Compendium of Recent Work, International Development Research Center, Ottawa, Canada, 90–94, 1977.

Hodnett, M.G., Oyama, M.D., Tomasella, J., de O Marques Filho, A., Comparisons of long-term soil water storage behavior under pasture and forest in three areas of Amazonia, Amazonian Deforestation and Climate, edited by Gash, J.H., Nobre, C.A., Roberts, J.M., Victoria, R.L., John Wiley & Sons, Chichester, 55–77, 1996.

Holland, E., Lamarque, J. –F., Modeling bio-atmospheric coupling of the nitrogen cycle through NO_x emissions and NO_y deposition, *Nutrient Cycling in Agroecosystems*, 48, 7–24, 1997.

Huebert, B.J., Roberts, C.H., The dry deposition of nitric acid to grass, *J. Geophys. Res.*, 90, 2085–2090, 1985.

Huemmrich, K.F., Goward, S.N., Spectral vegetation indexes and the remote sensing of biophysical parameters, Proceedings of the International Geoscience and Remote Sensing Symposium (IGARSS), Houston, Texas, 1017–1019, 1992.

Hungria, M., Vargas, M.A.T., Environmental factors affecting N-2 fixation in grain legumes in the tropics, with an emphasis on Brazil, *Field Crops Research*, 65, 151–164, 2000.

Hutchinson, G. L., Vigil, M. F., Doran, J. W., Kessavalou, A., Coarse scale soil-atmosphere NOx exchange modeling: status and limitations, *Nutrient Cycling in Agroecosystems*, 48, 25–35, 1997.

IPCC, Climate Change, 1994—Radiative Forcing of Climate Change and an Evaluation of the IPCC IS92 Emission Scenarios, Cambridge University Press, Cambridge, U.K, 1995.

Jacob, D. J., Wofsy, S. C., Budgets of reactive nitrogen, hydrocarbons, and ozone over the Amazon forest during the wet season, *J. Geophys. Res.*, *9*5, 16737–16754, 1990

Jacob, D. J., Bakwin, P. S., Cycling on NOx in tropical forest canopies, in Microbial Production and Consumption of Greenhouse Gases: Methane, Nitrogen Oxides and Halomethanes, edited by Rogers, J E., Whitman, W. B., Am. Soc. Microbiology, 237–253, 1991.

Johansson, C., Field measurements of emission of nitric oxide from fertilized and unfertilized forest soils in Sweden, *Journal of Atmospheric Chemistry*, 1, 429–442, 1984.

Johansson, C., Pine forest: a negligible sink for atmospheric NO_x in rural Sweden, *Tellus*, 39B, 426–438, 1987.

Johansson, C., Rodhe, H., Sanhueza, E., Emission of NO in a tropical savanna and a cloud forest during the dry season, *J. Geophys. Res.*, 93, 7180–7192, 1988.

Johansson, C., Sanhueza, E., Emissions of NO from savanna soils during the rainy season, *J. Geophys. Res.*, 93, 14193–14198, 1988.

Jones, J.A.A., Some limitations on the a/s index for predicting basin-wide patterns of soil water drainage, *Z. Geomorph, N.F.*, 60, 7–20, 1986.

Jordan, C.F., Caskey, W. Escalante, G., Herrera, R., Montagnini. F., Todd, R., Uhl., C., Nitrogen dynamics during conversion of primary Amazonian rain forest to slash and burn agriculture, 40, 131–139, *Oikos*, 1983.

Jordan, C.F., An Amazonian Rainforest: The structure and function of a nutrient stressed ecosystem and the impact of slash and burn agriculture, Parthenon Publishers, 1989.

Juo, A.S.R., Manu, A., Chemical dynamics in slash-and-burn agriculture, Agriculture, *Ecosystems & Environment*, 58, 49–60, 1996.

Kaplan, W.A., Wofsy, S.C., Keller, M., da Costa, J.M., Emission of NO and deposition of O_3 in a tropical forest system, *J. Geophys. Res.*, 93, 1389–1395, 1988.

Kauffman, J.B., Cummings, D.L., Ward, D.E., Babbitt, R., Fire in the Brazilian Amazon: 1. Biomass, nutrient pools, and losses in slashed primary forests, *Oecologia*, 104, 397–408, 1995.

Keller, M., Veldkamp, E., Weitz, A.M., Reiners, W.A., Effect of pasture age on soil trace-gas emissions from a deforested area of Costa Rica, *Nature*, 365, 244–246, 1993.

Keller, M., Reiners, W., Soil-atmosphere exchange of nitrous oxide, nitric oxide, and methane under secondary succession of pasture to forest in the Atlantic lowlands of Costa Rica, *Global Biogeochemical Cycles*, 8, 399–409, 1994.

Kelly, R.H., Parton, W.J., Hartman, M.D., Stretch, L.K., Ojima, D.S., Schimel, D.S., Intra-annual and interannual variability of ecosystem processes in shortgrass steppe, *J. Geophys. Res.*, 105, 20093–20100, 2000.

Kirkman, G.A., Piketh, S.J., Helas, G., Annegarn, H.J., Andreae, M.O., Seasonal Tropospheric Aerosol Characteristics over Southern Africa, *Journal of Aerosol Science*, 29, Suppl. 1, 555–557, 1998.

Kirkman, G.A., Piketh, S.J., Andreae, M.O., Annegarn, H.J., Helas, G., Distribution of aerosols, ozone, and carbon monoxide over southern Africa, *South African Journal of Science*, 96, 423–431, 2000.

Kisser, G., Bieniek, D., Ziegler, H., NO_2 binding to defined phenolics in the plant cuticle, *Naturwissenschaften*, 77, 492–493, 1990.

Klinge, H., Rodrigues, W.Q., Brunig, E., Fittkau, E.J., Biomass and structure in a central Amazonian rainforest, in Tropical Ecological Systems, edited by Golley, F.B, Medina, E., Springer Verlag, 115–122, 1975.

Kolar, J., *Stickoxide und Luftreinhaltung*, Springer Verlag, Heidelberg, 1990.

Kramlich, J.C, Linak, W.P., Nitrous oxide behavior in the atmosphere, and in combustion and industrial systems, *Prog. Energy Combust Science*, 20, 149–202, 1994.

Kramm, G., Müller, H., Fowler, D., Höfken, K.D., Meixner, F.X., Schaller, E., A modified profile method for determining the vertical fluxes of NO, NO_2, ozone and HNO_3 in the atmospheric surface layer, *Journal of Atmospheric Chemistry*, 13, 265–288, 1991.

Kramm, G., Beier, N., Foken , T., Müller, H., Schröder, P., Seiler, W., A SVAT scheme for NO, NO_2 and O_3–Model descriptions and test results, *Meteorol. Atmos. Phys.*, 61, 89–106, 1996.

Larcher, W., Ökophysiologie der Pflanzen, Verlag Eugen Ulmer, Stuttgart, 1994.

Lerdau, M.T., Munger, W.J., Jacob, D., The NO_2 flux conundrum, *Science,* 289, 2291–2293, 2000.

Lessa, A. S. N., Anderson, D.W., Moir, J., Fine root mineralization, soil organic matter and exchangeable cation dynamics in slash and burn agriculture in the semi-arid northeast of Brazil, *Agriculture, Ecosystems and Environment*, 59, 191–202, 1996.

Levine, J.S., Cofer, W., Sebacher, D., Rhinehart, R.P., Winstead, E.L., Sebacher, S., Hinkle, C.R., Scmalzer, P.A., Koller, M., The effects of fire on biogenic

emissions of methane and nitric oxide from wetlands, *J. Geophys. Res.*, 95, 1853–1864, 1990.

Levine, J.S., Cofer III, W. R., Cahoon, Jr., D. R., Winstead, E.L., Sebacher, D.I., Sebacher, S., Scholes, M. C., Parsons, D. A. B., Scholes, R. J., The impact of wetting and burning on biogenic soil emissions of nitric oxide (NO) and nitrous oxide (N_2O) in savanna grasslands in South Africa, *J. Geophys. Res.*, 101, 23689–23697, 1996.

Levine, J.S., Parsons, D.A.B., Zepp, R.G., Burke, R.A., Cahoon, D.R., Jr., Cofer, W.R., III, Miller, W.R., Scholes, M.C., Scholes, R.J., Sebacher, DI., Sebacher, S., Winstead, E.L., Southern African savanna grasslands as a source of atmospheric gases, Fire in the Southern African Savanna: Ecological and Environmental Perspectives, edited by van Wilgen, B.W., Andreae, M.O., Goldammer, J.G., Lindesay, J.A., Witwatersrand University Press, Johannesburg, South Africa, 135-160, 1997.

Lewis, W.M. Jr., Melack, J.M., McDowell, W. H., McClain, M., Richey, J.E., Nitrogen yields from undisturbed watersheds in the Americas, *Biogeochemistry*, 46, 149–162, 1999.

Li, C., Aber, J. D., Stange, F., Butterbach-Bahl, K., Papen, H., A process-oriented model of N_2O and NO emissions from forest soils, 1 Model development, *J. Geophys. Res*, 105, 4369–4384, 2000.

Lin, X., Trainer, M. Liu, S.C., On the non-linearity of the tropospheric ozone production, *J. Geophys. Res.*, 93, 15879–15888, 1988.

Linacre, E.T., A simple formula for estimating evaporation rates in various climates, using temperature data alone, *Agricultural Meteorology*, 18, 409–424, 1977.

Linn, D.M., Doran, J.W., Effect of water-filled pore space on carbon dioxide and nitrous oxide production in tilled and non-tilled soils, *Soil Sci. Soc. Am. J.*, 48, 1267–1272, 1984.

Liu, S., Reiners, W.A., Keller, M., Schimel, D.S., Model simulation of changes in N_2O and NO emissions with conversion of tropical rain forests to pastures in the Costa Rican Atlantic Zone, *Global Biogeochemical Cycles*, 13, 663–677, 1999.

Liu, S., Reiners, W.A., Keller, M., Schimel, D.S., Simulation of nitrous oxide and nitric oxide emissions from tropical primary forests in the Costa Rican Atlantic Zone, *Environmental Modelling & Software*, 15, 727–743, 2000.

Lloyd, J., Grace, J., Miranda, A.C., Meir, P., Wong, S.C., Miranda, B.S., Wright, I.R., Gash, J.H.C., Mcintyre, J., A Simple calibrated model of Amazon rainforest productivity based on leaf biochemical properties, *Plant, Cell & Environment*, 18, 1129–1145, 1995.

Ludwig, J., Untersuchungen zum Austausch von NO und NO_2 zwischen Atmosphäre und Biosphäre, Dissertation, Fakultät für Biologie, Chemie und Geowissenschaften, Universität Bayreuth, Germany, 1994.

Ludwig, J., Meixner, F.X., Vogel, B., Foerstner, J., Soil-air exchange of nitric oxide: an overview of processes, environmental factors, and modeling studies, *Biogeochemistry*, 52, 225–257, 2001.

Luedeke, M. K. B., Badeck, F.-W., Otto, R. D., Haeger, Ch., Doenges, Kindermann, S.,J., Wuerth, G., Lang , T., Jaekel, U., Klaudius, A., Ramge, P., Habermehl, St., Kohlmaier, G. H., The Frankfurt biosphere model: a global process-oriented model for the seasonal and long-term CO_2 exchange between terrestrial ecosystems and the atmosphere. Part I: Model description and illustrations, *Climate Research*, 4, 143–166, 1994.

Luizáo, F., Matson, P., Livingston, G., Luizáo, R., Vitousek, P., Nitrous oxide flux following tropical land clearing, *Global Biogeochemical Cycles*, 3, 281–285 1989.

Manabe, S., Climate and the Ocean Circulation: I. The Atmospheric Circulation and the Hydrology of the Earth's Surface, *Monthly Weather Review*, 97, No. 11, Nov. 1969.

Marufu, L., Photochemistry of the African troposphere – The influence of biomass burning, PhD Dissertation, Faculty of Nature and Astronomy, University of Utrecht, 1999.

Massman, W.J., Partitioning ozone fluxes to sparse grass and soil and the inferred resistance to dry deposition, *Atmospheric Environment*, 27, 167–174, 1993.

Mather, J.R., The Climatic Water Budget, Lexington Books, 1972.

Matson, P.A., Vitousek, P.M., Cross-system comparison of nitrous oxide flux in tropical forest ecosystems, *Global Biogeochemical Cycles*, 1, 163–170, 1987.

Matson, P.A., Vitousek, G.P., Schimel, D.S., Regional extrapolation of trace gas flux based on soils and ecosystems, in Exchange of Trace Gases between Terrestrial Ecosystems and the Atmosphere, edited by Andreae, M.O., Schimel, D.S., John Wiley and Sons, New York, 97–108, 1989.

Matson, P.A., Vitousek, P.M., Ecosystem approach to a global nitrous oxide budget, *Bioscience*, 40, 667–672, 1990.

Matson, P.A., Harris, R.C., Biogenic trace gases: Measuring emissions from soil and water, Methods in Ecology, Blackwell Science, 393 pp., 1995.

Matson, P., NO_x emissions from soils and its consequences for the atmosphere and biosphere: critical gaps and research directions for the future, *Nutrient Cycling in Agroecosystems*, 48, 1–6, 1997.

McKenney, D.J., Shuttleworth, K.F., Vriesacker, J.R., Findlay, W.I., Production and loss of nitric oxide from denitrification in anaerobic Brookstone clay, *Applied Environmental Microbiology*, 43, 534–541, 1982.

McWilliam, A.-L. C., Cabral, O.M.R., Gomes, B.M., Esteves, J.L., and Roberts, J.M., Forest and pasture leaf-gas exchange in south- west Amazonia, Amazonian Deforestation and Climate, edited by Gash, J.H.C., Nobre, C.A., Roberts, J., Victoria, R.L., John Wiley: Chichester, 265–286, 1996.

Meixner, F.X., Surface exchange of odd nitrogen oxides, *Nova Acta Leopoldina* NF 70, Nr. 288, 299-348, 1994a.

Meixner, F.X., Surface exchange of ammonia. Three different micrometeorological procedures applied, Physico-Chemical Behavior of Atmospheric Pollutants, edited by Angeletti, G., Restelli, G., Report EUR 15609, Office for Official Publications of the European Communities, Luxembourg, 749–754, 1994b.

Meixner, F.X., Fickinger, Th., Marufu, L., Serça, D., Nathaus, F.J., Makina, E., Mukurumbira, L., Andreae, M.O., Preliminary results on nitric oxide emission from a southern African savanna ecosystem, *Nutrient Cycling in Agroecosystems*, 48, 123–138, 1997.

Meixner, F.X., Eugster, W., Effects of landscape pattern and topography on emissions and transport, in: Integrating Hydrology, Ecosystem Dynamics, and Biogeochemistry in Complex Landscapes, edited by Tenhunen, J.D., Kabat, P., Dahlem Workshop Report, Chichester: John Wiley & Sons Ltd., 147–175, 1999.

Meixner, F.X., Gatti, L.V., Kirkman, G.A., Cordoba-Leal, A.M., Moura, M.L., Oliveira dos Santos, E., Andreae, M.O., Surface mixing ratios of NO, NO_x, and ozone at an west Amazonian pasture site during the 1999 wet-to-dry and dry-to-wet-transition periods, *Newsletter European Geophysical Society*, 74, 221, 2000.

Metherell, A.K., Harding, L.A., Cole, V.C., Parton, W.J., Century Soil Organic Model Environment Technical Documentation Report No. 4, USDA-ARS, Fort Collins, Colorado, 80523, 1993.

Millington, R.J., Gas diffusion in porous media, *Science*, *130*, 100–102, 1959.

Mintz, Y., Serafini, Y.V., A Global Monthly Climatology of Soil Moisture and Water Balance, *Climate Dynamics*, 8, 13–27, 1992.

Mintz, Y., Walker, G.K., Global fields of soil moisture and land surface evapotranspiration derived from observed precipitation and surface air temperature, *Journal of Applied Meteorology*, 32, 1305–1334, 1993.

Monteith, J.L., Principles of Environmental Physics, London, Edward Arnold, 1973.

Moran, E.F., Deforestation and land use in the Brazilian Amazon, *Human Ecology*, 2, 1–21, 1993.

Mosier, A.R., Parton, W.J., Valentine, D.W., Ojima, D.S., Schimel, D.S., Delgado, J.A., CH_4 and N_2O fluxes in the Colorado shortgrass steppe: 1. Impact of landscape and nitrogen addition, *Global Biogeochemical Cycles*, 10, 387–399, 1996.

Motavalli, P.P., Palm C.A., Parton, W.J., Elliot, E.T., Frey, S.D., Comparison of laboratory and modeling simulation methods for estimating soil carbon pools in tropical forest soils, *Soil Biology and Biogeochemistry*, 26, 935–944, 1994.

Motavalli, P.P., Palm C.A., Parton, W.J., Elliot, E.T., Frey, S.D., Soil pH and organic C dynamics in tropical forest soils: Evidence from laboratory and simulation studies, *Soil Biology and Biochemistry*, 27, 1589–1599, 1995.

Mroz, G.D., Jurgensen, M.F., Harvey, A.E., Larsen, M.J., Effects of fire on nitrogen in forest floor horizons, *Soil Science Society of America Journal*, 44, 395–400, 1980.

Müller, H., Meixner, F.X., Kramm, G., Fowler, D., Dollard, G.J., Possanzini, M., Determination of HNO_3 deposition by modified Bowen ratio and aerodynamic profile techniques, *Tellus*, 45B, 346-367, 1993.

Myneni, R.B., Willaims, D.L., On the relationship between FPAR and NDVI, *Remote Sensing Environment,* 40, 200–211, 1994.

Myneni, R., Running, S.W., Glassy, J., Votava, P., FPAR, LAI (ESDT: MOD15A2) 8-day Composite User's Guide, NASA MODIS Land Algorithm, NASA, 16 pp., 2000.

Neff, J.C., Keller, M., Holland, E.A., Weitz, A.W., Veldkamp, E., Fluxes of nitric oxide from soils following the clearing and burning of a secondary tropical rain forest, *J. Geophys. Res.*, 100, 913–25,922, 1995.

Neill, C., Piccolo, M. C., Steudler, P. A., Melillo, J. M., Feigl, B. J., Cerri, C. C., Nitrogen dynamics in soils of forests and active pastures in the western Brazilian Amazon basin, *Soil Biology & Biochemistry*, 27, 1167–1175, 1995.

Neill, C., Piccolo, M. C., Fray, B., Melillo, J. M., Stuedler, P. A., Moraes, J.F.L., Cerri, C. C., Forest- and pasture-derived carbon contributions to carbon stocks and microbial respiration of tropical pasture soils, *Oecologia*, 107, 113–119, 1996.

Neill C., Piccolo M.C., Cerri C.C., Steudler P.A., Melillo J.M., Brito M., Net nitrogen mineralization and net nitrification rates in soils following deforestation for pasture across the southwestern Brazilian Amazon basin landscape, *Oecologia*, 110, 243–252, 1997.

Neill C., Piccolo M.C., Mellillio J.M., Steudler P.A., Cerri C.C., Nitrogen dynamics in Amazon forest and pasture soils measured by N-15 pool dilution, *Soil Biology & Biochemistry*, 31, 567–572, 1999.

Nepstad, D.C., Moreira, AG., Alencar, A.A., Flames in the Rain Forest: Origins, impacts and alternatives to Amazonian Fire, Pilot Program to Conserve the Brazilian Rain Forest, Quick Printer, Brasilia, 1999a.

Nepstad, D.C., Verissimo, A., Alencar, A., Nobre C., Lima, E., Lefebvre, P., Schlesinger, P., Potter, C., Moutinho, P., Mendoza, E., Cochrane, M., Brooks, V., Large-scale impoverishment of Amazonian forests by logging and fire, *Nature,* 398, 505–508, 1999b.

Nyamapfene, K., Soils of Zimbabwe, Nehanda Publishers, Harare, 1991.

Nye, P.H., Greenland, D.J., The soil under shifting cultivation, Technical Comm No 51, Commonwealth Bureau of Soils. Harpenden, Commonwealth Agricultural Bureaux, Farnham Royal, Bucks England, 1960.

Oreskes, N., Shraker-Frechette, K., Belitz, K., Verification, validation, and confirmation of numerical models in the earth sciences, *Science*, 263, 641–646, 1994.

Otter, L.B., Yang, W.X., Scholes, M.C., Meixner. F.X., Nitric oxide emissions from a southern African savanna, *J. Geophys. Res.*, 104, 18471–18485, 1999.
Parkin, T.B., Spatial variability of microbial processes in soil – a review, *Journal of Environmental Quality*, 22, 409–417, 1993.
Palm, C.A., Swift, M.J., Woomer, P.L., Soil biological dynamics in slash-and-burn agriculture, *Agriculture Ecosystems and Environment*, 58, 61–74, 1996.
Parsons, D.A.B., Scholes, M. C., Scholes, R. J., Levine, J. S., Biogenic NO emissions from savanna soils as a function of fire regime, soil type, soil nitrogen and water status, *J. Geophys. Res.*, 101, 23683–23688, 1996.
Parton, W.J., Predicting soil temperatures in a shortgrass steppe, *Soil Science*, 138, 93–101, 1984.
Parton, W.J., Schimel, D.S., Cole, C.V., Ojima, D.S., Analysis of factors controlling soil organic matter levels in Great Plains grasslands, *Soil Science Society of America Journal*, 51, 1173–1179, 465, 1987.
Parton, W.J., Mosier, A.R., Ojima, D.S., Valentine, D.W., Schimel, D.S., Weier, K., Kulmala, A.E., Generalized model for N_2 and N_2O production from nitrification and denitrification, *Global Biogeochemical Cycles*, 10, 401–412, 1996.
Parton, W.J., Hartman, M.D., Ojima, D., Schimel, D., DAYCENT and its land surface submodel: description and testing, *Global Planetary Change*, 19, 35–48, 1998.
Parton, W.J., Holland, E., Del Grosso, S., Hartman, M.D., Martin, R., Arvin R. Mosier, Ojima, D.S., Schimel, D.S., Generalized model for NO_x and N_2O emissions from soils, *Global Biogeochemical Cycles*, submitted, 2000.
Pathre, U., Sinha, A.K., Shirke, P.A., Sane, P.V., Factors determining the midday depression of photosynthesis in trees under monsoon climate, *Trees*, 12, 472–481, 1998.
Piccolo, M..C., Neill C., Melillo J.M., Cerri C.C., ^{15}N Natural abundance in soils along forest-pasture chronosequences in the western Brazilian Amazon Basin, *Oceologia*, 112–117, 1994.
Piccolo, MC., Neill C., Cerri C.C., Steudler PA., N-15 natural abundance in forest and pasture soils of the Brazilian Amazon basin, *Plant & Soil*, 182, 249–258, 1996.
Pio, C.A., Feliciano, M.S., Vermeuelen, A.T., Sousa, E.C., Seasonal variability of ozone dry deposition under southern European climate conditions in Portugal, *Atmospheric Environment*, 34, 195–205, 2000.
Poth, M., Anderson, I.C., Miranda, H.S., Miranda, A.C., Riggan, P.J., The magnitude and persistence of soil NO, N2O, NH4, and CO2 fluxes from burned tropical savanna in Brazil, *Global biogeochemical Cycles*, 9, 503–513, 1995.
Potter, C. S., Matson, P. A., Vitousek, P. M., Davidson, E. A., Process modeling of controls on nitrogen trace gas emissions from soils worldwide, *J. Geophys. Res.*, 101, 1361–1377, 1996.
Potter, C.S., Davidson, E.A., Klooster, S.A., Nepstad, D.C., Negreiros, G.H., Brooks, V., Regional application of an ecosystem production model for

studies of biogeochemistry in Brazilian Amazonia, *Global Change Biology*, 4, 315–333, 1998.

Pulliam, W.M., Parton, W.J., Monthly water balance model applied to diverse ecosystems, *Water Resources Research*, submitted, 1998.

Raich, J.W, Russell, A.E, Vitousek, P.M., Primary productivity and ecosystem development along an electron gradient on Mauna Loa, Hawaii, *Ecology*, 78, 707–721, 1997.

Raich, J.W., Parton, W.J., Russell, AE., Sanford, R.L., Vitousek, P.M., Analysis of factors regulating ecosystem development on Mauna Loa using the Century model, *Biogeochemistry*, 51, 161–191, 2000.

Ramanathan, V., Callis, L., Cess, R., Hansen, J., Isaksen, I., Kuhn, W., Lacis, A., Luther, F., Mahlman, J., Reck, R., and Schlesinger, M., Climate Chemical Interactions and Effects of Changing Atmospheric Trace Gases, *Reviews in Geophysics*, 25, 1441–1482, 1987.

Reiners, W.A., Bouwman, A.F., Parsons, W.J.F., Keller, M., Tropical rain forest conversion to pasture: changes in vegetation and soil properties, *Ecological Applications*, 4, 363–377, 1994.

Remde, A., Slemr, F., Conrad, R., Microbial production and uptake of nitric oxide in soil, *FEMS Microbiology Ecology*, 62, 221–230, 1989.

Remde, A., Conrad, R., Role of nitrification and denitrification for NO metabolism, *Biogeochemistry*, 12, 189–205, 1991.

Remde A., Ludwig J., Meixner F. X., Conrad R., A study to explain the emission of nitric oxide from a marsh soil, *Journal of Atmospheric Chemistry*, 17, 249–275, 1993.

Rhoades, C.C., Coleman, D.C., Nitrogen mineralization and nitrification following land conversion in montane Ecuador, *Soil Biology & Biogeochemistry*, 32, 347–1354, 1999.

Roberts, D.A., Batista, G., Pereira, J., Waller, E., Nelson, B., Change identification using multitemporal spectral mixture analysis: Applications in Eastern Amazonia, Chapter 9 in Remote Sensing Change Detection: Environmental Monitoring Applications and Methods, edited by Elvidge, C., Lunetta. R., Ann Arbor Press, Ann Arbor, Mi, 137–161, 1998.

Roberts, D.A., Numata, I., Holmes, K., Batista, G., Krug, T., Chadwick, O.A., Large scale mapping of land-cover change in Rondônia using multitemporal spectral mixture analysis and decision tree classifiers, *J. Geophys. Res.*, submitted, 2001.

Robertson, G.P., Nitrification and denitrification in humid tropical ecosystems: potential controls on nitrogen retention, in Mineral Nutrients and Tropical Forest and Savanna Ecosystems, ed. J. Proctor, Oxford, Blackwell Scientific, 1989.

Rudolph, J., Conrad, R., Flux between soil and atmosphere, vertical concentration profiles in soil, and turnover of nitric oxide. II. Experiments with naturally layered soil cores, *Journal of Atmospheric Chemistry*, 23, 275–300, 1996.

Rummel, U., Ammann, C., Gut, A., Meixner, F.X., Andreae, M.O., Eddy covariance measurements of nitric oxide flux within an Amazonian rainforest, *J. Geophys. Res.*, submitted, 2001.

Salati, E., Sylvester-Bradley, R., Victoria, R.L., Regional gains and losses of nitrogen in the Amazon basin, *Plant and Soil*, 67, 367–376, 1982.

Sanchez, P.A., Villachioca, J.H., Bandy, D.E., Soil fertility after clearing a tropical rainforest in Peru, *Soil Science Society of America Journal*, 47, 1171-1178, 1983.

Sanhueza, E., Impact of human activity on NO soil fluxes, *Nutrient Cycling in Agroecosystems*, 48, 61-68, 1997.

Saxton, K.E., W.J., Rawls J.S., Romberger, R.I., Papendick, Estimating generalized soil-water characteristics from texture, *Soil Science Society of America Journal*, 50, 1031–1036, 1986.

Schimel, JP, Firestone, M.K., Killham, K.S., Identification of heterotrophic nitrification in a Sierran forest soil, *Applied and Environmental Microbiology*, 48, 802-806, 1984.

Schmidt, I., Bock, E., Anaerobic ammonia oxidation with nitrogen dioxide by *Nitrosomonas eutropha*, *Archives of Microbiology*, 167, 106–111, 1997.

Scholes, R.J., Ward, D., Justice, C.D., Emissions of trace gases and aerosol particles due to vegetation burning in southern-hemispheric Africa, *J. Geophys. Res.*, 101, 23677–23682, 1996.

Scholes, M.C., Martin, R., Scholes, R. J., Parsons, D., Winstead, E., NO and N_2O emissions from savanna soils following the first simulated rains of the season, *Nutrient Cycling in Agroecosystems*, 48, 115–122, 1997.

Scholes, M.C., Andreae, M.O., Biogenic and pyrogenic emissions form Africa and their impact on the global atmosphere, Ambio, 29, 23–29, 2000.

Schuster, M., Conrad, R., Metabolism of nitric oxide and nitrous oxide during nitrification and denitrification in soil at different incubation conditions, *FEMS Microbiology Ecology,* 101, 133–143, 1992.

Schwartz, S. E., Factors governing dry deposition of gases to surface water, Precipitation Scavenging and Atmosphere-Surface Exchange, edited by Schwartz, S.E., Slinn, W.G.N., Coords., II, Hemisphere Publishing Corporation, 789-801, 1992.

Sellers, P.J., Tucker, C.J., Collatz, G.J., Los, S.O., Justice, C.O., Dazlich, D.A., Randall, D.A., A global 1 by 1 NDVI data set for climate studies, Part 2: The generation of global fields of terrestrial biophysical parameters from the NDVI, *International Journal of Remote Sensing*, 15, 3519–3545, 1994.

Serça, D., Delmas, R., Jambert, C., Labroue, L., Emissions of nitrogen oxides from equatrorial rain forest in central Africa: origin and regulation of NO emission from soils, *Tellus*, 46B, 243-254, 1994.

Serça, D., Delmas, R., Le Roux, X., Parsons, D.A.B., Scholes, M.C., Abbadie, L., Lensi, R., Labroue, L., Variability of nitrogen monoxide emissions from African tropical ecosystems, *Global Biogeochemical Cycles*, 12, 637–651, 1998.

Seubert, C.E., Sanchez, P.A., Valverde, C., Effects of land clearing methods on soil properties and crop performance in an Ultisol of the Amazon jungle of Peru, Tropical Agriculture (Trinidad), 54, 307-321, 1977.

Sigler, J.M., Fuentes, J.D., Heitz, R.C., Garstang, M., Ozone dynamics and deposition processes at a deforested site in the Amazon basin, *Ambio*, submitted, 2000.

Silver, W.L., Neff, J., McGroddy, M., Veldkamp, E., Keller, M., Cosme, R., Effects of soil texture on belowground carbon and nutrient storage in a lowland Amazonian forest ecosystem, *Ecosystems*, 3, 193–209, 2000.

Singh, H.B., Reactive nitrogen in the troposphere chemistry and transport of NOx and PAN, *Environment Science Technology*, *21*, 320–327, 1987.

Skopp, J., Jawson, M.D., Doran, J.W., Steady-state aerobic microbial activity as a function of soil water content, *Soil Science Society of America Journal*, 54, 1619–1625, 1990.

Smith, K., Gholz, H.L., de Assis Oliveira, F., Litterfall and nitrogen-use efficiency of plantations and primary forest in the eastern Brazilian Amazon, *Forest Ecology and Management*, 109, 209–220, 1998.

Speight, J.G., The role of topography in controlling throughflow generation: a discussion, *Earth Surface Processes and Landforms*, 5, 187–191, 1980.

Stark, N., Jordan, C.F., Nutrient retention by the rootmass of an Amazonian rainforest, *Ecology*, 59, 434–437, 1978.

Stewart, J.W.B., Aselmann, I., Bouwman, A.F., Desjardins, R.L., Hicks, B.B., Matson, P.A., Rodhe, H., Schimel, D.S., Svensson, B.H., Wassmann, R., Whiticar, M.J., Yang, W.-X., Extrapolation of flux measurements to regional and global scales, in Exchange of Trace Gases between Terrestrial Ecosystems and the Atmosphere, edited by Andreae, M.O., Schimel, D.S., John Wiley and Sons, New York, 155–174, 1989.

Stromgaard, P., Biomass, growth, and burning of woodland in a shifting cultivation area of south central Africa, *Forest Ecology Management,* 12, 163–178, 1985.

Sylvester-Bradley, R., De Oliviera, L.A., De Podesta, J.A., St John, T.V., Nodulation of legumes, nitrogenase activity of roots, and occurrence of nitrogen-fixing Azospirillum spp. in representative soils in Central Amazonia, *Agro-Ecosystems*, 6, 249–266, 1980.

Thompson, J.G., Purves, W.D., A guide to the soils of Rhodesia, Technical handbook No.3, Rhodesia Agricultural Journal, Information Services, Salisbury, Rhodesia, 1978.

Thornthwaite, C.W., An approach toward a rational classification of climate, *Geographical Review*, 38, 55–94, 1948.

Tomasella, J., Hodnett, M.G., Estimating soil water retention characteristics from limited data in Brazilian Amazonia, *Soil Science*, 163, 190–202, 1998.

Torrance, J.D., Climate handbook of Zimbabwe, Department of Meteorological Services, 551.582(689.1), Salisbury, 1981.

Uhl, C., Jordan, C.F., Succession and nutrient dynamics following forest cutting and burning in the Amazon, *Ecology*, 65, 1476–1490, 1984.
van Cleemput, O., Beart, L., Theoretical considerations on nitrite self-decomposition reaction in soil, *Soil Science Society of America Journal*, 40, 322–324, 1976.
van Dijk, S., Meixner, F.X., Production and consumption of NO in forest and pasture soils from the Amazon basin: a laboratory study, *Water Air and Soil Pollution*, submitted, 2000a.
van Dijk, S.M., Meixner, F.X., Nitric oxide release from soils in the Amazon Basin: the effect of soil texture/structure on optimum moisture conditions, *Soil Science Society of America Journal.*, submitted, 2000b.
van Dijk, S.M., Gut, A., Kirkman, G.A., Gomes, B.M., Meixner, F.X., Andreae, M.O., Biogenic NO emissions from forest and pasture soils: Relating laboratory studies to field measurements, *J. Geophys. Res.*, submitted, 2001.
Valente, R.J., Thornton, F.C., Emissions of NO from soil at a rural site in Central Tennessee, *J. Geophys. Res.*, 98, 16745–16753, 1993
Veldkamp, E., Davidson, E., Erickson, H., Keller, M., Weitz, A., Soil nitrogen cycling and nitrogen oxide emissions along a pasture chronosequence in the humid tropics of Costa Rica. *Soil Biology & Biochemistry*, 3, 387–394, 1999.
Verchot, L.V., Davidson, E.A., Cattanio J.H., Ackerman I.L., Erickson H.E., Keller. M., Land use change and biogeochemical controls of nitrogen oxide emissions from soils in eastern Amazonia, *Global Biogeochemical Cycles*, 13, 31–46, 1999.
Villá-Guerrau de Arellano, J., Duynkerke, P. G., Influence of chemistry on the flux-gradient relationships for the NO-NO_3-NO_2 system, *Boundary Layer Meteorology*, 61, 375–387, 1992.
Vitousek, P.M., Matson, P.A. Disturbance, nitrogen availability and losses in an intensively managed loblolly pine plantation, *Ecology*, 66, 13360–13376, 1985.
Vitousek, P.M., Turner, D.R., Parton, W.J., Sanford, R.L., Litter decomposition on the Mauna Loa environmental matrix, Hawaii: Patterns, mechanisms and models, *Ecology*, 75, 418–429, 1994.
Vitousek, P.M, Hedin, L.O, Matson, P.A, Fownes, J.H, Neff, J.C., Within-system element cycles, input-output budgets and nutrient limitation, Successes, Limitations and Frontiers in Ecosystem Science, edited by Pace, M., Groffman, P,. Springer, N.Y., 432–451, 1997.
Weigand, C.L., Richardson, A.J., Escobar, D.E., Gebermann, A. H., Vegetation indices in crop assessments, *Remote Sensing Environment*, 35, 105–119, 1991.
Weitz, A.M., Veldkamp, E., Keller, M., Neff, J., Crill, P.M., Nitrous oxide, nitric oxide, and methane fluxes from soils following clearing and burning of tropical secondary forest, *J. Geophys. Res.*, 103, 28047–28058, 1998.
Welles, J.M., Norman, J.M., Instrument for Indirect Measurement of Canopy Architecture, *Agronomy Journal*, 83, 818–825, 1991.

Wesely, M.L., Hicks, B.B., Some factors that affect the deposition rates of sulfur dioxide and similar gases on vegetation, *J. Air Poll. Control Assoc.*, 27, 1110–1116, 1977.
Wesely, M. L., Parameterization of surface resistances to gaseous dry deposition in regional-scale numerical models, *Atmospheric Environment*, *2*3, 1293–1304, 1989.
Wesely, M.L., Hicks, B.B., A review of the current status of knowledge on dry deposition, *Atmospheric Environment*, 34, 2261–2282, 2000.
Wilks, D.S., Statistical Methods in the Atmospheric Sciences, Academic Press, San Diego, 439 pp., 1995.
Williams, E.J., Fehsenfeld, F.C., Measurement of soil nitrogen oxide emissions at three North American ecosystems, *J. Geophys. Res.*, 96, 1033–1042, 1991.
Williams, E.J., Parrish, D. D., Fehsenfeld, F.C., Determination of nitrogen oxide emission from soils: results from a grassland site in Colorado, United States, *J. Geophys. Res.*, 92, 2173–2179, 1987.
Williams, E.J., Parrish, D.D., Buhr, M.P., Fehsenfeld, F.C., Fall, R., Measurement of soil NOx emissions in central Pennsylvania, *J. Geophys. Res.*, 93, 9539–9546, 1988.
Williams, E.J., Guenther, A., Fehsenfeld, F.C., An inventory of nitric oxide emissions from soils in the United States, *J. Geophys. Res.*, 97, 7511–7519, 1992a.
Williams, E.J., Hutchinson, G.L., Fehsenfeld, F. C., NOx and N_2O emission from soil, *Global Biogeochemical Cycles*, 6, 351–388, 1992b.
Williams, M.R., Fisher, T.R., Melack, J.M., Solute dynamics in soil water and groundwater in a central Amazon catchment undergoing deforestation, *Biogeochemistry*, 38, 303–335, 1997.
Winer, A.M., Peters, J.W., Smith, J.P., Pitts Jr., J.N., Response of commercial chemiluminescent NO-NO_2 analyzers to other nitrogen-containing compounds, *Environmental Science & Technology*, 8, 1118–1121, 1974.
Yang, W.X, Meixner, F.X., Welling, M., Laboratory studies on the release of nitric oxide form a grassland soil (Marondera, Zimbabwe), *Annales Geophysicae*, 14(S II), C 472, 1996.
Yang, W.X, Meixner, F.X., Laboratory studies on the release of nitric oxide from subtropical grassland soils: The effect of soil temperature and moisture, Gaseous Nitrogen Emissions from Grasslands, edited by Jarvis, S.C., Pain, B.F., CAB International, Walling, New York, 67–70, 1997.
Yang, W.X., Otter, L.B., Li, X., Welling, M., van Dijk, S., Meixner, F.X., Methodology for the simultaneous measurement of NO_x and N_2O from soils, *Soil Science Society of America Journal*, submitted, 1998.
Yienger, J.J., Levy, H, Empirical model of global soil-biogenic NOx emissions, *J. Geophys. Res.*, 100, 11447–11464, 1995.
Zart, D., Bock, E., High rate of anaerobic nitrification and denitrification by *Nitrosomonas eutropha* grown in a fermenter with complete biomass retention in

the presence of gaseous NO_2 and NO, *Archives of Microbiology*, 169, 282–286, 1998.